energies

MDPI

Review

Recent Advances in the Development of Nanocatalysts for Direct Methanol Fuel Cells

Maria H. de Sá [1,2,*], Catarina S. Moreira [2,3], Alexandra M. F. R. Pinto [2,3,*] and Vânia B. Oliveira [2,3,*]

[1] CIQUP—Chemistry Research Centre of the University of Porto, Department of Chemistry and Biochemistry, Faculty of Sciences, University of Porto, Rua do Campo Alegre, 4169-007 Porto, Portugal
[2] CEFT—Transport Phenomena Research Centre, Faculty of Engineering, University of Porto, Rua Dr. Roberto Frias, 4200-465 Porto, Portugal
[3] AliCE—Associate Laboratory in Chemical Engineering, Faculty of Engineering, University of Porto, Rua Dr. Roberto Frias, 4200-465 Porto, Portugal
* Correspondence: mhsa@fe.up.pt (M.H.d.S.); apinto@fe.up.pt (A.M.F.R.P.); vaniaso@fe.up.pt (V.B.O.)

Abstract: Direct methanol fuel cells (DMFCs) have attracted much attention due to their potential application as a power source for portable devices. Their simple construction and operation, associated with compact design, high energy density, and relatively high energy-conversion efficiency, give the DMFCs an advantage over other promising energy production technologies in terms of portability. Nowadays, research on DMFCs has received increased attention in both academics and industries. However, many challenges remain before these systems become commercial, including their costs and durability. As a key material with a high-value cost, noble metal catalysts for both the anode and cathode sides face several problems, which hinder the commercialisation of DMFCs. This paper provides a detailed comprehensive review of recent progress in the development of nanocatalysts (NCs) for the anode and cathode reactions of DMFCs, based on Platinum, Platinum-hybrid, and Platinum-free materials. Particular attention is devoted to the systematisation of published experimental results tested in DMFC devices since 2015, with an emphasis on passive DMFC systems. In addition, a dedicated section was created to include modelling/theoretical studies. Some open problems and remaining challenges are also highlighted in the final section.

Keywords: direct methanol fuel cell; methanol oxidation reaction; oxygen reduction reaction; nanocatalysts; passive feed; modelling

Citation: de Sá, M.H.; Moreira, C.S.; Pinto, A.M.F.R.; Oliveira, V.B. Recent Advances in the Development of Nanocatalysts for Direct Methanol Fuel Cells. *Energies* **2022**, *15*, 6335. https://doi.org/10.3390/en15176335

Academic Editor: Jin-Soo Park

Received: 15 June 2022
Accepted: 25 August 2022
Published: 30 August 2022

1. Introduction

The direct methanol fuel cell (DMFC) is considered to be a suitable green power source for portable applications owing to its low operating temperature, high energy density, simplicity, and quick refuelling [1]. Moreover, methanol is an attractive fuel since it is abundantly available and is a liquid fuel, being more easily produced, stored, and handled than hydrogen. It also has a high energy density (4820 Wh L^{-1}) compared to hydrogen (180 Wh L^{-1}) [2] and a lower overall cost than hydrogen, considering production, storage, and transportation. Additionally, a DMFC has a higher electric energy efficiency than a proton-exchange membrane fuel cell (PEMFC) [2], being for these reasons the target fuel cell for small portable devices, overcoming the PEMFC limitations. In the presence of suitable catalysts, the conversion of the chemical energy of methanol (supplied directly to the DMFC) and an oxidant (oxygen from air) into electricity, heat, and water, is the fundamental electrochemical process occurring in the DMFC from [3]. The oxidation of the methanol to carbon dioxide occurs in the anode catalyst layer (CL), while at the cathode CL, the oxygen is reduced to water (as shown in Figure 1).

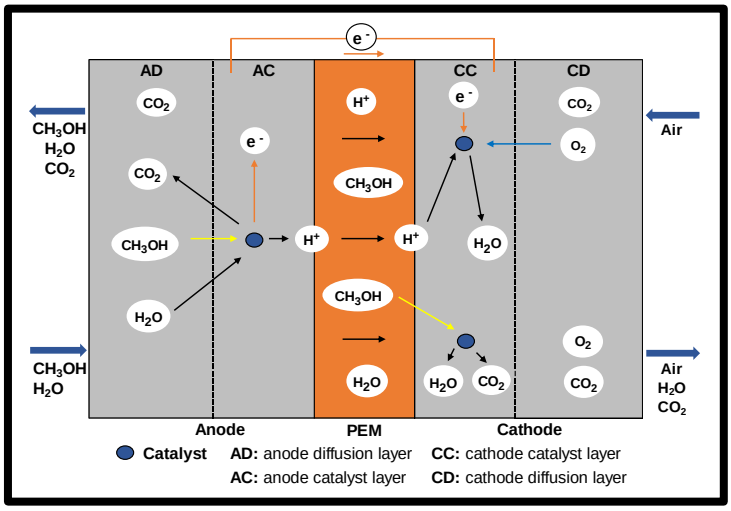

Figure 1. DMFC working scheme.

According to the process by which reactants reach the CLs, DMFCs are classified into two types: active and passive. In active DMFCs, the reactant flow is maintained by an external device (i.e., fan, blower, etc.) while in a passive supply, it is based on diffusion, capillary pressure, and natural convection [4]. Passive DMFCs are compact and do not require external energy to operate, presenting low parasitic power losses. Thus, these systems are a good option to replace the conventional batteries in portable electronic devices [5]. Moreover, due to their unique properties, these fuel cells can be used in remote areas where there is no electricity. Although, towards their commercialisation, it is crucial to achieve an optimum balance between cost, efficiency, and durability [6,7].

The anode and cathode CL structure is aimed to provide an abundant three-phase boundary (TPB), combining the reactant/product at the catalyst nanoparticles surface, carbon support (electron conductor), and Nafion® ionomer (proton conductor) in common sites. Hence, it is in the TPB that the electrochemical reactions actually occur, as illustrated for the cathode side in Figure 2.

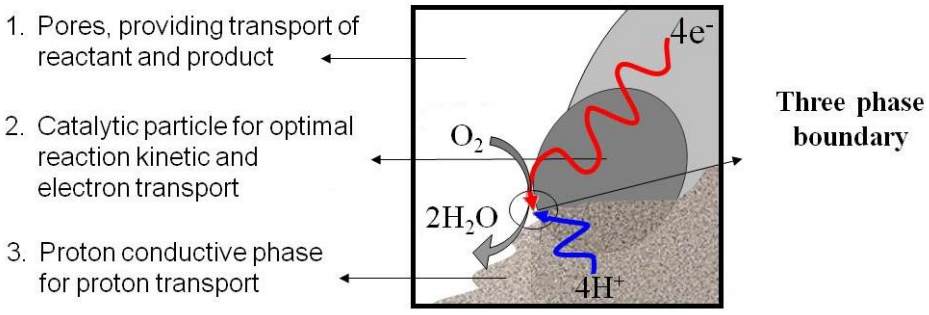

Figure 2. Schematic overview of the three-phase boundary for the cathode CL in a DMFC adapted from [8].

The International Union of Pure and Applied Chemistry (IUPAC) classifies porous materials into three categories according to the pore size, namely, micropores (<2 nm in diameter), mesopores (2–50 nm in diameter), and macropores (>50 nm in diameter) [9]. The catalyst layers (CLs) most commonly support carbon, mainly due to its low cost, chemical stability, high surface area, and affinity for supporting metallic nanoparticles (i.e., the catalyst), typically conductive carbon black (CB). Generally, when catalyst supports such as CB have an average pore diameter below 2 nm (micropores), fuel or gas supplies may not move smoothly in the resulting fuel cell environment, and the catalyst activity starts to be limited by mass transfer issues. Additionally, the micropores in the amorphous particles of CBs are poorly connected. Compared with CBs, mesoporous carbon materials (2–50 nm

in diameter) have fewer or no micropores on their higher surface areas, and mesopore sizes facilitate smooth mass transport and favour the high distribution of catalyst particles, yielding high limiting current values [10].

An ideal DMFC would supply any amount of current while maintaining a constant voltage, 1.21 V, obtained by thermodynamics. However, in a real fuel cell, this is not achieved due to three irreversible losses occurring during the process: activation, ohmic, and mass transport. Moreover, the open circuit voltage is lower than the thermodynamic value due to the methanol crossover. This phenomenon leads to inefficient fuel utilisation on the anode side and also poisons the cathode catalyst. The sluggish kinetics of electrochemical reactions, both anode and cathode, is another factor that declines the cell voltage [11,12]. Therefore, it was early recognised that the DMFC performance would be considerably improved if a methanol-impermeable membrane or a more active anode and methanol-tolerant cathode could be used [13].

Platinum-based nanoparticles (NPs) dispersed on a conductive carbon support, carbon black, have received substantial attention and are the most popular catalysts for DMFC (Pt–Ru on the anode side for the methanol oxidation reaction (MOR) and Pt on the cathode side for the oxygen reduction reaction (ORR)) [14–17]. Additional challenges related to the membrane composition, thickness, and properties are critically analysed in different review papers [18,19] and are out of the scope of this paper, which provides a detailed comprehensive review on recent progress in the development of different nanocatalysts (NCs) for DMFCs' electrodes. An overview of DMFC technology challenges, also detailing the factors and parameters affecting its widespread use, can be found in several scientific publications [2,20–27]. From these, it stems out that the high cost of Pt (Figure 3) and low electrocatalytic activity and durability of the catalysts remain as key problems for the commercialisation of DMFCs.

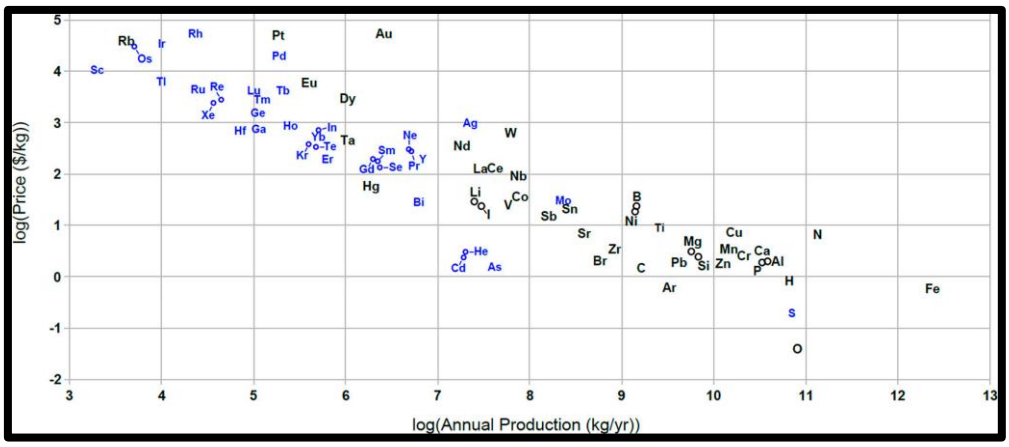

Figure 3. Price of different chemical elements (in USD/kg) versus their annual production (in kg/yr), retrieved from [28].

Due to its unique electron structure, Pt can either obtain or lose an electron from or to the ligands (such as methanol/oxygen and the intermediates) easily. The nanoscale materials have the advantage of inherent increased surface areas, allowing the maximised surface area of Pt per unit of Pt mass, thus better utilizing the high-value electro-active component. However, it is also known that their integrity is challenged by NP agglomeration, detachment, and dissolution during long-time DMFC operation, caused by their weak adsorption to the carbon support [29–31]. Moreover, the traditional carbon support by itself can also suffer from some corrosion processes under fuel cell operating conditions [14,32–35] which also affects the NCs' performance and durability.

All these factors are detrimental to the DMFC performance, which is most significantly affected by catalyst poisoning due to the strong adsorption of intermediary carbon monoxide and other carbonaceous species arising from methanol electrooxidation on pure

Pt. These species block the catalyst surface and retard the reaction kinetics, leading to rather low methanol oxidation activity [36]. The reaction mechanism of MOR in a pure Pt surface is therefore complex and can be summarised by the multi-path mechanism shown in Figure 4:

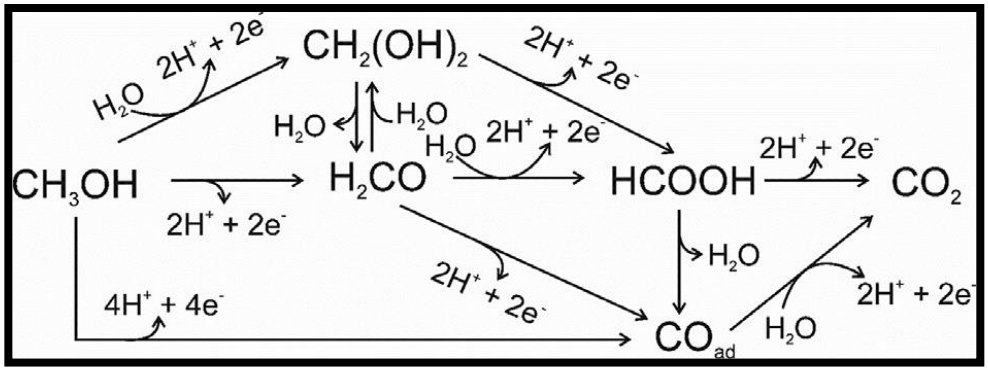

Figure 4. Possible pathways for MOR on pure Pt surfaces in acidic medium, retrieved from [36].

This has been regarded as a "dual/parallel path" mechanism, wherein one reaction path (as illustrated in the bottom) corresponds to the complete dehydrogenation of CH_3OH and yields the undesired intermediary adsorbed carbon monoxide (CO_{ad}); while in all the other possible paths, the incomplete oxidation occurs and leads to the formation of CO_2 through a different set of intermediates: formaldehyde (H_2CO) (available in the aqueous solution as methylene diol ($CH_2(OH)_2$) and formate (in the acidic form (HCOOH) in solution). These products are able to diffuse into the solution or to re-adsorb onto the catalyst surface and further react with the hydroxyl groups (from water) to form CO_2 [37]. The formation of hydroxyl groups by water activation on the Pt surface is a necessary step for the oxidative removal of adsorbed CO; however, it requires a high potential. In terms of MOR, such a high potential will limit the fuel cell application of a pure Pt catalyst, leading to significant overpotential and a loss in DMFC efficiency [38,39]. The solution has been to alloy the Pt with a second metal that can provide oxygenated species at lower potentials for the oxidative removal of adsorbed CO (e.g., Ru, Os, Sn, W, Mo, etc). Among them, the Pt–Ru-based alloy catalyst has been found to be the best active binary catalyst and is still the state-of-the-art anode catalyst for DMFC [21,40]. The enhanced activity of the Pt–Ru catalyst, when compared with Pt for MOR, has been attributed to both a bi-functional mechanism, where the Ru (more oxophilic than Pt) provides oxygenated species to oxidise (and thus remove) CO adsorbed on Pt at a lower potential than the CO_{ad} removal potential on bare Pt, and a ligand (electronic and strain effects) effect where the CO binding strength on Pt is weakened by the influence of the Ru [41]. These phenomena can be summarised as follows:

$$Pt + CH_3OH \rightarrow PtCO_{ad} + 4e^- + 4H^+ \quad (1)$$

$$Ru + H_2O \rightarrow Ru(OH)_{ad} + e^- + H^+ \quad (2)$$

$$PtCO_{ad} + Ru(OH)_{ad} \rightarrow CO_2 + Pt + Ru + e^- + H^+ \quad (3)$$

$PtCO_{ad}$ formation (Equation (1)) is the rate-determining step of the MOR [42]. Moreover, Ru dissolved from an anode (especially at high potentials experienced during start-up and shut-down DMFC) may diffuse across the membrane and cover active sites of the cathode catalyst, resulting in the severe degradation of ORR and DMFC efficiency [43–46]. Moreover, when Pt–Ru is used as an anode electrocatalyst, the power density of a DMFC is about a factor of 10 lower than that of a polymer electrolyte membrane fuel cell operated on hydrogen if the same Pt loading is used [47]. Therefore, it is of great urgency to design and fabricate catalysts with superior durability and improved corrosion resistance [48]. On the cathode side, pure Pt is considered the best electrocatalyst for ORR in DMFCs. However, due not only to its high cost and scarcity but also to its high susceptibility to the adverse

effect of methanol crossover from the anode and/or other intermediary species [49], an alternative should be found. The ORR at the Pt surface is also recognised as a complex process with sluggish kinetics, which involves two paths (the dissociative and associative), with the formation of adsorbed intermediary species at the surface of Pt. These reaction mechanisms of ORR in a pure Pt surface can be summarised by the scheme shown in Figure 5.

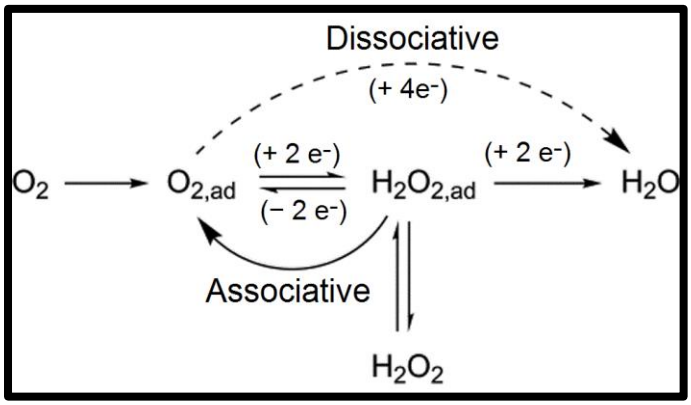

Figure 5. Possible pathways for ORR on pure Pt surfaces in acidic medium, adapted from [50].

The dissociative pathway is considered the "direct" form of four electron pathways since no H_2O_2 is formed during this process. In the associative pathway, the reaction intermediate ($H_2O_{2,ad}$) may be either desorbed from the metal surface and form H_2O_2 or reduced through additional two-electron transfer to form H_2O [50,51]. In fuel cells, the formation of water through the direct four-electron pathway is highly preferred since the generation of H_2O_2 can lead to the radical oxidative degradation of the membrane and the corrosion of the catalyst carbon support [52,53], which are highly undesirable and detrimental. However, water management is also key to the optimum reliability and durability of fuel cells. Furthermore, water crossover from the anode to the cathode exaggerates flooding at the cathode, which limits the mass transport of oxygen and decreases fuel cell performance [23,27,54–56]. Therefore, suitable pore structure and the appropriate hydrophilic/hydrophobic properties of the catalyst and CL should provide efficient water management, so that O_2 can have easy access to the surface of the catalysts and H_2O can be easily removed with minimal formation of H_2O_2 intermediate.

Hence, a large amount of effort is being invested in developing nanocatalysts that enhance the Pt utilisation efficiency or replace its use with other cost-effective materials, with outstanding electrocatalytic activities for MOR and ORR with higher methanol tolerance and durability in DMFCs.

Alternative supports for the catalyst have also been searched; however, the carbon-based ones have advantages in terms of cost and conductivity. In this way, a great concern of the development in the nanotechnology field, especially carbon nanomaterials synthesis, is to create more stable and active supported catalysts. Numerous studies of potential catalyst supports have been performed, but there are also studies on non-carbon materials. This has been the subject of recent extensive dedicated compilations provided in the literature [14,33,57] revealing the importance of the catalyst support in the improvement of the catalytic activity and enhancing the long-term stability and durability of the catalysts. The carbon supports can influence the NCs' properties such as metal particle size, morphology, metal dispersion, alloyed degree, and stability by providing proper loading sites. They should also provide pathways for both mass transport and CL electronic conductivity and NCs stability during the fuel cell operation.

The main goal of this review is to highlight recent advances in the most promising anode and cathode NCs tested in situ of Nafion®-based DMFCs. Moreover, it will give relevance to catalysts tested at low temperatures capable of being used in passive DMFCs. The optimisation of NCs' morphology and compositions becomes difficult to be obtained

because of the many possible combinations of different materials and supports. In order to rationalise the design of catalysts, further understand the different interactions involved, particularly at the atomic scale, and provide confirmation of experimental data or possible reaction mechanisms, the theoretical/simulation approach has been proven to be an important tool. Density Functional Theory (DFT) has captured a central role in this rapidly evolving field [58–61]. Further details on the subject concerning electrocatalysis for DMFCs will be addressed in Section 4 of this paper. Some open problems and continuing challenges are also highlighted in the final section.

2. Nanocatalysts for the Anode

The electrochemical methanol oxidation reaction has attracted great attention from scientists and researchers, and there has been a considerable effort to design catalysts for MOR that have the potential to enhance DMFC performance by overcoming the surface poisoning effects while reducing their cost. Different strategies have been adopted besides using metal NPs and these involve modifying the support materials in order to increase the stability and dispersion of NPs, combining the Pt with other metals and even the complete replacement of Pt by other cost-effective materials, as we present next. The main advantages and disadvantages of the different materials used as NCs for the anode side of a DMFC can be found in Figure 6. The focus will be given to the reaction usually performed in acidic solutions due to the acidic nature of the Nafion® membrane. However, in contrast to acidic DMFCs, it is known that MOR (and ORR) are improved in basic media since in alkaline solutions, specifically adsorbing spectator ions, they are much weaker than in acidic solutions, and there is a higher coverage of adsorbed hydroxyl groups at low potential, which is required for methanol oxidation [62]. However, the critical issue for alkaline fuel cells is the anion exchange membrane, which has low chemical stability [63]. One can find in the literature recent reviews for MOR catalysis [64–69] that can help to understand the context and impact of the following achievements in DMFC acidic medium.

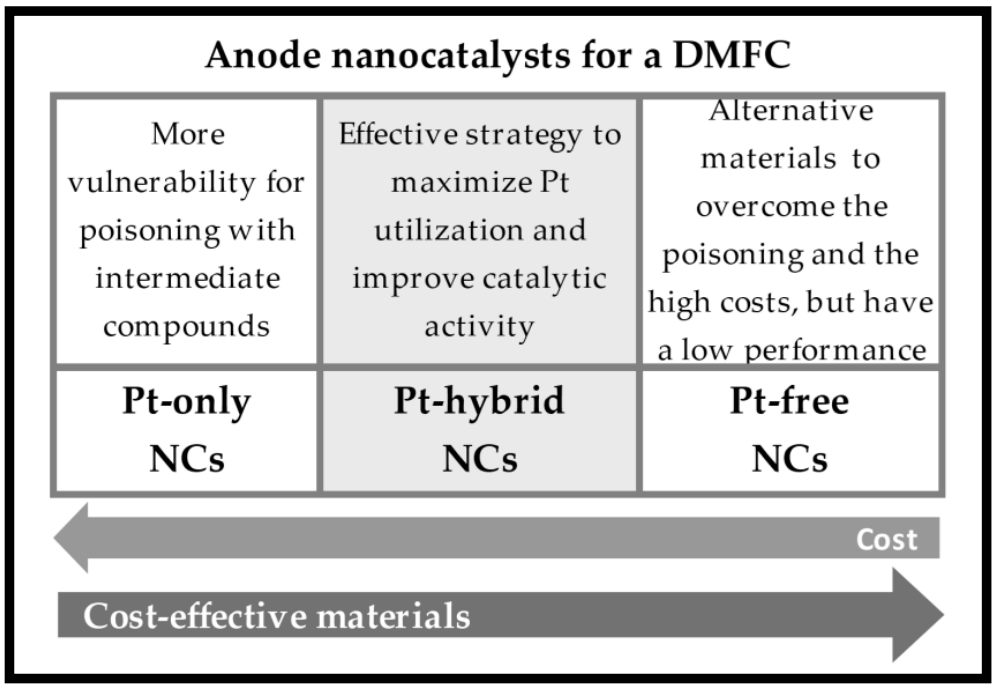

Figure 6. Main advantages and disadvantages of the different materials used as NCs for the anode side of a DMFC.

2.1. Pt-Only

Pt by itself presents strong differences in electrocatalytic behaviour, considering surface structure and crystallography since the CO-stripping reaction is surface-sensitive [70]. Several studies of the single-crystal surfaces of bulk Pt have shown that high-index planes generally exhibit much higher catalytic activity because there is a high density of atomic steps, edges, and kinks. They usually serve as active sites for breaking chemical bonds and forming oxygen-containing species compared to the terrace sites [62,71–74]. Furthermore, this ability has proven to be dependent on Pt particle size. In practical applications, Pt nanocrystals with high-energy surfaces of small sizes (sub-10 nm) have shown superior high-mass activity [75]. This can be attributed to the larger number density of surface defects, which becomes more pronounced with decreasing size. The adsorption of both CO_{ad} and OH_{ad} on Pt particles is greatly enhanced, leading to a decrease in electrocatalytic activity for MeOH oxidation due to restricted CO_{ad} surface mobility, as well as a size-dependent interaction between CO_{ad} and OH_{ad} [3,71,76–78]. Moreover, it is well-known that, depending on the size, shape, morphology, and nature of the support material, supported Pt nanostructures show improved catalytic performance since high efficiencies may be achieved. This occurs due to the unique properties of nanomaterials, which include the possibility of higher surface areas (due to better dispersion of the Pt), sufficient chemical resistivity, and superior mechanical strength, along with charge and mass transfer reaction paths (see references cited before). In this regard, we emphasise the recent advances in the architectures and nature of some carbon support nanomaterials that have shown potential to be used in DMFCs, including the three-dimensional spheres and zero-dimensional dots (when size is below 10 nm) (CSs & CDs) [79,80], one-dimensional nanotubes (CNTs) [81–83], layered configurations such as graphene (G) [84] and reduced graphene oxide (rGO) [85,86], two-dimensional materials, and combinations among them [87–90]. Other promissory results were also achieved with three-dimensional mesoporous carbon (MC) supports that ensure high surface areas [91–93], besides polymer modifications of the carbon supports with different morphologies and properties (stability and conductivity) favouring porosity, such as poly [2,2′-(2,6-pyridine)-5,5′-bibenzimidazole] (PyPBI) and CB [94], polyaniline (PANI) and rGO [95] or CNTs [96], polyvinylpyrrolidone (PVP) and GO [97] or CB [98], and/or acidification for further functionalisation [99–101]. In this way, it is possible to decrease the amount of catalyst used in the DMFC without losing performance by improving Pt NPs dispersion with a narrow diameter distribution in porous supports. This was also the motivation for performing metal hybrid modifications of the supports, taking advantage of nanomaterials like rGO/SnO_2 [102], TiN and $Ti_{0.9}Cu_{0.1}N$ [103], $Ti_{0.8}V_{0.2}N$ [104], CNTs@TiN [105], MoO_3/rGO [106], CNTs@TiCoN [107,108], PANI/TiO_2–C [108], TiO_2/graphitised nanodiamond (GND) [109], AlOOH-SiO_2/graphene [110], SiO_2/graphene [111], TiO_2@RFC (resorcinol-formaldehyde based carbon) [112], and TiO_2 nanotubes [113], among others.

All these studies have widened the scope of these materials for Pt catalysts of MOR and revealed, by electrochemical testing in the three-electrode system (ex situ fuel cell), a potential use as an alternative for DMFCs. From these kinds of tests, one also highlights the studies performed with zeolite NPs, porous crystalline aluminosilicate composites as Pt supports [114–117]. These have attracted much attention because of their unique geometrical configuration, structural features, and excellent physical properties, such as a very large specific surface area, nanometre-scale fine pores, and excellent structural stability. It shows a vital role of reducing the poisoning of the catalyst surface by adsorbed carbonaceous substances, which is beneficial for their use as catalyst supports. More detailed information about zeolite-modified electrodes for potential alcohol (methanol and ethanol) fuel cell application can be found in the review paper from Daas et al. [118].

The number of Pt-only catalysts for MOR really tested in DMFCs is very limited and focused on enhancing its catalytic performance by tuning the support. A blend of two different polymers was examined as a supporting material for dispersing Pt NPs [119], namely a novel electrospun chitosan (CH) and polyvinyl alcohol (PVA) with incorporated CuO and Co_3O_4 NPs based on *Sesbania sesban* plant (PVA-CuO-Co_3O_4) nanofibers. They

have unique properties such as a high surface area-to-volume ratio, high porosity, good thermal stability, and well-controlled composition. It also showed that CuO and Co_3O_4 metal oxides facilitate the oxidation of the adsorbed CO species and their removal from the Pt surface which leads to the enhanced catalytic activity for MOR. A real DMFC was designed, assembled and tested with Pt/PVA-CuO-Co_3O_4/CH as the anodic catalyst; however, no comparison with the commercial counterparts was provided by the authors.

A different study [120], using an N,F-codoped TiO_2 mixed carbon as the support of the Pt catalyst for MOR showed that it can effectively improve the catalyst activity and stability since it had a positive effect on reducing the particle size and improving the dispersion of obtained Pt NPs in the support. Furthermore, there was a strong electronic interaction between N,F-TiO_2 and Pt that was beneficial for weakening adsorption and facilitating the oxidative removal of CO on Pt-active sites. A DMFC employing the Pt–N,F$eTiO_2$/C anode catalyst had a power density that was 1.65 times that of analogous fuel cells employing a Pt/C commercial catalyst, confirming the potential of Pt-N,F$eTiO_2$/C as an anodic catalyst. For more details dealing with the methanol photo-oxidation on Pt/TiO_2 and Pt-M/TiO_2 (M = Ru, Ni) catalysts for DMFCs, highlighting the effect of TiO_2 morphology, NPs or 1D nanostructures, this can be found on the MOR activity under illumination in a recent detailed but concise review by Antolini [121]. This kind of catalyst is still under development, and the trend is to combine the Pt with other metals to reduce CO poisoning and the cost of the device.

2.2. Pt-Hybrid Metals

The use of bimetallic or multi-metallic Pt-based NCs has been known as an effective strategy to maximise Pt utilisation and improve catalytic activity as stated above. Thus, the study of new Pt-hybrid metallic electrocatalysts is very important for the development of improved DMFCs. Numerous studies on novel NCs for MOR with three-electrode system characterisation can be found in the scientific literature; however, we will focus on the ones reported with real DMFC application, since the three electrodes characterisation gives only the intrinsic activity of the catalysts, not taking into consideration the processes inherent to the real fuel cell environment. Figure 7 presents a performance comparison of the different Pt-hybrid materials used as nanocatalysts towards the MOR that will be explained in detail in this section. It should be noted that the maximum power density corresponds to the best performance obtained in each work. Other results can be found in detail in each reference. In spite of most significant recent progress and research, it is considered that currently there is still no better alternative to Pt–Ru electrocatalysts for MOR in DMFC [64,66,122].

2.2.1. Core-Shell Structured Catalysts

Major efforts are devoted to optimising this system with a focus on preparing NPs with controlled shape, size, composition, and structure. This is well detailed in the study presented by Xie et al. [48], which demonstrated that the atomically ordered Ru-core Pt-shell (Ru@Pt) NPs exhibited substantial enhancement in both activity and durability towards MOR in DMFC testing, compared with commercial Pt–Ru nano-alloy electrocatalysts, typically with the Pt:Ru atomic ratio of 1:1. The authors considered that in the commercial NCs, the Ru components are exposed directly to the redox environment. Therefore, substantial dissolution followed by the reconstruction and agglomeration of NPs occurs, while for the core–shell structured catalysts, the highly ordered Pt shell packing at the ordered Ru core surface can serve as a capsule to prevent the core from direct contact with the redox environment. Moreover, the ordered Ru core, due to its geometrical and internal confinement, improves the long-term stability of the catalysts, which is significant for the development of high-performance DMFCs with long-term durability. This kind of architecture was further explored to build selective electrocatalysts to run a DMFC at high concentrations of methanol, along with the combination of different precious metals [1]. For that, researchers have taken advantage of the strong electronic coupling effects in the Au@Ag_2S@Pt nanocomposites, where the core–shell Au@Ag_2S NPs are used as seeds

for the deposition of Pt metal in a core–shell-shell construction. These nanocomposites display superior activity for MOR, low activity for ORR, and better durability for MOR compared with commercial Pt/C. This strategy was also applied for the cathode side to develop core–shell Au@Pd NPs with thin Pd shells as selective electrocatalysts for ORR, based on the synergistic effect between Au and Pd components. Thus, the as-fabricated DMFC with core–shell-shell Au@Ag_2S@Pt nanocomposites at the anode and the core–shell Au@Pd NPs at the cathode maintains good performance at a methanol concentration of up to 15 M. This way, the authors claimed that this concept may shed some light on the design of more cost-effective and efficient DMFC systems. More information on the generic use of Ag-based catalysts in the heterogeneous selective oxidation of methanol and other alcohols can be found in the review from Torbina et al. [123].

2.2.2. Other Supports

The design of new supports has been an alternative strategy followed by different research groups to enhance the anode catalyst and also lower its cost. Regarding the carbon supports, in the last few years, the use of novel synthetic carbon supports has attracted much attention. It has been shown that the use of carbon materials with an ordered structure and high electrical conductivity improves the electrocatalysts' activity, lowers the loading of Pt–Ru, and increases the true surface area of the catalyst. As a result, electrocatalysts even more active than those supported on CBs can be produced. Among these, carbon nanofibers (CNFs) have shown to be an excellent carbon support for their suitable textural properties and their high electrical conductivity. However, it has also been shown that Pt–Ru catalysts supported on CNFs synthesised by different methods presented very different catalytic activity in a three-electrode system, even though similar metal content (20 wt.%) and a similar atomic ratio (Pt:Ru 1:1) can be obtained by all methodologies [124]. These same NCs, when tested as anodes in a DMFC, also showed different behaviour in agreement with the results achieved at the three-electrode system. The researchers demonstrated that CNFs' support may offer lower current resistance in comparison to the CB used as support in a commercial catalyst under specific conditions [125]. Moreover, for these same kinds of supports, it promises the modification with metal oxides like TiO_2, whose properties we have mentioned before, and CeO_2 is long recognised as one of the most attractive materials as a structural and electronic promoter of heterogeneous catalytic reactions [126,127]. A previous three-electrode system study showed significantly greater activity and stability for Pt–Ru NPs supported on a C-CeO_2 composite NFs (Pt–Ru/CECNFs) compared to the catalyst layer using a commercial Pt–Ru/C [128]. The increased activity was attributed to the strong interaction between the metal and oxide in the embedded CNF structure fabricated by electrospinning, and this has prompted the investigation for the optimised CeO_2 content of the CNF support of Pt–Ru catalyst in practical DMFC environment [129]. The researchers were able to run a DMFC with the Pt–Ru/CECNF exhibiting more than 2.5 times the maximum power density at half the Pt–Ru load of the commercial catalyst Pt–Ru/C. A similar strategy was followed for Pt–Ru NPs supported on C-TiO_2 composite NFs (Pt–Ru/TECNFs) [130–133]. The most recent studies showed that the Pt–Ru/TECNFs with different Pt–Ru contents (between 20 wt.% and 50 wt.%) presented higher mass activities compared to those of commercial Pt–Ru/C. However, the highest mass activity in DMFC testing was obtained by the catalyst with 30 wt.% which was about two times higher than the commercial one. With higher catalyst loading, the power density of the DMFC decreased due to the increased catalyst layer thickness which increased concentration overvoltage. Thus, showing that in the development of fuel cell electrocatalysts, the catalyst layer structure is also important, as well as the reactivity of the catalyst itself.

A previous evaluation of the Pt–Ru/C-TiO_2 anode electrocatalyst for DMFC applications has already pointed out that TiO_2 provides better performance as compared to the traditional commercial anode electrocatalyst [134]. TiO_2 materials were incorporated into commercial Pt–Ru/C anode electrocatalysts with different TiO_2 weight ratios (5, 15, and 25 wt.%) and tested as anodes of DMFCs under various operating conditions. The results

of these tests showed that the introduction of 5 wt.% of commercial TiO_2 into the commercial Pt–Ru/C anode electrocatalyst improves its stability characteristics significantly. Accordingly, to the authors, the performance decrease in DMFC with the increase in the amount of TiO_2 could be associated with the fact that an excessive amount of TiO_2 may prevent the transportation of the electrons to the Pt–Ru anode electrocatalyst by creating an additional barrier between the electrons and Pt–Ru. Furthermore, the additional OH species, which originate from the presence of TiO_2, may also obstruct the adsorption of CH_3OH by occupying the active areas. A recent work by Yang et al. [135] suggested a boron (B)-doped TiO_2 use as a co-catalyst for Pt/BC. The hybrid Pt–BTO_4/BC exhibited higher electrochemical activity, CO tolerance, and durability compared to the Pt–TiO_2/BC and Pt–Ru/C. The authors consider that the boron doping improves the electrocatalytic properties of these catalysts due to the strong adsorption ability of B to oxygen species, the increase in the oxygen vacancy concentration of TiO_2, and the downward shift of the d-band centre of Pt.

Titanium nitride (TiN) is another attractive support for the Pt–Ru electrocatalyst [136]. The TiN presents higher electrical conductivity and corrosion resistance compared to carbon. Though CB supports cost less than TiN NPs, increased durability obtained from the novel TiN NP supports can reduce the lifetime costs of the fuel cell system, with the increased advantage that for the same amount of loading and particle size, the number of Pt particles on the surface of the TiN NP support will be higher compared to a CB support of the same dimensions due to the difference in the density of TiN (5.1 g cm^{-3}) and C (1.9 g cm^{-3}) [137]. The tests on DMFC performance showed 56% improved maximum power density and superior electrochemical stability for an in-house synthesised (Pt–Ru/TiN) catalyst compared to that of commercial Pt–Ru. This was attributed to the uniform dispersion of Pt–Ru achieved on the nanostructured TiN yielding, higher electrochemical active surface area, and lower charge transfer resistance. Thus, it was demonstrated the potential of nanostructured TiN as a support for Pt–Ru-based anode electrocatalysts for DMFC applications despite its higher cost. More information about TiN and the other transition metal nitrides and carbides can be found in the reviews from Zhong et al. [138] and Ham et al. [139]. Mesoporous carbon nitride (MCN) is also an alternative material support for Pt–Ru as a result of its well-ordered porous structure with a conductive and basic CN network, which may be beneficial for the growth of small NPs in the pore channels. The presence of free NH_2 groups on the surface of the MCN has also been recognised as a help to stabilise the formed catalysts NPs inside the mesochannels and avoid the agglomeration. This was demonstrated by using Pt–Ru/MCN as an anode catalyst in ethanol [140] and most recently methanol [141] fuel cells, in comparison with the commercially available Pt–Ru-supported MWCNT and CB. Moreover, there were also reports that N atoms were highly important for the enhancement of stability in Pt–Ru electrocatalysts, mitigating both anode metal dissolution and Ru crossover [142,143]. This was the principle behind the design of new Pt–Ru electrocatalysts, with highly stable CO tolerance and durability, in which the Pt–Ru NPs are embedded in N-doped carbon layers derived from the carbonisation of PVP. This structure was assembled on previous PVP [144] or polybenzimidazole (PBI) [145]-coated CB in order to cap the micropores on CB before Pt–Ru deposition. The embedded Pt–Ru electrocatalysts were applicable in real DMFC operation, and their performance showed that they present a higher power density than the commercial Pt–Ru/CB. This was ascribed to the higher activity toward MOR and to the highly stable CO tolerance and durability gained using the N-doped carbon protective layers that decelerated the Ru dissolution.

A final selected example of the importance of the tuning of the catalyst and catalyst support is given by the work reported by Ganesan et al. [146]. These researchers showed that the electrodeposition of Pt–Ru alloy NPs on the surface of pyrolysed PANI and melamine on ZrO_2 enhances the catalyst utilisation and its durability. They considered that such behaviour was due to the formation of Pt shell with Ru core on the high surface area of pyrolysed ZrO_2/PANI-melamine during the pulse electrodeposition. The choice of ZrO_2 as the catalyst support was preferred for its enhanced performance and, particularly,

for its durability on methanol oxidation, reinforced by the fact that the pyrolysis of PANI and melamine on ZrO_2 forms a highly porous, graphene-like structure and improves the formation of particular C–N bonds. Due to the high surface area and stability of both the catalyst support and the catalyst, the loading of precious metals can be reduced in the DMFC anode. Compared to commercial catalysts, 98% of the Pt–Ru usage was reduced in this method, which was the first of its kind ever reported. The researchers assume that the cost and size of DMFCs can be reduced significantly using this catalyst. Hence, this type of ultra-low loading of the Pt–Ru catalyst has viable potential in commercializing DMFCs. The use of PANI as an efficient catalyst support material for improved deposition of Pt–Ru electrocatalyst NPs towards application in MOR was further investigated by Das et al. [147], showing that the enhanced dispersion of electrocatalysts resulted in suppression/elimination of the catalyst poisoning effect. For that, they used PANI different nanostructures, namely nanofibers (NFs) and nanowhiskers (NWs), and compared them with the commercial Vulcan® carbon supports. The obtained DMFC results followed the performance trend of Pt–Ru/PANI NWs > Pt–Ru/PANI NFs > Pt–Ru/C. Pt–Ru/PANI NWs also exhibited better stability, and the PANI NWs support exhibited better dispersion, higher utilisation of the deposited Pt–Ru catalyst NPs, and the lowest deposited catalyst particle size. Hence, this kind of support can be an effective route to reduce the loading and increase the efficiency of the state-of-the-art Pt–Ru catalyst. Further details on recent progress in nanocomposites based on conducting polymers can be found in recent reviews reported by Rhazi et al. [148], even if focused on their applications as electrochemical sensors, or the one by Pašti et al. [149] for electrochemical energy conversion and storage applications. Nevertheless, as stated before, from an economic viewpoint, it is also important to find alternatives to noble metal use as catalysts, and this has been the focus of several studies in the most recent years: combining the advantages of tuning proper catalyst supports with Pt-non-precious/noble metal hybrids. Veizaga et al. [150] verified the promoting synergetic effect of tin (Sn) in Pt anodic catalysts supported on MWCNTs (NT), mesoporous carbon, and Vulcan® carbon (VC) for DMFCs. They have shown that these Pt–Sn catalysts supported on VC and NT, when tested in a DMFC, gave a better power density than a commercial one, but only at low current densities. This was overcome by a different strategy presented by Amani et al. [151], by synthesising a Vulcan® carbon–polyaniline (C-PANI) composite to support Pt–Sn catalysts. This study will be discussed in Section 2.4.

It should be pointed out that, even if an effective DMFC efficiency is not reached, the possibility of using less expensive materials is a real gain. As an example, Maya-Cornejo et al. [152] reported the synthesis of a series of Pt–Ru and Pt–Mo bimetallic catalysts supported on single-wall carbon nanotubes (SWCNTs) for hydrogen and methanol electrooxidation in fuel cells applications. They concluded from their experimental and simulated polarisation curves obtained from DMFCs that Pt–Ru/SWCNT and Pt–Mo/SWCNT electrocatalysts exhibited higher power and current density values compared with the Pt/SWCNT electrocatalyst. Additionally, a previous study on nanosized Mo-doped CeO_2 co-catalysts [153] showed that the activity and stability of Pt for methanol oxidation can be significantly enhanced. CeO_2 is of particular interest due to its oxygen vacancy, i.e., oxygen storage capacity, able to supply sufficient OH_{ad} at low potential to efficiently eliminate the poisoning intermediates formed during methanol electrooxidation [154–156]. Other advantages are its lower price, as well as the good mechanical resistance and anticorrosion ability in acidic media; the major disadvantage is its low electrical conductivity, which is surpassed by the presence of other conducting metals [157]. Thus, the modification of Pt catalysts with Mo-doped CeO_2 materials with more oxygen vacancies and high electrical conductivity can effectively remove adsorbed intermediate species, resulting in remarkably improved electrocatalytic performance for methanol oxidation. Furthermore, a DMFC incorporating $Pt/Ce_{0.7}Mo_{0.3}O_{2-\delta}$–C as the anode catalyst exhibited a maximum power density 1.8 times higher than that of an analogous fuel cell using the commercial Pt/C. More information on the fundamentals and catalytic applications of CeO_2-based materials can be found in

the review paper of Montini et al. [158]. The review by Lykhach et al. [159] focuses on the recent efforts towards the fabrication of single-atom catalysts on nanostructured CeO_2 and their reactivity, in the prospect of their employment as anode catalysts. In a different work reported by Du et al. [160], a composite comprised of a CeO_2nanowire/MnO_2nanosheet heterogeneous structure was designed and synthesised by a facile hydrothermal approach. This system has shown improved catalytic properties by achieving more defective structures through the slight manganese (Mn) doping. However, to the best of our knowledge, no application of these kinds of materials as DMFC anodes has been implemented. Alternatively, the cost-effective transition metal Mn, particularly in its most common form, MnO_2, has also been combined with conductive carbon materials to overcome its poor electrical conductivity and has been proven that it can boost Pt electroactivity towards the MOR [161–163].

It is known that the oxidised form of graphene, i.e., rGO, acts as a conductive material to modulate the electrochemical reaction in a controlled fashion, with low-cost production and easy processability. Further information on the applications of rGO for electrocatalysis and fuel cell technology can be found in several recent review papers [164–169]. Herein, we highlight the fact that, in contrast to pristine graphene, the presence of functional groups such as -OH, -COOH, -CHO, and epoxides on rGO nanosheets provides sites for metal catalyst anchoring, and their 2D structure (high surface to volume ratio) allows higher loading of nanosize catalysts, contributing to higher current efficiency during MOR, as one can verify from the numerous different studies presented in the literature [86,97,170–177]. Furthermore, the hydrophilic nature of rGO promotes water activation at a lower potential and induces the oxidation of CO_{ad} on active Pt sites of pure Pt or Pt m NCs, by the bi-functional mechanism. Among numerous reported bimetallic Pt-based catalysts, Pt–Co is considered a better catalyst, as the incorporation of cobalt (Co) into the lattice of platinum introduces enhanced Pt d-band vacancies due to its oxophilic nature. The modified electronic structure of Pt–Co alloys affects the Pt–Pt bond distance, resulting in easier adsorption of oxygen moieties onto alloy NPs and reduced CO poisoning [178,179]. The synergistic effect of rGO and Pt–Co alloy to enhance the electrooxidation of methanol was taken into consideration by Baronia et al. [180,181]. Their results showed that the Pt–Co (1:9)/rGO catalyst had higher CO tolerance, resistance to methanol crossover, and higher power density, even when using 5 M methanol fuel feed, indicating its commercial potential as anode material in real DMFC devices. An efficient and CO-poisoning tolerant anode catalyst was proposed by Tian et al. [182], depositing Pt–Ru alloy nanoparticles on nanoporous gold film (NPG-Pt–Ru). NPG substrate plays dual functions in DMFC anodes, the synergetic effects with Pt–Ru nanoparticles, and the nanoscale and nature structure characteristics of NPG film. This last one provides a large specific surface area and rapid electron conduction in contrast with conventional carbon powder supports. The DMFC with NPG-Pt_2Ru_1 (0.2 mg_{Pt} cm^{-2} and 0.3 mg_{Au} cm^{-2}) achieved a maximum power density of 96 mW cm^{-2}, about a six-fold enhancement of the Pt efficiency of commercial Pt–Ru/C (1 mg_{Pt} cm^{-2}, 78 mW cm^{-2}). A group of researchers presented a Pt–Ru nanoalloy supported on porous graphitic carbon (PC) prepared by a simple method involving hydrogen co-reduction in the Pt and Ru precursors at 300 °C, followed by thermal treatment at 700 °C [183]. The high-temperature treatment promotes the development of a Pt–Ru/PC–H nanocatalyst with high electrocatalytic performance and CO tolerance. In a DMFC, this catalyst exhibited a maximum power density of 83.7 mW cm^{-2}, which is about 1.9 and 3.1 times more than commercial Pt–Ru/C and Pt/C, respectively.

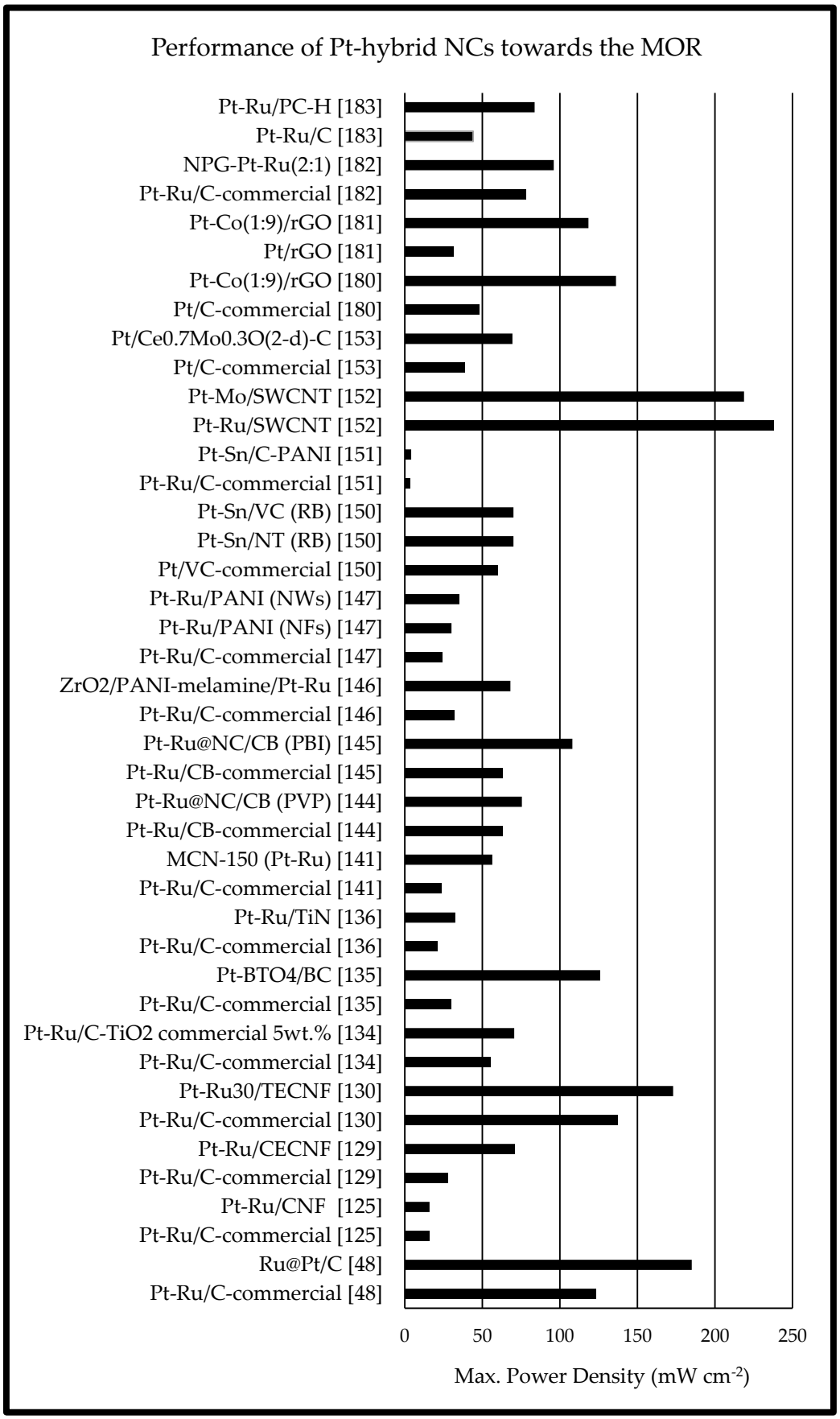

Figure 7. Performance comparison for different Pt-hybrid NCs towards the MOR.

2.3. Pt-Free

The search for cost-effective, non-precious metal or even metal-free catalysts efficient for fuel cell devices is a hot topic of research [184–188]. However, their use as anode catalysts in the acidic environment of DMFCs has not yet been successfully implemented, and only very few studies have been reported on the subject.

One of these studies [189] involved the fabrication of a cost-effective, non-noble metal supported on a conducting polymer composite such as copper/polypyrrole graphene oxide (Cu_2O/PPy-GO) as an anode catalyst for methanol oxidation in DMFC. The authors took advantage of the reactivity as well as the stability of cuprous oxide (Cu_2O); it can be improved by using a suitable supporting matrix system like GO with PPy, another conducting polymer, which can enhance the electro-chemically active surface area of catalysts and catalytic performance in DMFCs. The sponge-like porous structure of PPy in the Cu_2O/PPy-GO can trap the Cu_2O NPs within the boundary system, preventing their leaching into the solution. Hence, PPy-grafted GO as a support matrix for cuprous oxide contributes to the enhancement of the number of electrocatalytic active paths for efficient electron transfer. In addition, the GO sheets permitted the uniform dispersion of PPy and the synergetic effect employed between the active support, conducting polymer, and catalyst NPs of Cu_2O/PPy-GO, coupled with the close contact and substantial stabilisation influenced the highest DMFC performances. Thus, Cu_2O/PPy-GO NPs can be considered a cost-effective alternative for the Pt–Ru/C system to execute practical applications in DMFCs.

A similar approach was used with another cost-effective and abundant transition metal, nickel (Ni), by Das et al. [190]. It is well known that Ni NPs exhibit promising results in the MOR when used in combination with Pt since they promote electronic interaction and provide oxygen-containing groups (Ni (hydro)oxides) which enhance the rate of CO oxidation [191]. However, the prospect of using Ni alone as a catalyst under acidic conditions for methanol oxidation has been hindered by its relatively low stability in acidic medium, which the authors circumvented by using partially sulfonated PPy (SPPy) as a catalyst support. Since, in a previous study, using different support materials (Vulcan® carbon, PANI, and partially sulfonated PANI (SPANI)), they concluded that sulfonic acid ($-SO_3H$) dopant within the parent polymer interacts positively with the deposited catalyst particles, thus assisting in producing better dispersion, distribution, and utilisation of metal catalyst particles [192]. The results, thus obtained, were better than those obtained for the commercial Pt–Ru/C but not superior to the Cu_2O/PPy-GO system.

In effect, the route to cost-effective non-precious metal NCs as anode catalysts for DMFCs passes through the use of conducting polymers on their support, benefitting from their protonic and electronic conductivity, besides their large specific area, good mechanical strength, and excellent stability.

2.4. Passive Feed Systems

As passive DMFCs have a promising future, this section is intended to present the advances in anode NCs with the potential to be used in passive systems. An advantage of these systems is that they operate at room temperature; however, the catalysts tested at higher temperatures do not always have the same behaviour at room temperatures. Thus, the nanocatalysts tested in DMFCs at temperatures below 45 °C will be presented in this section and are summarised in Table 1.

Table 1. Comparison of DMFC performance towards MOR optimisation.

NCs	Pt Load (mg cm^{-2})	[CH_3OH] (M)	T (°C)	DMFC Mode	Max. Power Density (mW cm^{-2})	Ref.
Pt@RFC	0.75	1	40	Active	33.8	[193]
Pt–Ru/C-commercial	2.0				27.7	
Pt–Ru/CNF-BM	2.0	2	40	Active	(7.0)	[125]
Pt–Ru/CNF-SFM					(7.7)	
Pt–Ru/CNF-SFMTT					(7.2) [i]	
Pt–Ru/CNF-MeOH					(6.8)	
Pt–Ru/C-commercial					(5.4)	
Pt–Sn/C-PANI	4	2	(RT)	Passive	4	[151]
Pt–Ru/C-commercial					3.5 [i]	
Pt–MnO_2/rGO-L	2	2	60	Passive	26.31	[194]
Pt–MnO_2/rGO					21.11	
Pt/rGO					16.13	
Pt–Ru-Fe/NG	4 [§]	2	40	Active	57	[195]
Pt–Ru-Fe-Co/NG	4 [¢]	2	40	Active	68	[196]
Pt–Ru/NGA	2.5 [¥]	2	30	Active	32 [i]	[197]
Pt–Ru/GA					25 [i]	
Pt–Ru/C-commercial					23 [i]	
Pt/C-commercial	2.5				13 [i]	
Pt–$NiTiO_3$/C	0.5	0.5	45	Active	9.6	[198]
Pt–Ru/N-CNT	4	3	(RT)	Passive	26.10	[199]
Pt–Ru/CNT					22.12	
Pt–Ru/C					16.13	
Pt–Ru/C-commercial					2–17	

() values in mW mg^{-1}; RT: room temperature; [i] not specified, inferred from the plot; [¥] identified as "Pt–Ru"; [§] identified as "Pt–Ru–Fe"; [¢] identified as "Pt–Ru–Fe".

Li et al. [193] developed a novel structured catalyst with Pt nanoparticles partially embedded in porous resorcinol-formaldehyde-based carbon spheres (Pt@RFC) (with variation of the embedded architecture by controlling the reaction duration) in order to achieve a low Pt-loading and higher fuel cell performance. This new catalyst presented great enhancements in the electrocatalytic activity and stability towards MOR. Upon the integration of Pt@RFC into a DMFC, the device exhibited a comparable power density to the commercial Pt–Ru/C catalyst with only one-third of the noble metal loading, as well as a slower degradation rate of the catalyst due to a higher corrosion resistance. Calderón et al. [125] tested Pt–Ru catalysts supported on CNFs and demonstrated that the MEA containing the commercial catalyst Pt–Ru/C showed the lowest performance towards the MOR at 40 °C. These results were explained based on the higher conductivity of the CNFs over the carbon support. Amani et al. [151] synthesised a Vulcan® carbon–polyaniline (C-PANI) composite to support Pt–Sn catalysts that were used in a passive DMFC. The cell with the Pt–Sn(70:30)/C-PANI catalyst showed a higher power density and lower methanol crossover compared to the commercial Pt–Ru/C catalyst. Furthermore, they estimated that the presence of PANI in the anode catalyst layer reduced the methanol crossover up to 30% due to a synergism of the Vulcan® carbon and PANI, as well as to a faster MOR kinetic on the anode catalyst surface of the modified MEA. Therefore, the obtained results indicated that the synthesised Pt–Sn(70:30)/C-PANI catalyst may be a good candidate to replace the commercial Pt–Ru/C electrocatalysts. Yuan et al. [194] introduced MnO_2 as a co-catalyst and used graphene as a support for Pt NPs. By taking advantage of in situ carbonisation using L-ascorbic acid (L) as the carbon source, they were able to prepare a carbon riveted Pt–MnO_2/rGO-L that showed a higher electrochemical surface area and catalytic activity towards the MOR. This catalyst exhibited a stronger ability of CO poisoning and a better stability than the Pt–MnO_2/rGO and Pt/rGO catalysts. The authors concluded that the performance improvement of the proposed catalyst could be attributed to the synergistic effects between MnO_2 and Pt and the anchoring effect of L-ascorbic acid.

Rethinasabapathy et al. [195] focused their work on taking advantage of the synergetic effect of nitrogen-doping graphene support (NG) by the conversion of rGO, along with the bifunctional and ligand effects of Pt and Ru with low-cost iron (Fe). Further, to minimise the use of noble metals, they studied the incorporation of low-cost metals such as Co [196], showing that this kind of catalyst has the potential for both MOR and ORR with a remarkable reduction in the fuel cell costs. Zhao et al. presented, for the first time, N-doped graphene aerogel (NGA) with porous structures and uniformly distributed Pt–Ru NPs (Pt–Ru/NGA), which exhibited an unprecedented performance towards the MOR [197]. Notably, these 3D graphene-based NCs, with an easy synthesis and simple manufacturing process, showed high performances due to their high catalytic activity, good CO tolerance and excellent stability for methanol oxidation. The Pt–Ru/NGA catalysts are very promising for the replacement of the conventional carbon-based catalyst in practical fuel cell applications. Thiagarajan et al. studied the effect of adding $NiTiO_3$ to Pt/C and Pt–Ru/C catalysts on the DMFC performance [198]. The cell with Pt–$NiTiO_3$/C as the anode catalyst demonstrated almost twice the performance of the one with the conventional Pt/C catalyst. The power density improvement when Pt–Ru–$NiTiO_3$/C was used as the anode catalyst was ~22% regarding a Pt–Ru/C catalyst. These results are due to the strong interaction between Pt, Pt–Ru, and $NiTiO_3$, which promotes high stability and MOR activity. These studies were performed with a low Pt loading of 0.5 mg cm^{-2} and at a temperature of 80 °C. The effect of the temperature was also evaluated, and a test at 45 °C using Pt–$NiTiO_3$/C as an anode catalyst was also performed. Although the performance decreases with a decrease in the temperature, it is possible to operate the DMFC at 45 °C, where the use of $NiTiO_3$/C can become an alternative for passive feed systems. Fard et al. [199] studied the effect of using three different supports, CB, CNT, and nitrogen-doped carbon nanotubes (N-CNT), for the bimetallic catalyst Pt–Ru and Pt nanoparticles on the performance of a passive DMFC. The DMFC performance with Pt–Ru/N-CNT was 18% and 62% higher than a cell with P-Ru/CNT and Pt–Ru/CB, respectively. The maximum power density (26.1 mW/cm^2) was obtained for the cell with N-CNT as the support. Nitrogen doping enhanced the electrochemical and physical characteristics of the catalyst through increasing the electrical conductivity and the surface area, boosting interaction between the support and the metal.

These works showed promising catalysts to be used as anode catalysts in passive DMFCs, showing the importance of carrying on fuel cell tests at low temperatures.

3. Nanocatalysts for the Cathode

For the DMFC cathode, the fundamental challenges for NCs are how to enhance the sluggish oxygen reduction reaction kinetics and circumvent the parasitic methanol presence due to crossover, demonstrating, therefore, high methanol resistance. The methanol floods the cathode and limits the mass transport of O_2. Thus, methanol crossover causes a drastic decrease in cathode performance, which is generally overcome by using "excessive" amounts of noble metal catalysts. As explained before, among pure metals, Pt is the best electrocatalyst for ORR in DMFCs. However, it is costly and highly sensitive to the presence of even small amounts of fuel. As a result, there have been concerted efforts to improve its methanol tolerance and mass utilisation efficiency. Singh et al. [49] compiled an overview of all the advances in regard to the design, synthesis, and ORR activity of Pt-based cathodes for DMFCs during the period 2000–2013. In this review, we focus on the reported developments since 2015 for Pt-based cathodes used in DMFCs and their supports, as well as the recent advances reached for non-precious metal NCs, in a similar manner as performed before for MOR. It should be noted that the cathodes usually suffer from more severe corrosion and degradation because of the higher potential compared to anodes. Therefore, the development of more durable and efficient cathode materials should couple with the design of more durable and efficient anode catalysts [57]. For a broader vision on the subject of ORR catalysis, the following recent review papers can be very useful [28,59,198,200–203] as well as [204,205] if one is focused on Pt-based electrocatalysts.

Figure 8 summarises the main advantages and disadvantages of the different materials used as NCs for the cathode side of a DMFC.

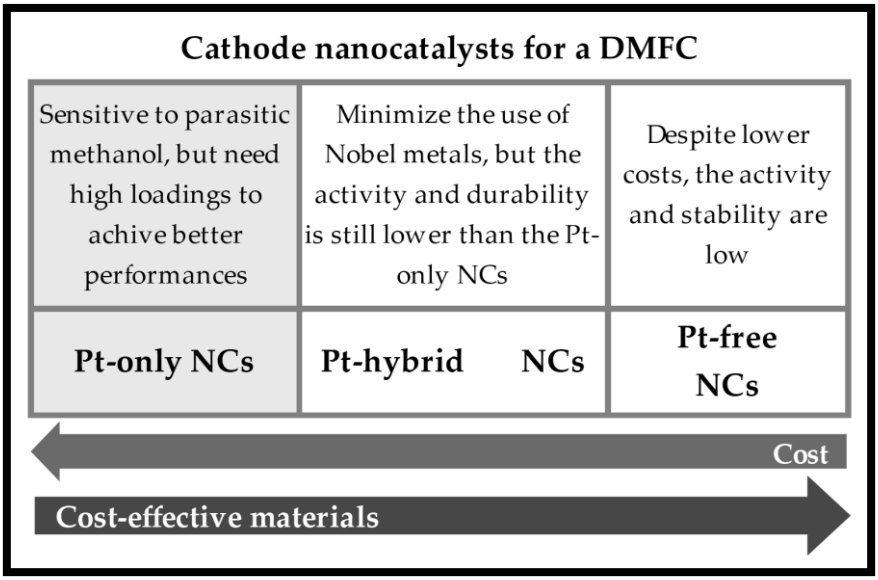

Figure 8. Main advantages and disadvantages of the different materials used as NCs for the cathode side of a DMFC.

3.1. Pt-Only

Most of the time, these studies aimed at variations in the hydrophobic/hydrophilic nature of electrode materials, as well as optimised pore structures, which help to create more pathways for water removal and reactant access to the catalyst active sites. As mentioned before, carbon supports are necessary to obtain a high dispersion and a narrow distribution of Pt NPs, which is the prerequisite to preparing high-performance catalysts and they should also present an adequate mesoporous structure with a pore size in the range of catalyst particles to favour catalyst stability and durability [10,206–209]. Thus, several studies recently reported in the literature covered this subject mainly focused on optimising the porosity of the materials for the cathode side of a DMFC. Figure 9 shows a performance comparison based on the maximum power density achieved, for the different Pt-only nanocatalysts used towards the ORR, which are presented in detail in this section.

One interesting example is given by Zhao et al. [210] who investigated the impact of the pore size (ranging from 4.0 nm to 8.1 nm) of ordered mesoporous carbon (OMC) FDU-15-supported Pt catalysts on ORR. They rationalised these findings, considering that the specific area of FDU-15 enlarges in response to an increase in the pore size, ensuring a better dispersion of Pt particles on the larger surface area of the FDU-15 samples. However, when the pore size of FDU-15 reaches a value greater than 6.5 nm, the particle size of the FDU-15-supported Pt catalysts becomes independent of the specific surface area of the FDU-15 sample. Their tests allowed to infer the relevant impact of the optimised pore size of OMC FDU-15-supported Pt NCs on ORR. A similar approach for the same type of ORR catalyst but with a different carbon support, hollow graphitised carbon spheres (HGS), but also with the mesoporous structure was presented by Tesfu-Zeru et al. [211]. At catalyst loading close to 1.5 mg_{Pt} cm^{-2}, MEA with HGS exhibited the best performances compared to MEA with Vulcan®-supported cathodes. This result is an indication of the optimal morphology of the HGS and allows for the better accessibility of catalyst active sites compared to the chain-like Vulcan® structure. However, at higher catalyst loadings, the reverse trend was observed. This was attributed to mass transport limitation in HGS-based CL, evidenced by electrochemical impedance spectroscopy (EIS). This way, the researchers were able to show that for DMFC applications, where the catalyst loading of at least 2 mg_{Pt} cm^{-2} is usually required to yield acceptable power densities, the diameter of HGS should preferentially lie

in the range of 50–100 nm in order to reduce dead volume, electrode thickness, and as a consequence, mass transport loss contribution in the cathode CL.

In the quest for the design of a low-cost and high-methanol-tolerant Pt cathodic electrocatalyst for DMFCs, Yang et al. [212] described a new methanol-tolerant electrocatalyst. It was fabricated from the chemical modification of CB by coating it with PVP after being wrapped in PBI. The PVP layer blocks the methanol adsorption and oxidation and slightly affects the O_2 diffusion and reduction due to the different sizes of methanol and oxygen. The PVP/Pt/PBI/CB NCs in the DMFC cathode showed four- and five-times higher performance when compared to non-coated and commercial electrocatalysts, respectively, even with 12 to 20 M methanol fed to the anode. This was an improvement in relation to their previous work [213] in which the Pt-NPs supported on MWNTs were coated by poly(vinylphosphonic acid) (PVPA) after being wrapped in a thin layer of PyPBI (1–2 nm). In the cathode of a DMFC, the polymer-coated electrocatalyst reached only a ~2.3 times higher power density compared to using the commercial when fed with 8 M methanol. Replacing the MWNTs with the less-expensive CB, the researchers showed that the PVP/Pt/PBI/CB NCs are a promising candidate for the cathode side of the DMFC, and these studies offer useful information for the preparation of effective methanol-tolerant electrocatalysts using the "polymer coating" strategy.

The effect of different structures of carbon supports for cathode catalysts on the performance of DMFC, like CB, MWNTs, and rGO, had already been reported by Liu et al. [214]. The authors explained that the significant differences in the DMFCs' performances are due to the compression ratios and hydrophilic/hydrophobic properties of CLs with different structures of carbon supports, which strongly affect electrochemical active sites and mass transport in cathodic CLs. The long-term testing of DMFCs indicated that Pt/MWNTs exhibited superior stability. Thus, the researchers found that MWNTs' support enhanced the formation of TPB and ordered CL, which favours the performance of fuel cells. Additionally, the results revealed that the Pt/MWNTs catalyst possesses 1.2 times higher durability than the Pt/C catalyst in DMFCs since it has a stronger corrosion resistance than CB. Based on an overall consideration of the power and lifetime of DMFC, they considered MWNTs as an "optimal" candidate among the three investigated carbon supports. One should point out that these tailoring effects do not restrain the NPs' support, but they were also explored for the NPs by themselves on the ORR progression under a DMFC environment. The understanding of particle size effects of catalyst NPs on their activity is one of the essential objectives in heterogeneous catalysis, particularly for ORR, and has been the subject of extensive research efforts. For a detailed review on tuning NPs into advance NCs for efficient ORR under fuel-cell reaction conditions, one can refer to the works of Guo et al. [215], Mistry et al. [216], and Lu et al. [217]. For a more generic approach, one refers to the paper from Calle-Vallejo et al. [218], which explains why conclusions from Pt model surfaces do not necessarily lead to enhanced NP catalysts for the ORR, or the paper from Tian et al. [74], which reports the synthesis of tetrahexahedral platinum nanocrystals with high-index facets and high electro-oxidation activity. Additionally, we also highlight a previous publication from Shao et al. [219], who studied the size-dependent specific and mass activities of the oxygen reduction in $HClO_4$ solutions on the Pt NPs in the range of 1–5 nm. They determined that mass activity increases two-fold from 1.3 to 2.2 nm and decreases as the particle size further increases. On the other hand, the specific activity increases rapidly four-fold as the particle grows to 2.2 nm and then slowly as particle size further increases. The maximal mass activity at 2.2 nm was well explained based on the DFT calculations also reported (further information on DFT can be found in the following section). The authors considered that the presence of the edge sites was the main reason for the low specific activity in NPs due to very strong oxygen binding energies at these sites. They also confirmed that the state-of-the-art Pt/C catalyst with an average particle size of 2.5 nm has almost the maximum mass activity that conventional Pt NPs can achieve. Hence, their results emphasised the importance of facet sites in the particles for ORR and clearly demonstrated that the catalytic activity highly depends on the shape and size of the NPs,

thus the importance of designing better catalysts, with size and shape controlled. Moreover, one should also point out the work performed by Li et al. [220] on synthesizing ultrafine jagged platinum nanowires, which enabled ultrahigh mass activity for the ORR (nearly double previously reported best values) and recognised as a promissory advance catalytic system to be translated to real fuel cell applications [221]. This work clearly demonstrated the advantages of hollow NPs in electrocatalysis, since they can expose a high proportion of active surfaces while saving the amounts of expensive precious metals. An extensive review on this topic was recently performed by Park et al. [222] as one advice reading for further complementary information on the subject. Kim et al. [223] proposed a simple hierarchical cathode structure consisting of unsupported Pt (Pt black) as the inner CL (sublayer close to the membrane) and carbon-supported Pt (Pt/C) as the outer CL (sublayer close to the gas diffusion layer). The same catalysts function as the CLs in a conventional MEA without any additive such as Pt–Ru, so the only difference was the cathode structural properties since the thickness of the Pt black layer (5.6 μm) is much thinner and less porous than the Pt/C layer (11.8 μm). Additionally, Pt black has a more hydrophilic surface than Pt/C due to the absence of carbon support. Their EIS studies showed that the charge transfer resistance for the MEA with its hierarchical structure is considerably lower, as it has more electrochemically active sites for the ORR. The researchers argue that the inner CL with the compact structure decreases the CL thickness and prevents the methanol contamination of the Pt sites as the cathode outer CL with the porous structure increases the electrochemically active surface area and reduces more oxygen owing to clean Pt sites free from the permeated methanol. They demonstrated that the newly developed MEA applied in DMFCs can maintain the high ORR activity of the cathode catalysts offsetting the adverse effect of methanol crossover. At a high methanol concentration (3 M), it showed a high maximum power density compared with the conventional devices. Unfortunately, so far as we know, there was no reference to the durability and long-term stability of this simpler solution.

The intrinsic three-dimensional nature of the CL is important and commonly overlooked in the electrode structure research that can affect the overall performance and cost of the fuel cell. Glass and Prakash [224] investigated the effect of the different individual CL thicknesses and loadings of the cathode DMFC. The drawdown method was performed at thicknesses varying from 1 mil to 8 mils, with Pt loadings ranging from 0.25 mg cm^{-2} to 2.0 mg cm^{-2}. They observed that the MEAs with thicker individual layers performed better overall than those prepared with thinner individual layers. One reason for that, according to the authors, is the tortuosity of the CLs in the MEAs. Thinner individual layers can lead to higher tortuosity and higher mass transfer resistance of the O_2 in the cathode CL, as verified in their EIS measurements. Another possible detrimental aspect linked with the higher tortuosity is the flooding caused by both water crossover as well as from the ORR. The higher tortuosity in the CLs leads to longer more winding pathways for the water to travel along, leading to an increase in flooding in the cathode compartment. This can possibly be a significant detriment to the overall fuel cell performance. Moreover, they reported that the maximum power density for the different loading levels followed an exponential decrease in Pt utilisation at the higher loading levels, indicating a loss in catalyst utilisation. Thus, the 4 mil layer thickness displayed a 95 % increase in power density over the 1 mil layers at a loading of 0.25 mg cm^{-2}, while this increase in performance decreases to around 5 % at the 2.0 mg cm^{-2} Pt loading. This trend can be due to the penetration depth of the gases flowing in the cathode side of the MEA. At higher loadings, only a fraction of the CL is electrochemically active, leading to lower catalyst utilisation and only minor increases in cell performance.

It is evident that the complexity of the numerous variables regarding the fuel cell CLs, even for Pt, make it the state-of-the-art, most-studied catalyst for the ORR. Further research is still needed to uncover and optimise the conditions of the cathode catalyst in order to achieve DMFCs with superior performance.

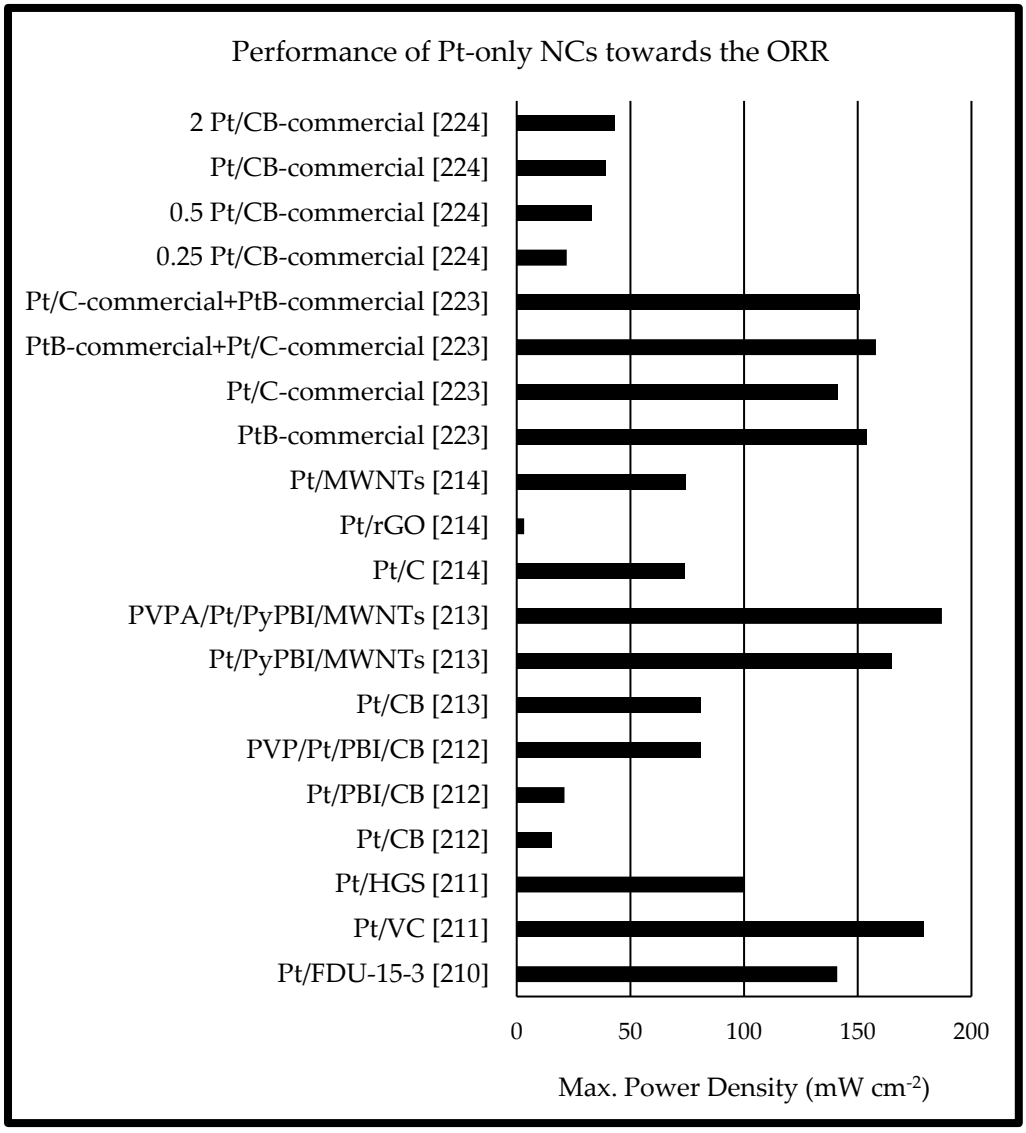

Figure 9. Performance comparison for different Pt-only NCs towards the ORR.

3.2. Pt-Hybrid Metals

The doping of Pt with other metals, as previously mentioned for MOR, is also an effective way of enhancing Pt catalytic activity towards ORR. As such, there have been intense research efforts to eliminate or substantially reduce the loadings of Pt in various catalytic systems. These efforts have resulted in a plethora of heterogeneous Pt-hybrid metals catalyst morphologies beyond the traditional supported spherical NP, that maximises activity and durability while minimizing precious metal loading.

A published work from Hunt and Román-Leshkov [225] describes the principles and methods for the rational design of core−shell nanoparticle catalysts with ultralow noble metal loadings, pointing out that in this way, the unique benefits of the many emerging noble metal architectures could be preserved while their fundamental limitations could be overcome through reformulation via a core−shell morphology. They considered that such core−shell architectures offer the promise of ultralow precious metal loadings, while ceramic cores (comprising elements from Groups 4, 5, and 6 of the periodic table with a nonmetal) hold the promise of thermodynamic stability and access to unique catalytic activity/tunability. Thus, they pave the way to design highly active, stable, and low-cost materials with high precious metal utilisation for both thermo- and electrocatalysis. This prospect of Pt-based nanostructures for the electrocatalytic reduction in oxygen is shared by

Wang et al. [204], who in their Viewpoint paper provided an assessment for the continued development of ORR electrocatalysts, focusing on recent advances and guidelines for maximizing the efficient use of Pt. Recent examples are discussed that demonstrated the growth of Pt shells on non-precious core materials, and they note promising gains in durability without significant sacrifice of the mass activity or cost. Hence, core–shell nanostructures can still possess the beneficial mechanisms of bimetallic catalysts, such as the strain effect arising from the lattice mismatch between the two dissimilar metals and additional ligand effects for cases where the precious metal shells are thin. These effects were first described by Stamenkovic et al. [226] in their paper focused on how variations in the electronic structure determine trends in the catalytic activity of the ORR across the periodic table. They show that Pt alloys involving 3D metals are better catalysts than Pt because the electronic structure of the Pt atoms on the surface of these alloys has been modified slightly. Based on that, they established an interesting volcano-shaped variation in the electrocatalytic activity (Figure 10). In this way, they have established a new approach for the screening of new catalysts for the ORR, by looking for surfaces that bind oxygen a little weaker than Pt or, specifically, for Pt overlayers or "skins", meaning surfaces with a downward shift of the Pt d states relative to the Fermi level, which results in increasing occupation and weaker adsorbate bonding.

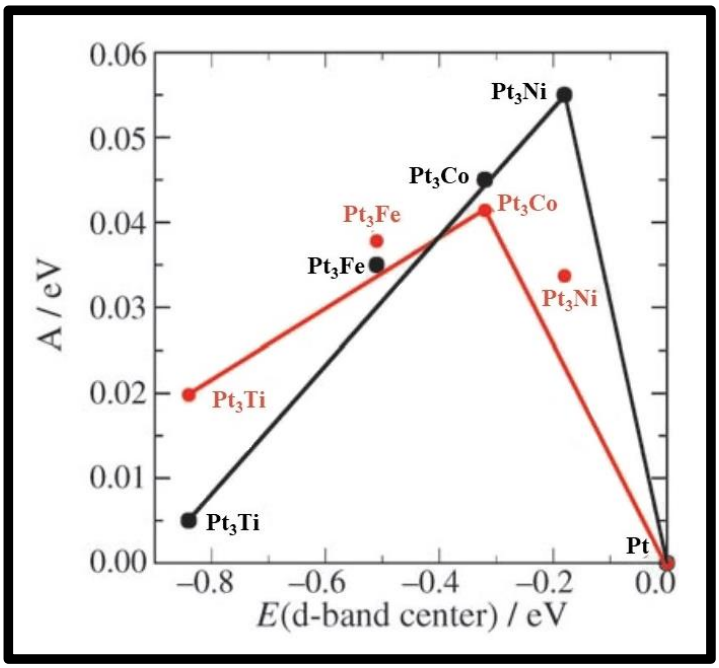

Figure 10. Activity versus the experimentally measured d-band centre, relative to platinum (activity predicted from DFT simulations is shown in black, and the measured activity is shown in red), retrieved from [226].

The general asymmetric volcano trend in the ORR activity was further improved by Calle-Vallejo et al. [227] in order to include graphitic materials with active sites composed of four nitrogen atoms and transition metal atoms belonging to groups 7 to 9 in the periodic table, which are active towards the ORR, and later on by Li et al. [228], to incorporate the site-blocking effect that dominates catalysts with low redox potential or strong binding energy. Early studies reported by Stamenkovic et al. [229] concerning the electrocatalytic trends on Pt_3M (M = Ni, Co, Fe, Ti, V) surfaces between the experimentally determined surface electronic structure (the d-band centre) and activity for the ORR confirmed this "volcano-type" behaviour, where the maximum catalytic activity is governed by a balance between the adsorption energies of the reactive intermediates and surface coverage by spectator (blocking surface) species. These were further incorporated in the study presented by Greeley et al. [230], who describe a new set of ORR electrocatalysts consisting of Pd

or Pt alloyed with early transition metals such as Sc or Y. These studies were prompted by the previous discovery that the Pt_3Ni [111] crystal surface can exhibit an exceptionally high ORR activity as reported by Stamenkovic et al. [231]; however, the demonstration of their practical viability, particularly both high initial Pt-normalised mass activity and high long-term stability in realistic fuel cells, still remains limited [232]. Ni and Co atoms are smaller than Pt atoms and therefore exert a compressive strain on the Pt surface atoms. Compression weakens the binding to the oxygen-containing reaction intermediates; thus, a mild weakening increases the catalytic activity of Pt for oxygen reduction [233]. Since these discoveries, Pt-based alloy nanomaterials have been extensively investigated, aiming to achieve the advanced catalytic performance in practical high-surface-area catalysts. Escudero-Escribano et al. [234] demonstrate how the lanthanide contraction can be used to control strain effects and tune the activity, stability, and reactivity of Pt_5M (M = lanthanum, cerium, samarium, gadolinium, terbium, dysprosium, thulium, or calcium) alloy electrocatalysts. Highly crystalline multimetallic nanoframes with 3D electrocatalytic surfaces were synthesised by Chen et al. [235] by exploiting the structural evolution of platinum–nickel (Pt–Ni) bimetallic nanocrystals. Furthermore, in a different study, Bu et al. [236] reported Pt–Pb/Pt core–shell nanoplates that exhibit large biaxial strains and boost oxygen reduction catalysis. Moreover, as referred before, the most recent developments point out hollow nanostructures as a novel NCs design motif (Figure 11) [222]. Hollow nanostructures can have metal alloy compositions, enabling very high catalytic activities requiring significantly lower amounts of expensive precious metals due to the high proportion of active surfaces. This includes hollow-structured Pt-based ORR catalysts that have shown significant activity enhancement as compared to commercial Pt/C. It is recognised however that are still great barriers to their application in fuel cells in terms of the performance and structural robustness during catalysis. Further efforts are necessary to overcome the limitations of Pt-based, hollow-structured ORR catalysts.

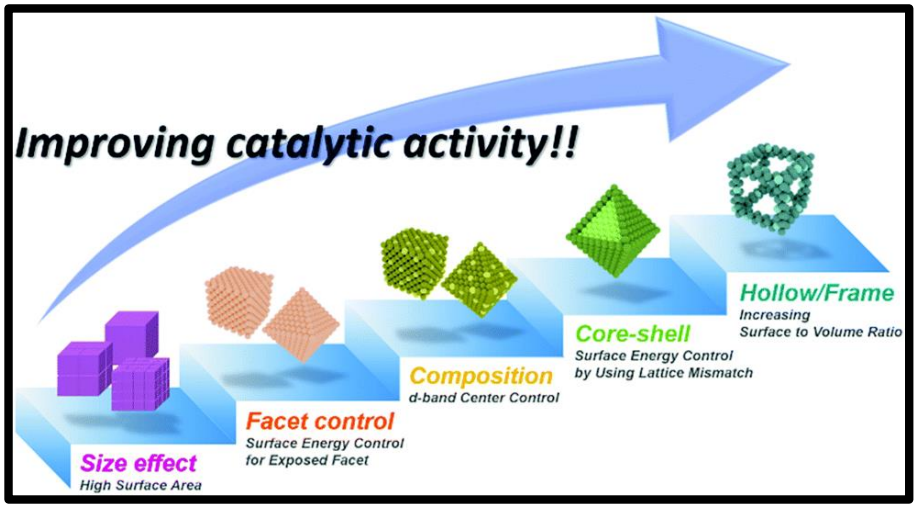

Figure 11. Schematic illustration of a brief history of the development of Pt-based ORR electrocatalysts, retrieved from [222].

Hence, the implementation of these new Pt-hybrid metal NCs in the cathodic CL of real DMFCs is not so much explored, since researchers in the field have focused their attention on non-precious metal catalyst alternatives (as will be demonstrated in the next section). Alternatives such as Pt–Ni alloy nanosheets [237] and Pd [238] are two examples tested in fuel cells and will be explored in this section as potential catalysts for passive DMFCs. Another different solution to improve DMFC efficiency was presented by Yan et al. [239] by using a novel cathode architecture involving an additional thin reaction layer (TRL) with 5–7 μm thickness, in contrast with the cathode CL that is approximately 50 μm. The TRL interfaced with the membrane in order to chemically oxidise the permeated methanol

at the cathode before reaching the effective cathode CL. This TRL is composed of Pt–Ru NCs supported on silica and Nafion® ionomer, in which the reaction between methanol and oxygen spontaneously takes place; hence, the permeated methanol can be chemically consumed before it reaches the cathode CL. It should be noted that, as the silica catalyst support is an electron insulator, triple-phase boundaries cannot be formed in the TRL, so there are no electron pathways. The experimental results obtained with DMFC fed with increasing methanol concentration (1 to 5 M) showed that the adoption of the proposed cathode not only increased the open-circuit voltage due to a reduced mixed-potential loss but also led to better performance, with the peak power density showing an increase for the higher methanol concentrations when compared with the conventional cathode with no TRL. Further electrochemical tests performed confirmed a decrease in the desorption peaks of the intermediates on the cathode catalyst (Pt) surfaces as a result of an alleviation in Pt-poisoning. Hence, accordingly to the authors, the overall fuel cell performance exhibits a substantial improvement. However, one has to notice that the TRL-modified MEA gained extra 15% catalyst loading, which was not compensated in the conventional MEA, as far as we can understand from the description provided. The above work presented has demonstrated the benefits of using Pt-hybrid metals; however, the number of tests in DMFC devices is not very prolific. These compounds still present some important limitations and due to the presence of Pt and other precious metals, the focus has been, as observed in the following section, on the study of non-precious metal catalysts.

3.3. Pt-Free

In recent years, there has been significant progress in replacing platinum group metals (PGMs) with earth-abundant materials for the cathodes of proton exchange membrane fuel cells [28,184,240–243]. As explained before, the ORR is very sensitive to the surface electronic properties and electronic surface atomic arrangement or coordination of the catalyst. The most active sites for ORR are commonly viewed as metal centres coordinated by nitrogen atoms bound to the carbon matrix [244–246]. Hence, among the studied catalyst formulations, heteroatom-doped carbon materials and metal/carbon hybrid materials with unique nanostructures and nitrogen-doped carbon structures were commonly used [183,247,248]. Typically, these kinds of electrocatalysts are produced by mixing an external carbon source, which acts as support, with a nitrogen precursor and a transition metal and then subject to pyrolysis or heat treatment. This process plays a crucial role in increasing the concentration of available ORR active sites while at the same time improves the catalyst stability since it favours proper metal–nitrogen coordination occurring on the carbon support as a result of the tuning of their micropore structures [249]. These carbon–nitrogen-based catalysts exhibit electrocatalytic activity due to the unique electronic interactions between the lone-pair electrons of nitrogen and the π-system of graphitic carbon. Unfortunately, most of the explored heat-treated, non-precious metal–nitrogen catalysts show relatively low activity and stability compared to Pt-based catalysts in the acidic operating environment of a real fuel cell. Their low activity implies the use of relatively thick cathodic CLs (Figure 12), which can lead to severe transport losses, and in turn limits high current density operation, thus presenting relatively low durability/stability of the device [183,239,250–252]. However, manipulating the ligand or increasing the electron-withdrawing properties of the graphitic environment surrounding the active sites can be effective ways to design better catalysts towards ORR [253–255]. Nevertheless, these novel materials, due to their unique intrinsic tolerance to methanol, are considered to provide a great opportunity to be used in DMFCs' acidic environment, enabling the implementation of cost-effective and tolerant methanol contamination cathodes [256].

Therefore, these are great challenges that need to be addressed, particularly in the fuel cell environment, where the high density of active sites and the 3D porous structure are favourable for active-site exposure and mass transfer. This benefits the penetration of electrolytes and the transportation of ions and O_2, thereby leading to high ORR activity, assuming that transport phenomena do not negatively affect the performance of the de-

vice. In this consideration, the engineering porosity and microarchitecture of the cathode CL in the fuel cell is critical, and Serov et al. [257] showed, for the first time, PGM-free cathodic CL morphology in an MEA for a H_2/air fuel cell. This pioneering work allows the researchers to identify morphology-dependent transport losses in the thick PGM-free electrodes [258] associated with the high hydrophobicity and water expulsion, creating additional space within the CL, which introduces longer pathways for all species' transport. Thus, these studies confirm the need to take a holistic approach (i.e., both catalyst and CL design) to enhance the development of low-cost, efficient, stable, and durable fuel cells, as discussed previously.

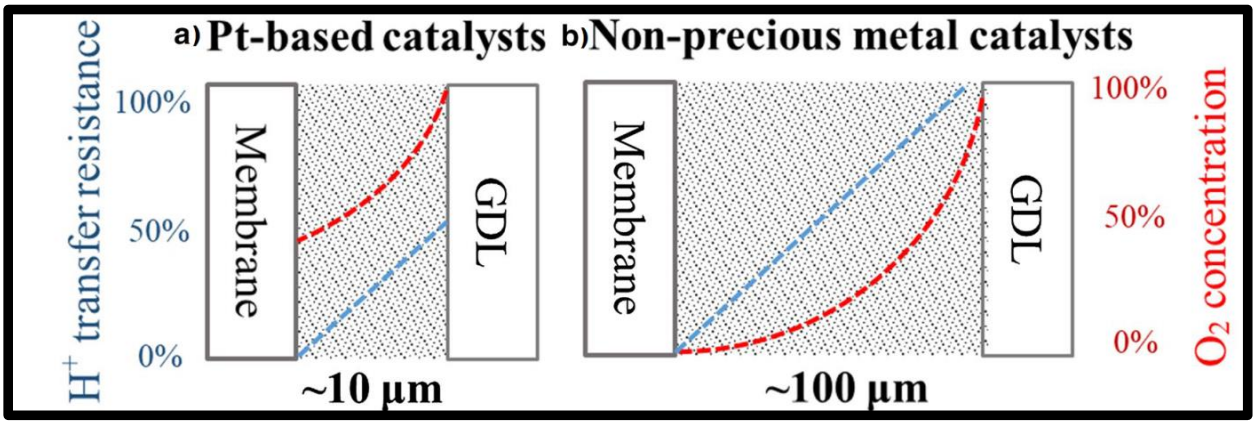

Figure 12. Comparison of O_2 and proton transfer between (**a**) thin Pt-based CL and (**b**) thick CL of PGM-free catalysts, adapted from [251].

3.3.1. Pd-Based

Regarding DMFCs, Pd has been considered an alternative material to catalyse ORR due to its similarities with Pt and lower cost, as pointed out in the review compiled by Gómez et al. [259]. However, the ORR activity of conventional Pd NPs is at least five times lower than their Pt counterparts [260], preventing their direct use as a replacement for Pt. Although, recent efforts are focused on developing more advanced Pd-based NCs, increasing their activity approaching surface modification, alloying, composition and morphology control, and support promotion, in a way similar to what happens with Pt [261,262]. Additionally, one has to keep in mind that all PGMs are extremely rare on Earth's surface. Pd has a lower cost than Pt because of limited use (low demand), not high supply, which in turn can limit its use in fuel cell technology. This way, the research is currently addressed to the development of PGM-free electrocatalysts, in particular transition metal–nitrogen–carbon (TM–N–C) materials, with the TM being Fe or Co. These are considered cheap and sustainable catalysts for the ORR in the acidic environment of the DMFCs [263,264]. An excellent mini-review presenting the analysis of this kind of catalysts mounted at the cathode of a DMFC or investigated in rotating disk electrode (RDE) configuration for the ORR in the presence of methanol was compiled recently by Lo Vecchio et al. [186].

Herein, we intend to confront these kinds of NCs with all the others, comparing their effective performance in real DMFC application, stability, and durability according to the information gathered from the different studies. To this end, we highlight the work reported by Gavidia et al. [265] who developed specific carbon-supported Pt-free catalysts (Pd, Pd–Fe, Pd–Ir, and Pd–Fe–Ir). The performance of the Pd–Fe–Ir/C catalyst was evaluated as cathode material in a DMFC and compared with commercial Pd/C and $Pd_{25}Pt_{75}$/C. A significant improvement in both power output and open circuit voltage (OCV), was given by the MEA with Pd–Fe–Ir/C. The researchers related these results to the "third-body effect" of methanol on the ternary catalyst surface, due to the presence of iron and iridium oxides, where the adsorbed molecules block the catalyst surface sites but do not oxidise, and consequently the mixed potential at the cathode could be avoided. Thus, the MEA

with a cathode containing Pd–Fe–Ir/C catalyst yielded elevated performance in DMFC, while the electrode cost was dramatically reduced. However, despite Pd–Fe–Ir/C's low Pd content, the presence of iridium results in a cost increase compared to the bimetallic Pd–Fe catalyst for equivalent Pd loadings in the electrode. Therefore, with a view to enhancing cost savings, the researchers decided to further study the DMFC performance of the synthesised bimetallic catalyst Pd–Fe/C cathode and Pd/C and compare them with carbon-supported Pd and Pt commercial catalysts [266]. These tests revealed enhanced performance from Pd–Fe/C, especially when operating with high methanol concentration (10 M). More specifically, the MEA based on Pd–Fe/C achieved 25% and 18% higher power density than those based on commercial Pd/C and Pt/C catalysts, respectively. A DMFC stability test was carried out for the best-performing cathode, Pd–Fe/C, to evaluate cell performance; it showed a 44% loss in the maximum power density after 16 h of operation at 0.4 V. Thus, the insertion of Fe into Pd NPs aids the electrocatalytic activity for the ORR, which was ascribed accordingly to the authors to the electronic conjugation by superficial iron oxide and metallic Pd, accompanied by the interplanar spacing decrease that they detected by XRD (X-ray diffraction) and TEM (Transmission Electron Microscopy) analysis. Hence, the authors concluded that the utilisation of partially oxidised surface species based on abundant transition metal alloys with cheaper Pt-free metals such as palladium offered a new path in the search for novel catalysts with high oxygen electro-reduction selectivity and low cost. In a similar study, but this time resourcing to Pd and Pd–Co alloys supported on carbon black as cathode catalysts for DMFCs [267], the researchers were able to evaluate their performance. The Pd-based electrodes have shown to be very appropriate for their use as cathode catalysts in DMFC in terms of a reduction in costs and an increase in the energy density of the device since they are much more tolerant to permeated methanol than a benchmark Pt/C catalyst. In fact, the cell based on the Pd/KB catalyst provided higher performance than that based on Pt/C at a high methanol concentration (>5 M). Additionally, the OCV of the cells based on the Pd/KB and Pd–Co/KB cathodes showed similar behaviour as the methanol concentration increased, whereas the reference cell equipped with the Pt/C cathode exhibited a significant decrease in OCV with methanol concentration. This result was another clear indication of the better tolerance toward the methanol crossover of the MEA based on Pd catalysts. Moreover, the durability tests highlighted the advantage of including a small amount of cobalt in the crystalline structure of Pd in terms of stability and resistance to corrosion phenomena. Thus, this study also reinforces that Pd-based electrodes represent a reliable way to minimise the cost of DMFCs, providing a higher performance than that of Pt-based electrodes at high methanol concentrations with inherently lower costs compared to their Pt counterparts. Both solutions (Pd–Co and Pd–Fe) present rather equivalent results, since one takes into consideration the different metal loading used in the studies.

3.3.2. Other Supports

In relation to the alternative lower-cost TM–N–C catalysts, several different studies reporting their use as cathode catalysts can be found in the literature in the most recent years. Hu et al. [268] used PANI nanofiber-derived catalysts as standard to evaluate the promotional effect of including other species like the phosphorus doping on the activity of the iron–nitrogen–carbon (Fe–N–C) catalyst for the ORR. Even the obtained doped and undoped catalysts exhibited mostly the same nanorod morphologies and structures; the phosphorus doping caused the catalyst to exhibit a much-enhanced ORR performance. The researchers considered that the phosphorus doping process might not have altered the nature of active sites but led to the increase in the ORR active site density and/or better dispersion of them on the catalyst surface. Furthermore, they tested the activity and stability of the Fe–NP–C catalyst in DMFCs and compared them with the Pt/C cathode-based fuel cell. However, even if the Fe–NP–C cell performance was rather stable and durable, the maximum current density and peak power density were about one-fourth of those for the Pt/C cathode-based cell due to the less efficient mass transport in the thick

Fe–NP–C catalyst layer, thus implying the further optimisation of the electrode fabrication for the Fe–NP–C catalyst to be a viable alternative as a cathode in a DMFC. Another variation to the PANI nanofiber-derived catalysts was reported by Karim et al. [269,270], who further study transition metal macrocycle-based catalysts. There are several types of macrocycles that have attracted attention, such as porphyrin (P), phthalocyanine (Pc), tetramethylphenylporphyrin (TMPP), phenanthroline (Phen) complexes, and others due to their reasonable activities, remarkable selectivities of the catalysis of ORRs, and high tolerance to methanol [271]. Cobalt phthalocyanine (CoPc) presents low reactivity towards the ORR, although it is highly inert to methanol, and in a previous theoretical study [272], the researchers showed that tungsten atom adsorption on CoPc can improve its ORR performance, and led to reaction pathways that produced water as the main product. The CoPc/C-$W_{18}O_{49}$ catalyst was also applied in DMFCs as the cathode catalyst, and the power density of the cell was higher than with non-platinum macrocycle-based catalysts with modified structures such as PANI-FeTsPc [273]. The use of $W_{18}O_{49}$ as a support enhanced the ORR activity of CoPc.

The importance of the support in these kinds of catalysts has been evidenced in various works. Negro et al. [274] reported Fe–N supported on graphitic carbon 3D nano-networks (Fe–N/CNN) as ORR catalysts. In previous studies, they have shown that CNNs can be successfully used as a more durable support for Pt catalysts compared to commercially used CNTs, while their performance is comparable to CNTs with a less expensive production. Therefore, they tested its behaviour in conjunction with Fe–N. They achieved 15 mW cm^{-2} at 90 °C, with a MeOH concentration of 2 M and they considered that this was an interesting alternative to state-of-the-art Pt-based electrocatalysts. However, the excellent result presented, where the resistance of the new catalyst to MeOH contamination is significant, with no direct comparison to the equivalent Pt/CNN catalyst in a DMFC environment. This was somewhat circumvented in the study provided by Li et al. [275], who studied Fe–N and a different carbon material, reduced graphene oxide (rGO), presenting a new method to prepare highly a porous graphene catalyst for the ORR cathode in DMFCs. This way, they showed that, while the morphology of 2D rGO was largely preserved, the resulting Fe–N–rGO catalyst provided a more unique porous structure. The performance of the Fe–N–rGO cathode exceeded the performance of the Pt/C cathode when the methanol feed concentration was higher than 2 M. Moreover, the OCV measured with the Fe–N–rGO catalyst was higher than that of Pt/C even at the lowest methanol feed concentration of 0.5 M. This work demonstrated the viable possibility of using Earth-abundant catalysts for DMFC technologies, particularly at higher methanol concentrations since one of the most desirable characteristics for a cathode catalyst in a DMFC is a high tolerance to the presence of methanol. Park et al. [276] reinforced these findings by resorting to a nano-sized graphene-based Fe/Co–N–C catalyst, derived from the heat treatment of a ball-milled GO. The results showed that the graphene-based catalyst (GbC) was capable of tolerating a highly concentrated methanol feed up to 10 M without a considerable activity loss from methanol crossover. Because of the trade-off effects from both the ionomer and catalyst contents in the electrode, the best performance was observed with an ionomer content and catalyst loading of 66.7 wt.% and 5.0 mg cm^{-2}, respectively. The maximum power density was ca. 32 mW cm^{-2} with a 1 M methanol feed concentration at a relatively low Pt–Ru content (2 $mg_{Pt–Ru}$ cm^{-2}). This performance is comparable to other high-performing Fe(Co)–N–C catalysts. However, even though it has a very outstanding methanol-tolerant property, the maximum power density at the optimised cathode compositions is still very low compared with that of Pt/C. Therefore, to successfully replace commercial Pt cathodes with graphene-derived Fe(Co)–N–C catalysts in DMFC systems, further activity improvement and additional stability issues need to be more clearly resolved in the near future.

3.3.3. Sacrificial Support Method

A strategy to improve both the activity and stability of TM–N–C catalysts derived from H_2-fed fuel cell research has been replacing the carbon support in the synthesis procedure

by a non-carbonaceous sacrificial support with an ordered structure (such as silica, alumina, zirconia), designated as a sacrificial support method (SSM) [277,278]. This sacrificial support is mixed with the precursor(s) containing nitrogen, carbon, and transition metal, and it is removed after the pyrolysis step, which results in a self-supported TM–N–C catalyst with high pore volume and good accessibility to active sites. This alternative synthesis was employed in the work reported by Videla et al. [279], who used iron phthalocyanine (FePc) as Fe–N–C source and templated with an ordered mesoporous silica (SBA-15) to synthesise a self-supported PGM-free catalyst for the ORR [280]. They showed that the resulting catalyst was composed of a self-standing Fe–N–C framework, which was not only methanol-tolerant but also active enough for fuel cell portable applications. The cathodic catalyst was not dramatically affected by the presence of methanol, showing only a 12% drop in maximum power density with the highest methanol concentration of 10 M fed at the anode. A 3D multi-dimensional DMFC model incorporating computational fluid dynamics (CFD) was also implemented in this study and it agreed with the experimental data. This showed that the presence of condensed water, and consequently the barrier effect, limited the ability for oxygen diffusion to reach the triple-boundary reactive phase on the active ensembles of the Fe–N–C catalyst, representing one of the major limitations of the cell performance using a non-noble catalyst on the cathode side. Wang et al. [281] recognised the importance of the matter and successfully promoted triple-phase interfaces in micropores of Fe–N–C catalysts by controlling the distribution of a hydrophobic additive, dimethyl silicon oil (DMS), not filling them fully. Such a proper distribution of DMS can help to form a robust triple-phase interface in micropores and prevent water flooding, but it cannot block O_2 transport seriously. They recognised that the main difficulty was that small-sized micropores (<2 nm) can also be easily fully filled by hydrophobic additives to block both O_2 and proton transport channels, which is not obvious for the mesopore and macropore characteristics of the traditional Pt/C catalyst layer. The key was then to control the DMS distribution on the Fe/N/C catalyst by screening the DMS molecular weights, size, and viscosity. This approach effectively addressed the problem of micropore water flooding of the Fe/N/C catalyst. They used an Fe–N–C catalyst derived from the pyrolysis of poly-m-phenylenediamine (PmPDA)—coated carbon black and $FeCl_3$, known to possess high activity for the ORR in acid medium [282]. The Fe–N–C(DMS) cathode exhibited good durability, with only a 12.7% voltage loss after a 20 h test at 0.10 A cm^{-2}, which is even superior to that of the Pt/C cathode (15%). When the methanol concentration was increased from 3 to 15 M, the Fe–N–C(DMS) cathode performance only showed a negligible decay (8%), whereas the bare Fe–N–C cathode exhibited a severe decay of 27%. The Pt/C cathode could not run at all when the methanol concentration was increased to 10 M due to the severe methanol crossover and mixed potential. This way, the proposed strategy was considered a contribution to engineering a microenvironment of catalyst active sites to boost the performance and durability of non-precious-metal catalysts for fuel cell devices. Another contribution was presented by Osmieri et al. [283] who synthesised an Fe–N–C catalyst by the impregnation of Fe(II)-phthalocyanine (Fe-Pc) on SBA-15 silica used as a sacrificial template, resulting in a material with an extremely high specific surface area and high microporosity (around 50%) (more details about the procedure can be found in their previous paper [284]). This catalyst presented a composite morphology where it was possible to identify the presence of longer nanotubes interconnecting different rod-like particles. The best results for the Fe–N–C catalyst as a DMFC cathode were obtained with no Vulcan addition, 50 wt.% Nafion® content, and a catalyst loading of 2.5 mg cm^{-2}. The maximum power density obtained in these conditions was 19.6 mW cm^{-2} (at 90 °C and using 2 M MeOH), which was close to the results obtained by other groups using similar Fe–N–C catalysts in similar testing conditions (FeAAPyr 2.7) [285] and (FeABZIM) [286], which will be explored in the next section. A short-term durability test was also performed, showing a deactivation of 64% in terms of the maximum power density, which the researchers ascribed to the flooding of the micropores and/or to the active site's deactivation. However, the performance loss of the Fe–N–C catalyst was considerably lower compared

to a commercial Pt/C catalyst after a 3 h test, making the Fe–N–C catalyst a potentially good candidate for Pt replacement in DMFC cathodes, since it leads to a considerable decrease in the total MEA cost. Nevertheless, the performance of this Fe–N–C catalyst in DMFCs is still lower than a commercial Pt/C catalyst, leaving open space for future work in performance improvement. The same researchers also reported their results concerning the investigation of the effect of four carbonaceous materials (acetylene black (AB), multi-walled carbon nanotubes (MWCNT), silica mesoporous nanoparticles (MPC), and silica nano-powder (CNS)) [287]. These were used as a support to synthesise Fe–N–C catalysts for the ORR by impregnation with a Fe(III)-1,10-phenanthroline (Phen) complex and subsequent pyrolysis in an inert atmosphere. As mentioned before, due to the fact that the Fe-Phen complex contains Fe, N, and C, with nitrogen atoms coordinating the metal, it has aroused the interest of researchers in the field of ORR catalysts as an alternative to Pt-based ones [288]. However, to achieve enhanced catalytic performance, particularly in the fuel cell environment, it is necessary to assure the good mass transport of reactants and products, and a possible approach is to properly tune the structural features of the carbonaceous support, as these researchers showed. The ORR activity performance of the catalysts prepared is related to the different structural features of the carbonaceous support materials, such as the specific surface area and the pore size distribution, and to the weight loss during the pyrolysis. These characteristics play an important role, particularly in acidic environments, like in DMFCs, as evidenced by the results obtained when tested as cathodes in real fuel cell devices. The DMFC prepared using Fe–N/MPC1 had a maximum power density of about 73% of that of commercial Pt/C, whereas Fe–N/MPC2 showed a slightly lower performance, with about 57% maximum power density compared to Pt/C. This fact could be explained by the higher microporosity of Fe–N/MPC2, which can be problematic in fuel cell operation because it is subjected to water flooding. Fe–N/CNS, Fe–N/MWCNT, and Fe–N/AB catalysts have considerably lower performance; thus, a short-term durability test in DMFCs was carried out only for the two most-performing catalysts (Fe–N/MPC1 and Fe–N/MPC2). The results obtained with the two Fe–N/MPC catalysts are considerably better compared to that of Pt/C and the Fe(II)-phthalocyanine-based catalyst they synthesised and we presented before [283]. Hence, it evidenced their high methanol tolerance and consequent higher durability compared to Pt/C catalysts. Nevertheless, these Fe–N–C catalysts still need improvements since their ORR electroactivity in acidic media compared to commercial Pt/C is low. It should be pointed out that these results clearly show that if one only cares about the cost reduction, choosing, for example, a carbon black support (e.g., AB), the risk of producing a catalyst with a too-poor final ORR activity is high. Hence, much attention must be paid to the choice of an adequate C-support and its synthesis. In this regard, the use of a sacrificial template such as a mesoporous silica to obtain the final desired structural features was demonstrated to be effective. Another system studied was the highly active Fe–N–C catalyst derived from the pyrolysis of a nitrogen-containing charge transfer organic salt: nicarbazin (N,N′-bis(4-Nitrophenyl)urea compound with 4,6-dimethyl-2-pyrimidinone) and Fe salt, denoted as Fe–NCB [289]. Accordingly, computational calculations (DFT) demonstrated that Fe–N4 and Fe–N2C2 active sites preferentially adsorb oxygen with much higher energy than methanol, ethanol, and products of partial ethanol oxidation (0.73–1.16 eV stronger adsorption), while nitrogen–carbon related sites (pyridinic and graphitic nitrogen) are much less selective towards ORR. The feasibility of DMFC operation based on high methanol concentration (up to 17 M) due to the utilisation of Fe–N–C cathode catalyst was demonstrated. Hence, the researchers proposed a new strategy for the commercialisation of direct alcohol fuel cells (DAFCs), considering that using noble metals only at the anode side (in combination with other cheaper ad-metals like Ru or Sn) and highly tolerant PGM-free catalysts (M-N-C) in the cathode allows the extension of the device energy density compared to PGM-based catalysts at both electrodes. Moreover, in the pursuit to achieve a large-scale commercialisation of cost-effective DMFCs, Lo Vecchio et al. [290], in a recent published work, reported a new template-free procedure leading to low-cost Me–N–C (Me = Fe or Co) electrocatalysts derived from EDTA (ethylene

diamine tetra acetic acid). These cathode catalysts were prepared by chelating the metal with the biological environmentally friendly nitrogen precursor EDTA, followed by deposition on a high surface carbon support (Ketjenblack, KB). Four samples, CoNC8, CoNC10, FeNC8, and FeNC10, were investigated in a DMFC under reliable conditions (low-Pt loading at the anode). These tests showed that FeNC8 was the best-performing low-cost cathode catalyst in terms of higher ORR activity and methanol tolerance, achieving a maximum power density of 10.5 $mW \cdot cm^{-2}$ when using MeOH 2M and 90 °C. This was correlated to the fact that it also showed the largest percentage of C-N defects, pyridinic/pyrrolic ratio, and N–Fe interaction. Instead, in this work, the metals are derived from metal nitrates, the nitrogen precursor was a low-cost and easily available bio-compound (EDTA), and a template-free preparation procedure was involved. So, as the researchers recognised, the optimisation of the synthesis procedure is necessary in order to obtain more active ORR catalysts based on non-noble metals and earthly abundant compounds, but this can be a more sustainable route to that.

3.3.4. PGM-Free Materials

A research paper integrated, for the first time, a PGM-free (Fe–N–C) electrocatalyst, commercially available on market into the cathodic layer of a DMFC [291]. The authors tested the effect of catalyst loading, ionomer content, and methanol concentration at two temperatures (60 °C and 90 °C). A high cathodic catalyst loading of 6 mg cm^{-2} demonstrated counteraction of the increases methanol crossover rate by the use of high fuel concentrations. Regarding the ionomer content, the best compromise between the increased catalytic sites number and the suitable conductivity of the layer was obtained with 45 wt.% Nafion. The highest power density (≈76 mW cm^{-2}) was provided with Fe–N–C loading of 6 mg cm^{-2} for a methanol concentration of 2 M at 90 °C. This catalyst allows reaching the best performances recorded for PGM-free cathode in a DMFC under similar conditions. Xu et al. presented a novel Fe–N–C catalyst (ZIF/MIL-10-900), which is derived from a mixture of ZIF-8 and MIL-101(Fe) precursors and atomically dispersed FeN_4 structures [292]. The authors verified that ZIF-8-derived support provides abundant specific surface area and nitrogen, while MIL-101(Fe) supply iron to from the atomically dispersed active sites. The proposed catalyst exhibited comparable ORR activity, better stability, and superior methanol tolerance compared to the commercial Pt/C, with a maximum power density 2.8-fold higher in the same conditions. It was demonstrated to be a promising alternative to precious metals for DMFC cathodes. All these findings clearly indicate that heteroatom-doped carbon nanomaterials of the type transition metal–nitrogen–carbon (TM–N–C) are promising non-PGM electrocatalysts for ORR in acidic fuel cells and, in this way, pave the way to more efficient, stable, and cost-effective DMFCs. Lastly, particular attention should be paid to the catalyst layer porosity and TBP interaction since they affect the mass transfer and utilisation of active sites in the CL, which further determines the fuel-cell performance and durability. To address such challenges, further efforts should be attempted toward understanding the fundamental problems of catalyst layers and finding the best solutions to solve or minimise them. This route implies a holistic approach by developing new NCs and tailoring the design of the electrodes.

3.4. Passive Feed Systems

The developments on cathode nanocatalysts for DMFC devices operating at temperatures below 45 °C will be presented in this section and summarised in Table 2, since they may be suitable for passive systems, where the operating temperature is lower.

Table 2. Comparison of DMFC performance towards ORR optimisation.

NCs	Pt Load (mg cm^{-2})	[CH_3OH] (M)	T (°C)	DMFC Mode	Max. Power Density (mW cm^{-2})	Ref.
Pt/C-commercial	2	2	25	Passive	30.2	[293]
Pt/C (DLC1)	1				29.1	
Pt/C (DLC2)	2				39.4	
Pt/C-commercial	0.83	2	25	Passive	15.5	[294]
Pt/C-commercial	1				17.4	
Pt/C-commercial	2				25.4	
Pt/C (S-Pt)	0.12				15.1	
Pt/C (D-Pt)	0.22				20.8	
Pt/CFX (O_2 LF)	4	1	30	Active	23	[295]
Pt/C (O_2 LF)					14 [i]	
Pt/C	1	2	25	Passive	16.2	[296]
Pt/MWNTs (3:1)					14.7	
Pt/MWNTs (1:1)					18.1	
Pt/MWNTs (1:2)					28.5	
Pt/MWNTs (1:3)					24.2	
Pt/MWNTs (1:2)	0.5				19.2	
$Pd_{19}Pt_1$/C	2.8 *	2	30	Active	45 [i]	[238]
$Pd_{19}Pt_1$/C		4			40 [i]	
$Pd_{19}Pt_1$/C		6			35 [i]	
Pt/C		2			30 [i]	
Pt/C		4			23 [i]	
Pt/C		6			15 [i]	
Pt NSs/C	1.0	2	25	Passive	30.6	[237]
Pt–Ni NSs/C	0.8				32.2	
Pt/C	1.0				17.4	
Pt/C	2.0				29.9	
Pt–Ni NTs	1.0	4	RT	Passive	25.1	[297]
Pt/C					18.6	
FeAAPyr 7.4	7.4 ***	10	30	Active	(9) [i]	[285]
FeAAPyr 2.7	2.7 ***				(7) [i]	
Pt/C	1				(5) [i]	
FeABZIM	3.0 ***	10	30	Active	6.7	[286]
Fe–N–C (S)	2.97	1	25	Active	1.5 [i]	[298]
	1.74				2 [i]	
Fe–N–C (S)	2.97		40		4 [i]	
	1.74				4 [i]	

* identified as "metal"; *** identified as "catalyst"; [i] not specified, inferred from the plot; () values in W g^{-1} Pt MEA.

In order to reduce the Pt catalyst loading in the cathode side of passive DMFCs, Pu et al. [293] reported a reduction of up 50% by using Pt nanorod assemblies (linear aggregates of Pt NPs in the range of 30–60 nm) in a double-layered configuration (DLC). A DMFC with a conventional cathode based on a commercial Pt/C was used as a reference to evaluate the potential of the DLC for the reduction in the Pt loading and the system costs. The improved performance of the DLC was ascribed to an increase in the catalyst utilisation and a decrease in the charge-transfer resistance in the cell, confirmed by the EIS data. Based on that, the authors considered that the Pt nanorod-based systems have a great potential in reducing the DMFC costs. Wang et al. [294] used an ordered nanostructured cathode based on controlled, vertically-aligned Pt nanotubes fabricated by combining the sacrificial template method and in situ galvanic replacement for ultra-low Pt-loading passive DMFCs. The proposed catalyst exhibited an electrochemical specific area which is three times higher than that of conventional Pt/C, and when used for the ORR, exhibited similar activity but better durability than the commercial catalyst. By using vertically aligned Pt nanotubes, it was possible to reduce the Pt loading by approximately one-seventh without sacrificing the fuel cell performance. This method may provide a new way to fabricate ordered nanostructured cathodes for ultra-low Pt-loading fuel cells. Viva et al. [295] studied the

use of fluorinated carbon as a Pt support (Pt/CF_x) in comparison to a commercial Pt/C catalyst. Overall, the Pt was well dispersed on the CF_x support, with a homogeneous average particle size of 4.5 nm (smaller than the commercial unmodified Pt/C). Further electrochemical characterisation showed that the ORR with Pt/CF_x proceeds mostly to water, with a yield of >99%, and the amount of H_2O_2 generated was smaller than that usually reported for Pt/C (2–4%). When the Pt/CF_x was used in the cathode of a DMFC, it was observed that there was an improvement in the performance and an increase of 60 to 70% in the peak power density at low O_2 and air flows. Moreover, the results showed that the cell performance using Pt/CF_x does not decrease as abruptly as the one using a commercial catalyst when the O_2 flow decreases. This was explained by the fact that the fluorinated carbon surface extends the O_2 residence time as it flows through the cell compartment improving the reaction kinetics. They considered that further experiments need to be carried out, and the new support is an interesting option for decreasing the amount of Pt in the fuel cell cathodes. Pu et al. [296] used a new MEA with an MWCNT–Pt nanocomposite cathode catalyst in a passive DMFC. This new cathode catalyst layer has a 3D network structure that requires a significantly lower Pt loading while maintaining a similar performance than the one obtained with a conventional MEA with twice the Pt loading. The enhanced performance was attributed to the discontinuous distributions of the Pt MWCNT structures and the formation of a cross-twined network within the cathode CL. The EIS data showed that the new cathode CL decreases the charge transfer resistance of the ORR and greatly increases the catalyst utilisation in comparison with the conventional MEA.

Choi et al. [238] prepared a carbon-supported Pd-rich Pd–Pt bimetallic nanoparticle electrocatalyst with a metal content of 60% that was used as cathode catalyst in a DMFC. The results demonstrated that when Pd-rich electrocatalysts ($Pd_{19}Pt_1$ NPs) were used, the cell performance decreased slightly with an increase in the methanol concentration (from 2 to 6 M), while the one using a Pt electrocatalyst decreased rapidly. Additionally, by the rotating disk electrode measurements, it was possible to see that the Pd-rich electrocatalysts have an excellent methanol tolerance compared to Pd-free Pt electrocatalysts. Thus, the authors considered that Pd-rich Pd–Pt electrocatalysts could be a viable candidate to minimise the use of Pt in the DMFC cathodes, especially for highly concentrated methanol solutions.

Wang et al. [237] reported a study using interconnected nanoparticle-stacked two-dimensional Pt and porous Pt–Ni alloy nanosheets (NSs) as cathode electrocatalysts in passive DMFCs. The cell with Pt NSs (1.0 mg_{Pt} cm^{-2}) and porous Pt–Ni NSs (0.8 mg_{Pt} cm^{-2}) exhibited excellent performance, with satisfactory stability at 25 °C, which was slightly higher than the one with Pt (2.0 mg_{Pt} cm^{-2}). The performance improvement of the cells with Pt NSs and porous Pt–Ni NSs was attributed to higher electrocatalytic activity and a lower charge transfer resistance of the cathodic CL, confirmed by EIS. This technique also showed that the Pt–Ni NS-modified MEA shows a much smaller charge transfer resistance than that of Pt NS, which may be due to the porous structure of Pt–Ni NSs that could be beneficial to expose the active sites and provide additional channels for mass transport.

Fan et al. [297] used a Pt–Ni alloy nanotube catalyst towards the ORR in a passive DMFC, obtaining a maximum power density 35% higher than the one obtained with Pt/C. This catalyst exhibited enhanced ORR activity and excellent durability, which was attributed to the Pt–Ni alloy effect and the hollow nanotube structure effect, respectively. This study revealed an interesting alternative to decrease the use of noble metals in these devices.

Sebastián et al. [285] synthesised and tested a highly active non-PGM catalyst for the ORR by modified SSM in order to control the morphology and hydrophobicity of the transition metal–nitrogen–carbon material (M–N–C). This catalyst was evaluated by SEM (Scanning electron microscopy), TEM, and BET (Brunauer–Emmett–Teller), and the catalyst's activity towards the ORR and tolerance to methanol poisoning were studied by RDE. This catalyst was used in the cathode of a DMFC working at different methanol concentrations (1 to 10 M) and operating temperatures (30 to 90 °C). The results showed that the Fe-AAPyr catalyst has an extraordinarily high tolerance to methanol crossover,

with no significant decay of performance up to a methanol concentration of 10 M. The durability tests showed a DMFC performance decay of up to 70% after 100 h of operation. Despite the lower performance when the cell was operated at 30 °C, the cell performance with the proposed catalyst was better than the one using Pt/C, being a good alternative to passive systems. Considering that the Fe-AAPyr cost is two orders of magnitude lower than Pt, this catalyst can be used as a highly active, methanol-tolerant and inexpensive catalyst in DMFC systems. The same authors investigated alternative synthesis procedures to develop an improved catalyst based on Fe–N–C for the ORR, one of them being derived from pyrolysed Fe-aminobenzimidazole (Fe-ABZIM), a highly nitrogen-rich organic precursor [286]. This formulation consisted of a well-developed 3D porous structure with a high density of active sites, presenting higher activity towards the ORR than the Fe-AAPyr catalyst [285]. The Fe-ABZIM catalyst showed a remarkably high tolerance to methanol, resulting in higher ORR performance compared to Pt/C, even in real DMFC operating conditions. Moreover, the durability tests showed an enhanced performance behaviour with the operating time, reaching a power density decay of about 40% after 100 h of operation, similar to that obtained by a commercial Pt-based catalyst. Martinaiou et al. [298] also reported a study with a non-precious metal catalyst, Fe–N–C, which was prepared using polyaniline, dicyandiamide, and iron acetate as precursors. The activity and the influence of the methanol concentration on the catalyst performance were tested in a half-cell set up in acidic media. The influence of the operating temperature (from room temperature to 80 °C) on the catalyst activity (in the absence of methanol) was also studied in order to estimate its activation energy. When the catalyst was used in a DMFC, the cell performance was as good as the one obtained with other Fe–N–C catalysts. However, a comparison with the conventional Pt/C catalyst was not performed, and the maximum power density decreased by 85% during the DMFC operation. Mössbauer spectroscopy measurements indicated that the decrease in the catalytic performance seems to go along with the demetallation of the FeN4 sites and the subsequent formation of iron and iron oxide clusters. Thus, Fe–N–C (S) is a promising cathode catalyst for the DMFCs; however, the stability needs to be improved, and the factors that contribute to its degradation should be investigated.

Many efforts have been made to replace the traditional Pt/C catalyst in the DMFCs, being the catalysts tested at low temperatures a promising alternative for passive systems. Even so, it is essential to continue the research in this area towards the development of catalysts with higher performances and durability and lower costs.

4. Theoretical/Modelling Approaches

Over the last decade, theory and modelling have become increasingly powerful in fuel cell electrocatalysis. For further insights into such an extensive and challenging subject, one can reference the compilation of Eslamibidgoli et al. [61], which focused on the first principles of electrochemical modelling but put emphasis on aspects beyond the capabilities of DFT, including metal charging and solvent effects. The electronic properties derived from DFT calculations can provide information concerning the energy gaps between the highest occupied molecular orbital (HOMO) and lowest unoccupied molecular orbital (LUMO), which in turn can be related to the stability of the materials. Despite its limitations, one should note that, due to the enhanced ability of DFT to scale with the number of electrons, it has captured a central role in this rapidly evolving field. This is also recognised by an excellent review provided by Seh et al. [299]. The authors explained how design strategies for state-of-the-art, heterogeneous electrocatalysts can be rationalised based on combining theory and experiments toward developing improved catalysts. A case study presented by Ismail et al. [300] showing how the effects of catalyst agglomerate shape in polymer electrolyte fuel cells can be investigated by a multi-scale modelling framework is also mentioned. This way, they presented a catalyst synthesis process more modelling-led and significantly saved cost and time by reducing the amount of experimental trial-and-error to improve the performance of the fuel cell. Finally, among many others, one highlights also the pioneering work of Zawodzinski et al. [301], who evidenced the synergy that can be

established between theoretical and experimental studies for fuel cell electrocatalysts in an integrated approach.

In a prospective DMFC context, a pertinent review of data regarding Ru–Pt catalysts was performed by Moura et al. [58]. The authors aimed to present a coherent frame of the recent experimental and computational breakthroughs for Ru–Pt catalytic activity towards the MOR in an inclusive perspective, filling the gap of the transversal analysis. This way, they analysed the various recent theoretical approaches for determining the pathway of methanol oxidation and systematised their validation with the experimental data. A short overview of the current research of catalysts for the MOR in DMFC, merging the experimental and theoretical aspects, was also reported by Karim et al. [302]. Several metal alloys and catalyst supports have been reviewed in this paper together with a discussion about the durability of the catalysts. In addition, the DFT study to find the most stable condition of methanol adsorption is highly encouraged. The researchers pointed out that the determination of the mechanism reaction using DFT is important since different pathways will give different activation energy during the MOR. Additionally pertinent are the numerical modelling and simulations of DMFC systems under various ambient temperatures and operating conditions [303–306]. This kind of study is also important in optimising each component and understanding the internal processes (mass and heat transport). Since most of these processes are difficult to follow directly in experiments, mathematical models can be applied to obtain hints for the development of DMFC optimal control and operating strategies. However, this perspective is out of the scope of the present paper.

The aim of this section is to grasp how the theoretical insights from the structure–catalytic activity relationship of the NCs can be used to optimise the development of cost-effective materials and the performance of real DMFCs. One example of this approach can be found in the first principles study on the CO removing mechanism on Pt-decorated oxygen-rich anode surfaces (Pt_2/o-MO_2(110), M = Ru and Ir) in DMFC reported by Liu et al. [307]. The authors applied DFT to investigate the adsorption of CO and H_2O on pristine Pt_2/MO_2(110) and the oxygen-rich Pt_2/o-MO_2(110) surfaces. They found that the application of the oxygen-rich surfaces significantly reduces the adsorption energies of CO and H_2O molecules as well as the major reaction barrier reactions forming CO_2. Their detailed analyses of the electronic interaction between the catalysts and adsorbates indicated that Pt_2/o-MO_2(110) may be a promising DMFC anode material since it reduces the CO poison problem. Thus, they successfully explained the previous experimental observations [308] of better Pt dispersion with the inclusion of RuO_2 and IrO_2 species and the high catalytic performance of the MOR with efficient CO removal. Another theoretical study on the kinetic energy of a novel metal composite for anode catalysts in DMFCs was reported by Basri et al. [309]. They intended to investigate the doping effect of adding Ni and Fe to Pt–Ru in order to improve the MOR kinetics. They analysed the NCs structures using Materials Studio DMol3, a modelling program that uses DFT, to simulate chemical processes and predict the properties of the material. The simulation results indicated that Pt–Ru–Ni–Fe had the potential to improve the performance of the catalyst due to the lower calculated adsorption energies and the presence of Fe^{2+} and Ni^{2+} ions, which increased the electron density. Theoretical studies showed that Pt–Ru–Fe–Ni/MWCNTs had more favourable energy values than Pt–Ru/MWCNTs. The optimum geometry for the CNT was experimentally confirmed from Raman analysis. Therefore, the researchers concluded that Pt–Ru–Fe–Ni/MWCNTs are more stable and should have a higher reaction rate than Pt–Ru/MWCNTs. Moreover, this enhanced stability should be responsible for the increased durability of the Pt–Ru–Fe–Ni catalyst in comparison to Pt in fuel cells. A similar study, in order to understand the basic interfacial properties of the catalyst–catalyst support, but this time employing nitrogen-doped, partially-exfoliated carbon nanotubes (PECNTs) as anode catalyst support materials for DMFCs was reported by Ghosh and Ramaprabhu [310]. They presented evidence that the MOR kinetics can be increased by employing PECNTs, wherein the partial exfoliation of CNT gave rise to

abundant straight edges, which possess superior electron-donating properties and could also act as active anchoring sites for catalyst dispersion. Further, DFT calculations revealed that doping nitrogen in the PECNT framework significantly reduced the LUMO–HOMO energy gap. The physical properties elucidated a significant enhancement in the specific surface area and an increment of about ten times in pore size. This increment led to improved methanol diffusion, thereby resulting in an increase in the number of TPB and MOR kinetics at the anode. They also verified that the enhancement in diffusion coefficient led to a reduction in the mass transfer loss during DMFC measurement, which resulted in a maximum power density of 92 mW cm^{-2} at 80 °C. These results clearly indicated a promising application of PECNTs as a catalyst support and confirmed the theoretical findings. Liu et al. [311], exploring high-activity electrocatalysts for ORRs, also supported their experimental findings by DFT by using DMol3 to perform geometry optimisation and total energy calculations. They presented the advantages of using N-doped hierarchical porous carbon nanosheets (N-HPCNSs) in the cathode of various fuel cell devices, including DMFC. This was considered to be a template-free, economic, and environmentally friendly strategy for the scalable synthesis of N-HPCNSs with biomass water lettuces as the carbon precursor. The N-HPCNSs were demonstrated to possess 3D hierarchical porous structures with a high surface area and uniform N-doping. A systematic electrochemical study revealed that the N-HPCNSs not only hold numerous active sites but also manifest high intrinsic activity for each of the active sites toward ORRs in pH-universal electrolytes of alkali, acid, and neutral. All the experimental and theoretical results gathered by the researchers pointed to the increase in surface area and porosity of the N-HPCNSs as the additional factors in enhancing the activity of ORRs. With the N-HPCNSs as cathode electrocatalysts, three types of home-made fuel cells were set up that run in alkaline, acidic, and neutral media, i.e., a Zn-air alkaline fuel cell, a direct methanol fuel cell, and a microbial fuel cell, respectively. Here, we refer only to the results obtained with the DMFC type. The N-HPCNSs–DMFC presented an OCV of around 0.654 V and a P_{max} of 3.815 W m^{-2} at the current density of 15.51 A m^{-2}. These values indicated a performance close to the Pt/C-DMFC (OCV = 0.566 V, P_{max} = 4.111 A m^{-2}) and better methanol tolerance. The 330 h durability test performed indicated that the N-HPCNSs-modified DMFC is capable of producing steady electricity upon long-term operation, further demonstrating its potential to replace the high-cost Pt-based electrocatalysts for practical applications. Owing to the multiple attracting features, including high catalytic activity, good durability, low cost, and scalable production, the as-developed pH-universal N-HPCNS electrocatalysts presented in this study may open a promising avenue for developing the next-generation cathode electrocatalysts for fuel cells of practical significance.

5. Concluding and Perspectives

In recent years, there has been tremendous progress in the nanomaterial field, and employing NCs with tailored size and surface configurations is now routine. These technologies allow the enhancement of the intrinsic catalytic activity of the materials and their utilisation as electrodes, with a particular impact in the domain of the fuel cells where the scarcity, high cost, and poor long-term stability of Pt and Pt-based catalysts (the most widely used) are the main obstacles for the large-scale commercialisation of these devices.

In fact, the rational design and sophisticated fabrication of catalytic nanomaterials are becoming two of the top priorities in heterogeneous catalysis, with the potential to allow the precise control of the nanostructure of solid catalysts to be used as electrodes in the fuel cells and to deepen the understanding of the catalytic processes. In this way, the concept of morphology-dependent NCs provides a new strategy for finely tuning catalytically active sites.

The results reviewed herein demonstrate that there has been significant progress for both MOR and ORR, and the development of ultra-low but highly efficient Pt or Pt-based materials, as well as alternative Pt-free catalysts on real DMFC devices is a reality. The focus of the discussion was to shed light on the current status of the different

development approaches of the materials and an understanding of how their integration as electrodes of the DMFC affects the durability and stability of the catalyst layer and ultimately the performance of the device. The high density of active sites, the 3D porous structure, favourable for active-site exposure and mass transfer, as well as the synergism of physical morphology and chemical reactivity are the common elements for efficient catalytic performance.

It is clear that progress in the science of catalyst layer design is dependent on excellent electrode structuring, where, ideally, the catalyst is optimally dispersed in the layer and fully utilised, while the support is stable, and the ionomer-to-catalyst ratio is appropriate. This way, creating optimised TPB interfaces without limiting mass or charge transport, minimizing the methanol crossover, and flooding effects. To achieve this goal, proper structuring of the catalyst layer is fundamental. Hence, focus should be put towards rational design and the fundamental understanding of the catalyst layer morphology (experimental and theoretical) coupled with in and ex situ analysis of its performance on real DMFC devices. Thus, the finding of an optimum structure that balances the cost, efficiency, and durability of DMFCs can be achieved.

Author Contributions: Conceptualization, M.H.d.S.; resources, V.B.O. and A.M.F.R.P.; writing—original draft preparation, M.H.d.S. and C.S.M.; writing—review and editing, M.H.d.S., C.S.M., V.B.O. and A.M.F.R.P.; supervision, V.B.O.; funding acquisition, V.B.O. All authors have read and agreed to the published version of the manuscript.

Funding: This work was financially supported by: Project PTDC/NewPortCell-POCI-01-0145-FEDER-032116—funded by FEDER funds through COM-PETE2020-Programa Operacional Competitividade e Internacionalização (POCI) and by national funds (PIDDAC) through FCT/MCTES. This work was financially supported by LA/P/0045/2020 (ALiCE), UIDB/00532/2020 and UIDP/00532/2020 (CEFT), funded by national funds through FCT/MCTES (PIDDAC).

Conflicts of Interest: The authors declare no conflict of interest. The funders had no role in the design of the study; in the collection, analyses, or interpretation of data; in the writing of the manuscript, or in the decision to publish the results.

References

1. Feng, Y.; Liu, H.; Yang, J. A selective electrocatalyst–based direct methanol fuel cell operated at high concentrations of methanol. *Sci. Adv.* **2017**, *3*, e1700580. [CrossRef]
2. Dias, V.; Pochet, M.; Contino, F.; Jeanmart, H. Energy and Economic Costs of Chemical Storage. *Front. Mech. Eng.* **2020**, *6*, 21. [CrossRef]
3. Zhao, X.; Yin, M.; Ma, L.; Liang, L.; Liu, C.; Liao, J.; Liu, T.; Xing, W. Recent advances in catalysts for direct methanol fuel cells. *Energy Environ. Sci.* **2011**, *4*, 2736–2753. [CrossRef]
4. Falcão, D.S.; Pereira, J.P.; Rangel, C.M.; Pinto, A.M.F.R. Development and performance analysis of a metallic passive micro-direct methanol fuel cell for portable applications. *Int. J. Hydrogen Energy* **2015**, *40*, 5408–5415. [CrossRef]
5. Munjewar, S.S.; Thombre, S.B.; Mallick, R.K. Approaches to overcome the barrier issues of passive direct methanol fuel cell—Review. *Renew. Sustain. Energy Rev.* **2017**, *67*, 1087–1104. [CrossRef]
6. Braz, B.A.; Moreira, C.S.; Oliveira, V.B.; Pinto, A.M.F.R. Effect of the current collector design on the performance of a passive direct methanol fuel cell. *Electrochim. Acta* **2019**, *300*, 306–315. [CrossRef]
7. Siwal, S.S.; Thakur, S.; Zhang, Q.B.; Thakur, V.K. Electrocatalysts for electrooxidation of direct alcohol fuel cell: Chemistry and applications. *Mater. Today Chem.* **2019**, *14*, 100182. [CrossRef]
8. Mo, J.; Kang, Z.; Retterer, S.T.; Cullen, D.A.; Toops, T.J.; Green, J.B., Jr.; Mench, M.M.; Zhang, F.-Y. Discovery of true electrochemical reactions for ultrahigh catalyst mass activity in water splitting. *Sci. Adv.* **2016**, *2*, e1600690. [CrossRef]
9. Xu, Y.; Zhang, B. Recent advances in porous Pt-based nanostructures: Synthesis and electrochemical applications. *Chem. Soc. Rev.* **2014**, *43*, 2439–2450. [CrossRef]
10. Wang, Y.J.; Fang, B.; Li, H.; Bi, X.T.; Wang, H. Progress in modified carbon support materials for Pt and Pt-alloy cathode catalysts in polymer electrolyte membrane fuel cells. *Prog. Mater. Sci.* **2016**, *82*, 445–498. [CrossRef]
11. Kamarudin, S.K.; Achmad, F.; Daud, W.R.W. Overview on the application of direct methanol fuel cell (DMFC) for portable electronic devices. *Int. J. Hydrogen Energy* **2009**, *34*, 6902–6916. [CrossRef]
12. Xia, Z.; Zhang, X.; Sun, H.; Wang, S.; Sun, G. Recent advances in multi-scale design and construction of materials for direct methanol fuel cells. *Nano Energy* **2019**, *65*, 104048. [CrossRef]

13. Hogarth, M.P.; Hards, G.A. Direct Methanol Fuel Cells: Technological Advances and Further Requirements. *Platinum Metals Rev.* **1996**, *40*, 150–159.
14. Ramli, Z.A.C.; Kamarudin, S.K. Platinum-Based Catalysts on Various Carbon Supports and Conducting Polymers for Direct Methanol Fuel Cell Applications: A Review. *Nanoscale Res. Lett.* **2018**, *13*, 1–25. [CrossRef] [PubMed]
15. Basri, S.; Kamarudin, S.K.; Daud, W.R.W.; Yaakob, Z.; Kadhum, A.A.H. Novel Anode Catalyst for Direct Methanol Fuel Cells. *Sci. World J.* **2014**, *2014*, 547604. [CrossRef] [PubMed]
16. Salgado, J.R.C.; Alcaide, F.; Álvarez, G.; Calvillo, L.; Lázaro, M.J.; Pastor, E. Pt–Ru electrocatalysts supported on ordered mesoporous carbon for direct methanol fuel cell. *J. Power Sources* **2010**, *195*, 4022–4029. [CrossRef]
17. Basri, S.; Kamarudin, S.K.; Daud, W.R.W.; Yaakub, Z. Nanocatalyst for direct methanol fuel cell (DMFC). *Int. J. Hydrogen Energy* **2010**, *35*, 7957–7970. [CrossRef]
18. Ogungbemi, E.; Ijaodola, O.; Khatib, F.N.; Wilberforce, T.; El Hassan, Z.; Thompson, J.; Ramadan, M.; Olabi, A.G. Fuel cell membranes—Pros and cons. *Energy* **2019**, *172*, 155–172. [CrossRef]
19. Farooqui, U.R.; Ahmad, A.L.; Hamid, N.A. Graphene oxide: A promising membrane material for fuel cells. *Renew. Sustain. Energy Rev.* **2018**, *82*, 714–733. [CrossRef]
20. Fadzillah, D.M.; Kamarudin, S.K.; Zainoodin, M.A.; Masdar, M.S. Critical challenges in the system development of direct alcohol fuel cells as portable power supplies: An overview. *Int. J. Hydrogen Energy* **2019**, *44*, 3031–3054. [CrossRef]
21. Munjewar, S.S.; Thombre, S.B.; Mallick, R.K. A comprehensive review on recent material development of passive direct methanol fuel cell. *Ionics* **2017**, *23*, 1–18. [CrossRef]
22. Chen, X.; Li, T.; Shen, J.; Hu, Z. From structures, packaging to application: A system-level review for micro direct methanol fuel cell. *Renew. Sustain. Energy Rev.* **2017**, *80*, 669–678. [CrossRef]
23. Shrivastava, N.K.; Thombre, S.B.; Chadge, R.B. Liquid feed passive direct methanol fuel cell: Challenges and recent advances. *Ionics* **2016**, *22*, 1–23. [CrossRef]
24. Velisala, V.; Srinivasulu, G.N.; Reddy, B.S.; Rao, K.V.K. Review on challenges of direct liquid fuel cells for portable application. *World J. Eng.* **2015**, *12*, 591–605. [CrossRef]
25. Falcão, D.S.; Oliveira, V.B.; Rangel, C.M.; Pinto, A.M.F.R. Review on micro-direct methanol fuel cells. *Renew. Sustain. Energy Rev.* **2014**, *34*, 58–70. [CrossRef]
26. Kumar, P.; Dutta, K.; Das, S.; Kundu, P.P. An overview of unsolved deficiencies of direct methanol fuel cell technology: Factors and parameters affecting its widespread use. *Int. J. Energy Res.* **2014**, *38*, 1367–1390. [CrossRef]
27. Oliveira, V.B.; Falcão, D.S.; Rangel, C.M.; Pinto, A.M.F.R. Water management in a passive direct methanol fuel cell. *Int. J. Energy Res.* **2013**, *37*, 991–1001. [CrossRef]
28. Shao, M.; Chang, Q.; Dodelet, J.P.; Chenitz, R. Recent Advances in Electrocatalysts for Oxygen Reduction Reaction. *Chem. Rev.* **2016**, *116*, 3594–3657. [CrossRef]
29. Schoekel, A.; Melke, J.; Bruns, M.; Wippermann, K.; Kuppler, F.; Roth, C. Quantitative study of ruthenium cross-over in direct methanol fuel cells during early operation hours. *J. Power Sources* **2016**, *301*, 210–218. [CrossRef]
30. Meier, J.C.; Galeano, C.; Katsounaros, I.; Witte, J.; Bongard, H.J.; Topalov, A.A.; Baldizzone, C.; Mezzavilla, S.; Schüth, F.; Mayrhofer, K.J.J. Design criteria for stable Pt/C fuel cell catalysts. *Beilstein J. Nanotechnol.* **2014**, *5*, 44–67. [CrossRef]
31. Oh, H.S.; Lim, K.H.; Roh, B.; Hwang, I.; Kim, H. Corrosion resistance and sintering effect of carbon supports in polymer electrolyte membrane fuel cells. *Electrochim. Acta* **2009**, *54*, 6515–6521. [CrossRef]
32. Cherevko, S. Stability and dissolution of electrocatalysts: Building the bridge between model and 'real world' systems. *Curr. Opin. Electrochem.* **2018**, *8*, 118–125. [CrossRef]
33. Du, L.; Shao, Y.; Sun, J.; Yin, G.; Liu, J.; Wang, Y. Advanced catalyst supports for PEM fuel cell cathodes. *Nano Energy* **2016**, *29*, 314–322. [CrossRef]
34. Samad, S.; Loh, K.S.; Wong, W.Y.; Lee, T.K.; Sunarso, J.; Chong, S.T.; Daud, W.R.W. Carbon and non-carbon support materials for platinum-based catalysts in fuel cells. *Int. J. Hydrogen Energy* **2018**, *43*, 7823–7854. [CrossRef]
35. Mohanta, P.; Regnet, F.; Jörissen, L. Graphitized Carbon: A Promising Stable Cathode Catalyst Support Material for Long Term PEMFC Applications. *Materials* **2018**, *11*, 907. [CrossRef]
36. Cuesta, A. Electrooxidation of C1 organic molecules on Pt electrodes. *Curr. Opin. Electrochem.* **2017**, *4*, 32–38. [CrossRef]
37. Kübler, M.; Jurzinsky, T.; Ziegenbalg, D.; Cremers, C. Methanol oxidation reaction on core-shell structured Ruthenium-Palladium nanoparticles: Relationship between structure and electrochemical behavior. *J. Power Sources* **2018**, *375*, 320–334. [CrossRef]
38. Tiwari, J.N.; Tiwari, R.N.; Singh, G.; Kim, K.S. Recent progress in the development of anode and cathode catalysts for direct methanol fuel cells. *Nano Energy* **2013**, *2*, 553–578. [CrossRef]
39. Liu, H.; Song, C.; Zhang, L.; Zhang, J.; Wang, H.; Wilkinson, D.P. A review of anode catalysis in the direct methanol fuel cell. *J. Power Sources* **2006**, *155*, 95–110. [CrossRef]
40. Falcão, D.S.; Silva, R.A.; Rangel, C.M.; Pinto, A.M.F.R. Performance of an Active Micro Direct Methanol Fuel Cell Using Reduced Catalyst Loading MEAs. *Energies* **2017**, *10*, 1683. [CrossRef]
41. Olu, P.Y.; Ohnishi, T.; Mochizuki, D.; Sugimoto, W. Uncovering the real active sites of ruthenium oxide for the carbon monoxide electro-oxidation reaction on platinum: The catalyst acts as a co-catalyst. *J. Electroanal. Chem.* **2018**, *810*, 109–118. [CrossRef]
42. Sahin, O.; Kivrak, H. A comparative study of electrochemical methods on Pt–Ru DMFC anode catalysts: The effect of Ru addition. *Int. J. Hydrogen Energy* **2013**, *38*, 901–909. [CrossRef]

43. Bresciani, F.; Rabissi, C.; Zago, M.; Gazdzicki, P.; Schulze, M.; Guétaz, L.; Escribano, S.; Bonde, J.L.; Marchesi, R.; Casalegno, A. A combined in-situ and post-mortem investigation on local permanent degradation in a direct methanol fuel cell. *J. Power Sources* **2016**, *306*, 49–61. [CrossRef]
44. Mehmood, A.; Scibioh, M.A.; Prabhuram, J.; An, M.G.; Ha, H.Y. A review on durability issues and restoration techniques in long-term operations of direct methanol fuel cells. *J. Power Sources* **2015**, *297*, 224–241. [CrossRef]
45. Bresciani, F.; Rabissi, C.; Casalegno, A.; Zago, M.; Marchesi, R. Experimental investigation on DMFC temporary degradation. *Int. J. Hydrogen Energy* **2014**, *39*, 21647–21656. [CrossRef]
46. Piela, P.; Eickes, C.; Brosha, E.; Garzon, F.; Zelenay, P. Ruthenium Crossover in Direct Methanol Fuel Cell with Pt–Ru Black Anode. *J. Electrochem. Soc.* **2004**, *151*, 2053–2059. [CrossRef]
47. Antolini, E.; Salgado, J.R.C.; Gonzalez, E.R. Carbon supported Pt75M25 (M = Co, Ni) alloys as anode and cathode electrocatalysts for direct methanol fuel cells. *J. Electroanal. Chem.* **2005**, *580*, 145–154. [CrossRef]
48. Xie, J.; Zhang, Q.; Gu, L.; Xu, S.; Wang, P.; Liu, J.; Ding, Y.; Yao, Y.F.; Nan, C.; Zhao, M.; et al. Ruthenium-platinum core-shell nanocatalysts with substantially enhanced activity and durability towards methanol oxidation. *Nano Energy* **2016**, *21*, 247–257. [CrossRef]
49. Singh, R.N.; Awasthi, R.; Sharma, C.S. Review: An Overview of Recent Development of Platinum-Based Cathode Materials for Direct Methanol Fuel Cells. *Int. J. Electrochem. Sci.* **2014**, *9*, 5607–5639.
50. Gómez-Marín, A.M.; Rizo, R.; Feliu, J.M. Some reflections on the understanding of the oxygen reduction reaction at Pt(111). *Beilstein J. Nanotechnol.* **2013**, *4*, 956–967. [CrossRef]
51. Holton, O.T.; Stevenson, J.W. The Role of Platinum in Proton Exchange Membrane Fuel Cells Evaluation of platinum's unique properties for use in both the anode and cathode of a proton exchange membrane fuel cell. *Platin. Met. Rev* **2013**, *57*, 259–271. [CrossRef]
52. Chen, C.; Fuller, T.F. Modeling of H_2O_2 formation in PEMFCs. *Electrochim. Acta* **2009**, *54*, 3984–3995. [CrossRef]
53. Borup, R.; Meyers, J.; Pivovar, B.; Kim, Y.S.; Mukundan, R.; Garland, N.; Myers, D.; Wilson, M.; Garzon, F.; Wood, D.; et al. Scientific aspects of polymer electrolyte fuel cell durability and degradation. *Chem. Rev.* **2007**, *107*, 3904–3951. [CrossRef]
54. Zainoodin, A.M.; Kamarudin, S.K.; Daud, W.R.W. Electrode in direct methanol fuel cells. *Int. J. Hydrogen Energy* **2010**, *35*, 4606–4621. [CrossRef]
55. Zhao, T.S.; Xu, C.; Chen, R.; Yang, W.W. Mass transport phenomena in direct methanol fuel cells. *Prog. Energy Combust. Sci.* **2009**, *35*, 275–292. [CrossRef]
56. Knights, S.D.; Colbow, K.M.; St-Pierre, J.; Wilkinson, D.P. Aging mechanisms and lifetime of PEFC and DMFC. *J. Power Sources* **2004**, *127*, 127–134. [CrossRef]
57. Huang, Y.; Babu, D.D.; Wu, M.; Wang, Y. Synergistic Supports Beyond Carbon Black for Polymer Electrolyte Fuel Cell Anodes. *ChemCatChem* **2018**, *10*, 4497–4508. [CrossRef]
58. Moura, A.; Fajín, J.; Mandado, M.; Cordeiro, M. Ruthenium–Platinum Catalysts and Direct Methanol Fuel Cells (DMFC): A Review of Theoretical and Experimental Breakthroughs. *Catalysts* **2017**, *7*, 47. [CrossRef]
59. Lv, H.; Li, D.; Strmcnik, D.; Paulikas, A.P.; Markovic, N.M.; Stamenkovic, V.R. Recent advances in the design of tailored nanomaterials for efficient oxygen reduction reaction. *Nano Energy* **2016**, *29*, 149–165. [CrossRef]
60. Holby, E.F.; Zelenay, P. Linking structure to function: The search for active sites in non-platinum group metal oxygen reduction reaction catalysts. *Nano Energy* **2016**, *29*, 54–64. [CrossRef]
61. Eslamibidgoli, M.J.; Huang, J.; Kadyk, T.; Malek, A.; Eikerling, M. How theory and simulation can drive fuel cell electrocatalysis. *Nano Energy* **2016**, *29*, 334–361. [CrossRef]
62. Spendelow, J.S.; Wieckowski, A. Electrocatalysis of oxygen reduction and small alcohol oxidation in alkaline media. *Phys. Chem. Chem. Phys.* **2007**, *9*, 2654–2675. [CrossRef] [PubMed]
63. Kakati, N.; Maiti, J.; Lee, S.H.; Jee, S.H.; Viswanathan, B.; Yoon, Y.S. Anode catalysts for direct methanol fuel cells in acidic media: Do we have any alternative for Pt or Pt–Ru? *Chem. Rev.* **2014**, *114*, 12397–12429. [CrossRef] [PubMed]
64. Gong, L.; Yang, Z.; Li, K.; Xing, W.; Liu, C.; Ge, J. Recent development of methanol electrooxidation catalysts for direct methanol fuel cell. *J. Energy Chem.* **2018**, *27*, 1618–1628. [CrossRef]
65. Yang, L.; Ge, J.; Liu, C.; Wang, G.; Xing, W. Approaches to improve the performance of anode methanol oxidation reaction—a short review. *Curr. Opin. Electrochem.* **2017**, *4*, 83–88. [CrossRef]
66. Tolmachev, Y.V.; Petrii, O.A. Pt–Ru electrocatalysts for fuel cells: Developments in the last decade. *J. Solid State Electrochem.* **2017**, *21*, 613–639. [CrossRef]
67. Mansor, M.; Timmiati, S.N.; Lim, K.L.; Wong, W.Y.; Kamarudin, S.K.; Kamarudin, N.H.N. Recent progress of anode catalysts and their support materials for methanol electrooxidation reaction. *Int. J. Hydrogen Energy* **2019**, *44*, 14744–14769. [CrossRef]
68. Shang, C.; Wang, E. Recent progress in Pt and Pd-based hybrid nanocatalysts for methanol electrooxidation. *Phys. Chem. Chem. Phys.* **2019**, *21*, 21185–21199. [CrossRef]
69. Tian, H.; Yu, Y.; Wang, Q.; Li, J.; Rao, P.; Li, R.; Du, Y.; Jia, C.; Luo, J.; Deng, P.; et al. Recent advances in two-dimensional Pt based electrocatalysts for methanol oxidation reaction. *Int. J. Hydrogen Energy* **2021**, *46*, 31202–31215. [CrossRef]
70. Ciapina, E.G.; Santos, S.F.; Gonzalez, E.R. Electrochemical CO stripping on nanosized Pt surfaces in acid media: A review on the issue of peak multiplicity. *J. Electroanal. Chem.* **2018**, *815*, 47–60. [CrossRef]

71. Lai, S.C.S.; Lebedeva, N.P.; Housmans, T.H.M.; Koper, M.T.M. Mechanisms of carbon monoxide and methanol oxidation at single-crystal electrodes. *Top. Catal.* **2007**, *46*, 320–333. [CrossRef]
72. Kamyabi, M.; Martínez-Hincapié, R.; Feliu, J.; Herrero, E. Effects of the Interfacial Structure on the Methanol Oxidation on Platinum Single Crystal Electrodes. *Surfaces* **2019**, *2*, 177–192. [CrossRef]
73. Iwasita, T. Electrocatalysis of methanol oxidation. *Electrochim. Acta* **2002**, *47*, 3663–3674. [CrossRef]
74. Tian, N.; Zhou, Z.Y.; Sun, S.G.; Ding, Y.; Zhong, L.W. Synthesis of tetrahexahedral platinum nanocrystals with high-index facets and high electro-oxidation activity. *Science* **2007**, *316*, 732–735. [CrossRef]
75. Sheng, T.; Xu, Y.F.; Jiang, Y.X.; Huang, L.; Tian, N.; Zhou, Z.Y.; Broadwell, I.; Sun, S.G. Structure Design and Performance Tuning of Nanomaterials for Electrochemical Energy Conversion and Storage. *Acc. Chem. Res.* **2016**, *49*, 2569–2577. [CrossRef] [PubMed]
76. Bayati, M.; Abad, J.M.; Nichols, R.J.; Schiffrin, D.J. Substrate structural effects on the synthesis and electrochemical properties of platinum nanoparticles on highly oriented pyrolytic graphite. *J. Phys. Chem. C* **2010**, *114*, 18439–18448. [CrossRef]
77. Andreaus, B.; Maillard, F.; Kocylo, J.; Savinova, E.R.; Eikerling, M. Kinetic modeling of COad monolayer oxidation on carbon-supported platinum nanoparticles. *J. Phys. Chem. B* **2006**, *110*, 21028–21040. [CrossRef]
78. Mukerjee, S.; McBreen, J. Effect of particle size on the electrocatalysis by carbon-supported Pt electrocatalysts: An in situ XAS investigation. *J. Electroanal. Chem.* **1998**, *448*, 163–171. [CrossRef]
79. Pan, D.; Li, X.; Zhang, A. Platinum assisted by carbon quantum dots for methanol electro-oxidation. *Appl. Surf. Sci.* **2018**, *427*, 715–723. [CrossRef]
80. Sha, R.; Solomon Jones, S.; Badhulika, S. Controlled synthesis of platinum nanoflowers supported on carbon quantum dots as a highly effective catalyst for methanol electro-oxidation. *Surf. Coat. Technol.* **2019**, *360*, 400–408. [CrossRef]
81. Liang, L.; Xiao, M.; Zhu, J.; Ge, J.; Liu, C.; Xing, W. Low-temperature synthesis of nitrogen doped carbon nanotubes as promising catalyst support for methanol oxidation. *J. Energy Chem.* **2019**, *28*, 118–122. [CrossRef]
82. Huang, M.; Zhang, J.; Wu, C.; Guan, L. Networks of connected Pt nanoparticles supported on carbon nanotubes as superior catalysts for methanol electrooxidation. *J. Power Sources* **2017**, *342*, 273–278. [CrossRef]
83. Zhu, Z.; Bukowski, B.; Deskins, N.A.; Zhou, H.S. Bamboo shaped carbon nanotube supported platinum electrocatalyst synthesized by high power ultrasonic-assisted impregnation method for methanol electrooxidation and related density functional theory calculations. *Int. J. Hydrogen Energy* **2015**, *40*, 2216–2224. [CrossRef]
84. Zhang, X.; Yuan, W.; Duan, J.; Zhang, Y.; Liu, X. Graphene nanosheets modified by nitrogen-doped carbon layer to support Pt nanoparticles for direct methanol fuel cell. *Microelectron. Eng.* **2015**, *141*, 234–237. [CrossRef]
85. Radhakrishnan, T.; Sandhyarani, N. Three dimensional assembly of electrocatalytic platinum nanostructures on reduced graphene oxide—An electrochemical approach for high performance catalyst for methanol oxidation. *Int. J. Hydrogen Energy* **2017**, *42*, 7014–7022. [CrossRef]
86. Yu, M.; Wu, X.; Zhang, J.; Meng, Y.; Ma, Y.; Liu, J.; Li, S. Platinum nanoparticles-loaded holey reduced graphene oxide framework as freestanding counter electrodes of dye sensitized solar cells and methanol oxidation catalysts. *Electrochim. Acta* **2017**, *258*, 485–494. [CrossRef]
87. Li, X.; Lv, Y.; Pan, D. Pt catalysts supported on lignin-based carbon dots for methanol electro-oxidation. *Colloids Surf. A Physicochem. Eng. Asp.* **2019**, *569*, 110–118. [CrossRef]
88. Mu, X.; Xu, Z.; Ma, Y.; Xie, Y.; Mi, H.; Ma, J. Graphene-carbon nanofiber hybrid supported Pt nanoparticles with enhanced catalytic performance for methanol oxidation and oxygen reduction. *Electrochim. Acta* **2017**, *253*, 171–177. [CrossRef]
89. Yang, Z.; Luo, F. Pt nanoparticles deposited on dihydroxy-polybenzimidazole wrapped carbon nanotubes shows a remarkable durability in methanol electro-oxidation. *Int. J. Hydrogen Energy* **2017**, *42*, 507–514. [CrossRef]
90. Hong, T.Z.; Xue, Q.; Yang, Z.Y.; Dong, Y.P. Great-enhanced performance of Pt nanoparticles by the unique carbon quantum dot/reduced graphene oxide hybrid supports towards methanol electrochemical oxidation. *J. Power Sources* **2016**, *303*, 109–117. [CrossRef]
91. An, G.H.; Jo, H.G.; Ahn, H.J. Surface effect of platinum catalyst-decorated mesoporous carbon support using the dissolution of zinc oxide for methanol oxidation. *Appl. Surf. Sci.* **2019**, *473*, 511–515. [CrossRef]
92. Zhang, C.; Wang, G.; Zhang, X.; Zhang, Y. High-loading Pt nanoparticles on mesoporous carbon with large mesopores for highly active methanol electro-oxidation. *J. Solid State Electrochem.* **2016**, *20*, 1705–1712. [CrossRef]
93. Kasturi, P.R.; Selvan, R.K.; Lee, Y.S. Pt decorated: Artocarpus heterophyllus seed derived carbon as an anode catalyst for DMFC application. *RSC Adv.* **2016**, *6*, 62680–62694. [CrossRef]
94. Yang, Z.; Hafez, I.H.; Berber, M.R.; Nakashima, N. An Enhanced Anode based on Polymer-Coated Carbon Black for use as a Direct Methanol Fuel Cell Electrocatalyst. *ChemCatChem* **2015**, *7*, 808–813. [CrossRef]
95. Eris, S.; Daşdelen, Z.; Yıldız, Y.; Sen, F. Nanostructured Polyaniline-rGO decorated platinum catalyst with enhanced activity and durability for methanol oxidation. *Int. J. Hydrogen Energy* **2018**, *43*, 1337–1343. [CrossRef]
96. Li, X.; Wei, J.; Chai, Y.; Zhang, S.; Zhou, M. Different polyaniline/carbon nanotube composites as Pt catalyst supports for methanol electro-oxidation. *J. Mater. Sci.* **2015**, *50*, 1159–1168. [CrossRef]
97. Daşdelen, Z.; Yıldız, Y.; Eriş, S.; Şen, F. Enhanced electrocatalytic activity and durability of Pt nanoparticles decorated on GO-PVP hybride material for methanol oxidation reaction. *Appl. Catal. B Environ.* **2017**, *219*, 511–516. [CrossRef]
98. Sun, J.; Ling, Y.; Zhang, Q.; Yu, X.; Yang, Z. Simultaneous enhancements in stability and CO tolerance of Pt electrocatalyst by double poly(vinyl pyrrolidone) coatings. *RSC Adv.* **2017**, *7*, 29839–29843. [CrossRef]

99. Eris, S.; Daşdelen, Z.; Sen, F. Enhanced electrocatalytic activity and stability of monodisperse Pt nanocomposites for direct methanol fuel cells. *J. Colloid Interface Sci.* **2018**, *513*, 767–773. [CrossRef]
100. Eris, S.; Daşdelen, Z.; Sen, F. Investigation of electrocatalytic activity and stability of Pt@f-VC catalyst prepared by in-situ synthesis for Methanol electrooxidation. *Int. J. Hydrogen Energy* **2018**, *43*, 385–390. [CrossRef]
101. Mondal, S.; Malik, S. Easy synthesis approach of Pt-nanoparticles on polyaniline surface: An efficient electro-catalyst for methanol oxidation reaction. *J. Power Sources* **2016**, *328*, 271–279. [CrossRef]
102. Sha, R.; Badhulika, S. Facile synthesis of three-dimensional platinum nanoflowers on reduced graphene oxide—Tin oxide composite: An ultra-high performance catalyst for methanol electro-oxidation. *J. Electroanal. Chem.* **2018**, *820*, 9–17. [CrossRef]
103. Yu, F.; Xie, Y.; Tang, H.; Yang, N.; Meng, X.; Wang, X.; Tian, X.L.; Yang, X. Platinum decorated hierarchical porous structures composed of ultrathin titanium nitride nanoflakes for efficient methanol oxidation reaction. *Electrochim. Acta* **2018**, *264*, 216–224. [CrossRef]
104. Zhang, B.; Pan, Z.; Yu, K.; Feng, G.; Xiao, J.; Wu, S.; Li, J.; Chen, C.; Lin, Y.; Hu, G.; et al. Titanium vanadium nitride supported Pt nanoparticles as high-performance catalysts for methanol oxidation reaction. *J. Solid State Electrochem.* **2017**, *21*, 3065–3070. [CrossRef]
105. Liu, G.; Pan, Z.; Zhang, B.; Xiao, J.; Xia, G.; Zhao, Q.; Shi, S.; Hu, G.; Xiao, C.; Wei, Z.; et al. A novel TiN coated CNTs nanocomposite CNTs@TiN supported Pt electrocatalyst with enhanced catalytic activity and durability for methanol oxidation reaction. *Int. J. Hydrogen Energy* **2017**, *42*, 12467–12476. [CrossRef]
106. Hao, Y.; Wang, X.; Zheng, Y.; Shen, J.; Yuan, J.; Wang, A.J.; Niu, L.; Huang, S. Uniform Pt Nanoparticles Incorporated into Reduced Graphene Oxides with MoO3 as Advanced Anode Catalysts for Methanol Electro-oxidation. *Electrochim. Acta* **2016**, *198*, 127–134. [CrossRef]
107. Zhan, G.; Fu, Z.; Sun, D.; Pan, Z.; Xiao, C.; Wu, S.; Chen, C.; Hu, G.; Wei, Z. Platinum nanoparticles decorated robust binary transition metal nitride–carbon nanotubes hybrid as an efficient electrocatalyst for the methanol oxidation reaction. *J. Power Sources* **2016**, *326*, 84–92. [CrossRef]
108. Yang, F.; Ma, L.; Gan, M.; Zhang, J.; Yan, J.; Huang, H.; Yu, L.; Li, Y.; Ge, C.; Hu, H. Polyaniline-functionalized TiO_2-C supported Pt catalyst for methanol electro-oxidation. *Synth. Met.* **2015**, *205*, 23–31. [CrossRef]
109. Zhao, Y.; Wang, Y.; Zang, J.; Lu, J.; Xu, X. A novel support of nano titania modified graphitized nanodiamond for Pt electrocatalyst in direct methanol fuel cell. *Int. J. Hydrogen Energy* **2015**, *40*, 4540–4547. [CrossRef]
110. Vu, T.H.T.; Tran, T.T.T.; Le, H.N.T.; Tran, L.T.; Nguyen, P.H.T.; Essayem, N. Pt-AlOOH-SiO_2/graphene hybrid nanomaterial with very high electrocatalytic performance for methanol oxidation. *J. Power Sources* **2015**, *276*, 340–346. [CrossRef]
111. Vu, T.H.T.; Tran, T.T.T.; Le, H.N.T.; Tran, L.T.; Nguyen, P.H.T.; Nguyen, H.T.; Bui, N.Q. Solvothermal synthesis of Pt-SiO_2/graphene nanocomposites as efficient electrocatalyst for methanol oxidation. *Electrochim. Acta* **2015**, *161*, 335–342. [CrossRef]
112. Li, K.; Xiao, M.; Jin, Z.; Zhu, J.; Ge, J.; Liu, C.; Xing, W. Advanced architecture carbon with in-situ embedded ultrafine titanium dioxide as outstanding support material for platinum catalysts towards methanol electrooxidation. *Electrochim. Acta* **2017**, *235*, 508–518. [CrossRef]
113. Sui, X.L.; Wang, Z.B.; Xia, Y.F.; Yang, M.; Zhao, L.; Gu, D.M. A rapid synthesis of TiO_2 nanotubes in an ethylene glycol system by anodization as a Pt-based catalyst support for methanol electrooxidation. *RSC Adv.* **2015**, *5*, 35518–35523. [CrossRef]
114. Medina Ramirez, A.; Ruiz Camacho, B.; Villicaña Aguilera, M.; Galindo Esquivel, I.R.; Ramírez-Minguela, J.J. Effect of different zeolite as Pt supports for methanol oxidation reaction. *Appl. Surf. Sci.* **2018**, *456*, 204–214. [CrossRef]
115. Medina Ramírez, A.; Villicaña Aguilera, M.; López-Badillo, C.M.; Ruiz-Camacho, B. Synthesis of FAU zeolite-C composite as catalyst support for methanol electro-oxidation. *Int. J. Hydrogen Energy* **2017**, *42*, 30291–30300. [CrossRef]
116. Daas, B.M.; Ghosh, S. Electro-oxidation of Methanol and Ethanol Catalyzed by Pt/ZSM-5/C. *Electroanalysis* **2017**, *29*, 2516–2525. [CrossRef]
117. Yao, J.; Yao, Y. Investigation of zeolite supported platinum electrocatalyst for electrochemical oxidation of small organic species. *Int. J. Hydrogen Energy* **2016**, *41*, 14747–14757. [CrossRef]
118. Daas, B.M.; Ghosh, S. Fuel cell applications of chemically synthesized zeolite modified electrode (ZME) as catalyst for alcohol electro-oxidation—A review. *J. Electroanal. Chem.* **2016**, *783*, 308–315. [CrossRef]
119. Ekrami-Kakhki, M.S.; Naeimi, A.; Donyagard, F. Pt nanoparticles supported on a novel electrospun polyvinyl alcohol-CuO–Co 3 O 4 /chitosan based on Sesbania sesban plant as an electrocatalyst for direct methanol fuel cells. *Int. J. Hydrogen Energy* **2019**, *44*, 1671–1685. [CrossRef]
120. Li, G.; Yao, S.; Zhu, J.; Liu, C.; Xing, W. The enhancement effect of nitrogen, fluorine-codoped titanium dioxide on the carbon supported platinum nano-catalyst for methanol electrooxidation reaction. *J. Power Sources* **2015**, *278*, 9–17. [CrossRef]
121. Antolini, E. Photo-assisted methanol oxidation on Pt–TiO_2 catalysts for direct methanol fuel cells: A short review. *Appl. Catal. B Environ.* **2018**, *237*, 491–503. [CrossRef]
122. Antolini, E. Evaluation of the Optimum Composition of Low-Temperature Fuel Cell Electrocatalysts for Methanol Oxidation by Combinatorial Screening. *ACS Comb. Sci.* **2017**, *19*, 47–54. [CrossRef] [PubMed]
123. Torbina, V.V.; Vodyankin, A.A.; Ten, S.; Mamontov, G.V.; Salaev, M.A.; Sobolev, V.I.; Vodyankina, O.V. Ag-Based Catalysts in Heterogeneous Selective Oxidation of Alcohols: A Review. *Catalysts* **2018**, *8*, 447. [CrossRef]

124. Calderón, J.C.; García, G.; Calvillo, L.; Rodríguez, J.L.; Lázaro, M.J.; Pastor, E. Electrochemical oxidation of CO and methanol on Pt–Ru catalysts supported on carbon nanofibers: The influence of synthesis method. *Appl. Catal. B Environ.* **2015**, *165*, 676–686. [CrossRef]
125. Calderón, J.C.; García, G.; Querejeta, A.; Alcaide, F.; Calvillo, L.; Lázaro, M.J.; Rodríguez, J.L.; Pastor, E. Carbon monoxide and methanol oxidations on carbon nanofibers supported Pt–Ru electrodes at different temperatures. *Electrochim. Acta* **2015**, *186*, 359–368. [CrossRef]
126. Trovarelli, A. Catalytic properties of ceria and CeO_2-Containing materials. *Catal. Rev. Sci. Eng.* **1996**, *38*, 439–520. [CrossRef]
127. McFarland, E.W.; Metiu, H. Catalysis by doped oxides. *Chem. Rev.* **2013**, *113*, 4391–4427. [CrossRef]
128. Feng, C.; Takeuchi, T.; Abdelkareem, M.A.; Tsujiguchi, T.; Nakagawa, N. Carbon-CeO_2 composite nanofibers as a promising support for a PtRu anode catalyst in a direct methanol fuel cell. *J. Power Sources* **2013**, *242*, 57–64. [CrossRef]
129. Kunitomo, H.; Ishitobi, H.; Nakagawa, N. Optimized CeO_2 content of the carbon nanofiber support of PtRu catalyst for direct methanol fuel cells. *J. Power Sources* **2015**, *297*, 400–407. [CrossRef]
130. Tsukagoshi, Y.; Ishitobi, H.; Nakagawa, N. Improved performance of direct methanol fuel cells with the porous catalyst layer using highly-active nanofiber catalyst. *Carbon Resour. Convers.* **2018**, *1*, 61–72. [CrossRef]
131. Abdullah, N.; Kamarudin, S.K.; Shyuan, L.K.; Karim, N.A. Fabrication and Characterization of New Composite TiO_2 Carbon Nanofiber Anodic Catalyst Support for Direct Methanol Fuel Cell via Electrospinning Method. *Nanoscale Res. Lett.* **2017**, *12*, 1–11. [CrossRef] [PubMed]
132. Zheng, Y.; Chen, H.; Dai, Y.; Zhang, N.; Zhao, W.; Wang, S.; Lou, Y.; Li, Y.; Sun, Y. Preparation and characterization of Pt/TiO_2 nanofibers catalysts for methanol electro-oxidation. *Electrochim. Acta* **2015**, *178*, 74–79. [CrossRef]
133. Ito, Y.; Takeuchi, T.; Tsujiguchi, T.; Abdelkareem, M.A.; Nakagawa, N. Ultrahigh methanol electro-oxidation activity of PtRu nanoparticles prepared on TiO_2-embedded carbon nanofiber support. *J. Power Sources* **2013**, *242*, 280–288. [CrossRef]
134. Ercelik, M.; Ozden, A.; Seker, E.; Colpan, C.O. Characterization and performance evaluation of Pt[sbnd]Ru/C[sbnd]TiO_2 anode electrocatalyst for DMFC applications. *Int. J. Hydrogen Energy* **2017**, *42*, 21518–21529. [CrossRef]
135. Yang, Z.; Shi, Y.; Wang, X.; Zhang, G.; Cui, P. Boron as a superior activator for Pt anode catalyst in direct alcohol fuel cell. *J. Power Sources* **2019**, *431*, 125–134. [CrossRef]
136. Patel, P.P.; Datta, M.K.; Jampani, P.H.; Hong, D.; Poston, J.A.; Manivannan, A.; Kumta, P.N. High performance and durable nanostructured TiN supported Pt50-Ru50 anode catalyst for direct methanol fuel cell (DMFC). *J. Power Sources* **2015**, *293*, 437–446. [CrossRef]
137. Avasarala, B.; Haldar, P. On the stability of TiN-based electrocatalysts for fuel cell applications. *Int. J. Hydrogen Energy* **2011**, *36*, 3965–3974. [CrossRef]
138. Zhong, Y.; Xia, X.; Shi, F.; Zhan, J.; Tu, J.; Fan, H.J. Transition Metal Carbides and Nitrides in Energy Storage and Conversion. *Adv. Sci.* **2016**, *3*, 1500286. [CrossRef]
139. Ham, D.; Lee, J. Transition Metal Carbides and Nitrides as Electrode Materials for Low Temperature Fuel Cells. *Energies* **2009**, *2*, 873–899. [CrossRef]
140. Goel, J.; Basu, S. Effect of support materials on the performance of direct ethanol fuel cell anode catalyst. *Int. J. Hydrogen Energy* **2014**, *39*, 15956–15966. [CrossRef]
141. Bello, M.; Zaidi, S.M.J.; Al-Ahmed, A.; Basu, S.; Park, D.H.; Lakhi, K.S.; Vinu, A. Pt–Ru nanoparticles functionalized mesoporous carbon nitride with tunable pore diameters for DMFC applications. *Microporous Mesoporous Mater.* **2017**, *252*, 50–58. [CrossRef]
142. Corpuz, A.R.; Olson, T.S.; Joghee, P.; Pylypenko, S.; Dameron, A.A.; Dinh, H.N.; O'Neill, K.J.; Hurst, K.E.; Bender, G.; Gennett, T.; et al. Effect of a nitrogen-doped PtRu/carbon anode catalyst on the durability of a direct methanol fuel cell. *J. Power Sources* **2012**, *217*, 142–151. [CrossRef]
143. Corpuz, A.R.; Wood, K.N.; Pylypenko, S.; Dameron, A.A.; Joghee, P.; Olson, T.S.; Bender, G.; Dinh, H.N.; Gennett, T.; Richards, R.M.; et al. Effect of nitrogen post-doping on a commercial platinum-ruthenium/carbon anode catalyst. *J. Power Sources* **2014**, *248*, 296–306. [CrossRef]
144. Ling, Y.; Yang, Z.; Yang, J.; Zhang, Y.; Zhang, Q.; Yu, X.; Cai, W. PtRu nanoparticles embedded in nitrogen doped carbon with highly stable CO tolerance and durability. *Nanotechnology* **2018**, *29*, 055402. [CrossRef]
145. Yang, Z.; Cai, W.; Zhang, Q.; Ling, Y.; Yu, X.; Zhang, Y. Stabilization of PtRu electrocatalyst by nitrogen doped carbon layer derived from carbonization of poly(vinyl pyrrolidone). *Int. J. Hydrogen Energy* **2017**, *42*, 12583–12592. [CrossRef]
146. Ganesan, A.; Narayanasamy, M.; Shunmugavel, K.; Jayanthi Chinnappa, I. Ultra low loading of anode catalyst for direct methanol fuel cells with ZrO_2/ pyrolysed (PANI-melamine) as catalyst support. *Int. J. Hydrogen Energy* **2016**, *41*, 8963–8977. [CrossRef]
147. Das, S.; Dutta, K.; Kundu, P.P.; Bhattacharya, S.K. Nanostructured Polyaniline: An Efficient Support Matrix for Platinum-Ruthenium Anode Catalyst in Direct Methanol Fuel Cell. *Fuel Cells* **2018**, *18*, 369–378. [CrossRef]
148. El Rhazi, M.; Majid, S.; Elbasri, M.; Salih, F.E.; Oularbi, L.; Lafdi, K. Recent progress in nanocomposites based on conducting polymer: Application as electrochemical sensors. *Int. Nano Lett.* **2018**, *8*, 79–99. [CrossRef]
149. Pašti, I.A.; Janošević Ležaić, A.; Gavrilov, N.M.; Ćirić-Marjanović, G.; Mentus, S.V. Nanocarbons derived from polymers for electrochemical energy conversion and storage—A review. *Synth. Met.* **2018**, *246*, 267–281. [CrossRef]
150. Veizaga, N.S.; Rodriguez, V.I.; Rocha, T.A.; Bruno, M.; Scelza, O.A.; de Miguel, S.R.; Gonzalez, E.R. Promoting Effect of Tin in Platinum Electrocatalysts for Direct Methanol Fuel Cells (DMFC). *J. Electrochem. Soc.* **2015**, *162*, F243–F249. [CrossRef]

151. Amani, M.; Kazemeini, M.; Hamedanian, M.; Pahlavanzadeh, H.; Gharibi, H. Investigation of methanol oxidation on a highly active and stable Pt–Sn electrocatalyst supported on carbon-polyaniline composite for application in a passive direct methanol fuel cell. *Mater. Res. Bull.* **2015**, *68*, 166–178. [CrossRef]
152. Maya-Cornejo, J.; Garcia-Bernabé, A.; Compañ, V. Bimetallic Pt-M electrocatalysts supported on single-wall carbon nanotubes for hydrogen and methanol electrooxidation in fuel cells applications. *Int. J. Hydrogen Energy* **2018**, *43*, 872–884. [CrossRef]
153. Zhang, G.; Yang, Z.; Zhang, W.; Wang, Y. Nanosized Mo-doped CeO_2 enhances the electrocatalytic properties of the Pt anode catalyst in direct methanol fuel cells. *J. Mater. Chem. A* **2017**, *5*, 1481–1487. [CrossRef]
154. Du, H.; Wan, T.; Qu, B.; Scott, J.; Lin, X.; Younis, A.; Chu, D. Tailoring the multi-functionalities of one-dimensional ceria nanostructures via oxygen vacancy modulation. *J. Colloid Interface Sci.* **2017**, *504*, 305–314. [CrossRef] [PubMed]
155. Puigdollers, A.R.; Schlexer, P.; Tosoni, S.; Pacchioni, G. Increasing oxide reducibility: The role of metal/oxide interfaces in the formation of oxygen vacancies. *ACS Catalysis* **2017**, *7*, 6493–6513. [CrossRef]
156. Figueroba, A.; Bruix, A.; Kovács, G.; Neyman, K.M. Metal-doped ceria nanoparticles: Stability and redox processes. *Phys. Chem. Chem. Phys.* **2017**, *19*, 21729–21738. [CrossRef]
157. Chu, Y.-Y.; Wang, Z.-B.; Jiang, Z.-Z.; Gu, D.-M.; Yin, G.-P. A Novel Structural Design of a Pt/C-CeO_2 Catalyst with Improved Performance for Methanol Electro-Oxidation by β-Cyclodextrin Carbonization. *Adv. Mater.* **2011**, *23*, 3100–3104. [CrossRef]
158. Montini, T.; Melchionna, M.; Monai, M.; Fornasiero, P. Fundamentals and Catalytic Applications of CeO_2-Based Materials. *Chem. Rev.* **2016**, *116*, 5987–6041. [CrossRef]
159. Lykhach, Y.; Bruix, A.; Fabris, S.; Potin, V.; Matolínová, I.; Matolín, V.; Libuda, J.; Neyman, K.M. Oxide-based nanomaterials for fuel cell catalysis: The interplay between supported single Pt atoms and particles. *Catal. Sci. Technol.* **2017**, *7*, 4315–4345. [CrossRef]
160. Du, H.; Wang, Y.; Arandiyan, H.; Younis, A.; Scott, J.; Qu, B.; Wan, T.; Lin, X.; Chen, J.; Chu, D. Design and synthesis of CeO_2 nanowire/MnO_2 nanosheet heterogeneous structure for enhanced catalytic properties. *Mater. Today Commun.* **2017**, *11*, 103–111. [CrossRef]
161. Videla, A.; Osmieri, L.; Esfahani, R.; Zeng, J.; Francia, C.; Specchia, S. The Use of C-MnO_2 as Hybrid Precursor Support for a Pt/C-MnxO1+x Catalyst with Enhanced Activity for the Methanol Oxidation Reaction (MOR). *Catalysts* **2015**, *5*, 1399–1416. [CrossRef]
162. Abdel Hameed, R.M.; Fetohi, A.E.; Amin, R.S.; El-Khatib, K.M. Promotion effect of manganese oxide on the electrocatalytic activity of Pt/C for methanol oxidation in acid medium. *Appl. Surf. Sci.* **2015**, *359*, 651–663. [CrossRef]
163. Sun, Q.; Park, S.J.; Kim, S. Preparation and electrocatalytic oxidation performance of Pt/MnO_2-graphene oxide nanocomposites. *J. Ind. Eng. Chem.* **2015**, *26*, 265–269. [CrossRef]
164. Jin, H.; Guo, C.; Liu, X.; Liu, J.; Vasileff, A.; Jiao, Y.; Zheng, Y.; Qiao, S.Z. Emerging Two-Dimensional Nanomaterials for Electrocatalysis. *Chem. Rev.* **2018**, *118*, 6337–6408. [CrossRef]
165. Yadav, R.; Subhash, A.; Chemmenchery, N.; Kandasubramanian, B. Graphene and Graphene Oxide for Fuel Cell Technology. *Ind. Eng. Chem. Res.* **2018**, *57*, 9333–9350. [CrossRef]
166. Wang, C.; Astruc, D. Recent developments of metallic nanoparticle-graphene nanocatalysts. *Prog. Mater. Sci.* **2018**, *94*, 306–383. [CrossRef]
167. Ambrosi, A.; Chua, C.K.; Latiff, N.M.; Loo, A.H.; Wong, C.H.A.; Eng, A.Y.S.; Bonanni, A.; Pumera, M. Graphene and its electrochemistry-an update. *Chem. Soc. Rev.* **2016**, *45*, 2458–2493. [CrossRef]
168. Navalon, S.; Dhakshinamoorthy, A.; Alvaro, M.; Garcia, H. Metal nanoparticles supported on two-dimensional graphenes as heterogeneous catalysts. *Coord. Chem. Rev.* **2016**, *312*, 99–148. [CrossRef]
169. Lawal, A.T. Graphene-based nano composites and their applications. A review. *Biosens. Bioelectron.* **2019**, *141*, 111384. [CrossRef]
170. Guo, M.; Tu, Q.; Wang, L.; Tang, Y.; Song, H.; Zhou, J.; Zhang, Z.; Wang, Y.; Liu, C. Hollow Pt skim-sandwiched Cu spheres supported on reduced graphene oxide-carbon nanotube architecture for efficient methanol electrooxidation. *Int. J. Hydrogen Energy* **2019**, *44*, 6886–6895. [CrossRef]
171. Salarizadeh, P.; Askari, M.B.; Beheshti-Marnani, A.; Seifi, M.; Rozati, S.M.; Rohani, T.; Askari, N.; Salarizadeh, N.; Mohammadi, S.Z. Synthesis and characterization of (Co, Fe, Ni) 9 S 8 nanocomposite supported on reduced graphene oxide as an efficient and stable electrocatalyst for methanol electrooxidation toward DMFC. *J. Mater. Sci. Mater. Electron.* **2019**, *30*, 3521–3529. [CrossRef]
172. Org, W.E.; Lu, F.; Zhang, C.; Cheng, J.; Zhu, C.; Zhang, H.; Cheng, X. Electrochemical Science Ball-like Pt Nanoparticles on GO-modified Carbon Fiber Cloth with High Electrocatalytic Activity for Methanol Oxidation. *Int. J. Electrochem. Sci.* **2018**, *13*, 9007–9016. [CrossRef]
173. Zhang, X.; Zhang, J.; Huang, H.; Jiang, Q.; Wu, Y. Platinum nanoparticles anchored on graphene oxide-dispersed pristine carbon nanotube supports: High-performance electrocatalysts toward methanol electrooxidation. *Electrochim. Acta* **2017**, *258*, 919–926. [CrossRef]
174. Jovanovic, Z.; Bajuk-Bogdanović, D.; Jovanović, S.; Mravik, Z.; Kovač, J.; Holclajtner-Antunović, I.; Vujković, M. The role of surface chemistry in the charge storage properties of graphene oxide. *Electrochim. Acta* **2017**, *258*, 1228–1243. [CrossRef]
175. Wang, H.; Xue, Y.; Zhu, B.; Yang, J.; Wang, L.; Tan, X.; Wang, Z.; Chu, Y. CeO_2 nanowires stretch-embedded in reduced graphite oxide nanocomposite support for Pt nanoparticles as potential electrocatalyst for methanol oxidation reaction. *Int. J. Hydrogen Energy* **2017**, *42*, 20549–20559. [CrossRef]

176. Ji, Y.; Hou, M.; Zheng, Y.; Chen, W.; Wang, Z. A 3D network structured reduced graphene oxide/PtRu alloyed composite catalyst in-situ assembled via particle-constructing method. *Colloids Surf. A Physicochem. Eng. Asp.* **2019**, *561*, 292–300. [CrossRef]
177. Iqbal, M.; Dinh, D.K.; Abbas, Q.; Imran, M.; Sattar, H.; Ul Ahmad, A. Controlled Surface Wettability by Plasma Polymer Surface Modification. *Surfaces* **2019**, *2*, 349–371. [CrossRef]
178. Qian, W.; Hao, R.; Zhou, J.; Eastman, M.; Manhat, B.A.; Sun, Q.; Goforth, A.M.; Jiao, J. Exfoliated graphene-supported Pt and Pt-based alloys as electrocatalysts for direct methanol fuel cells. *Carbon N. Y.* **2013**, *52*, 595–604. [CrossRef]
179. Antolini, E.; Salgado, J.R.C.; Gonzalez, E.R. The stability of Pt-M (M = first row transition metal) alloy catalysts and its effect on the activity in low temperature fuel cells. A literature review and tests on a Pt-Co catalyst. *J. Power Sources* **2006**, *160*, 957–968. [CrossRef]
180. Baronia, R.; Goel, J.; Kaswan, J.; Shukla, A.; Singhal, S.K.; Singh, S.P. PtCo/rGO nano-anode catalyst: Enhanced power density with reduced methanol crossover in direct methanol fuel cell. *Mater. Renew. Sustain. Energy* **2018**, *7*, 1–13. [CrossRef]
181. Baronia, R.; Goel, J.; Tiwari, S.; Singh, P.; Singh, D.; Singh, S.P.; Singhal, S.K. Efficient electro-oxidation of methanol using PtCo nanocatalysts supported reduced graphene oxide matrix as anode for DMFC. *Int. J. Hydrogen Energy* **2017**, *42*, 10238–10247. [CrossRef]
182. Tian, M.; Shi, S.; Shen, Y.; Yin, H. PtRu alloy nanoparticles supported on nanoporous gold as an efficient anode catalyst for direct methanol fuel cell. *Electrochim. Acta* **2019**, *293*, 390–398. [CrossRef]
183. Zhang, J.; Qu, X.; Han, Y.; Shen, L.; Yin, S.; Li, G.; Jiang, Y.; Sun, S. Engineering PtRu bimetallic nanoparticles with adjustable alloying degree for methanol electrooxidation: Enhanced catalytic performance. *Appl. Catal. B Environ.* **2020**, *263*, 118345. [CrossRef]
184. Banham, D.; Choi, J.; Kishimoto, T.; Ye, S. Integrating PGM-Free Catalysts into Catalyst Layers and Proton Exchange Membrane Fuel Cell Devices. *Adv. Mater.* **2019**, *31*, 1804846. [CrossRef]
185. Yang, L.; Shui, J.; Du, L.; Shao, Y.; Liu, J.; Dai, L.; Hu, Z. Carbon-Based Metal-Free ORR Electrocatalysts for Fuel Cells: Past, Present, and Future. *Adv. Mater.* **2019**, *31*, 1804799. [CrossRef]
186. Lo Vecchio, C.; Sebastián, D.; Lázaro, M.; Aricò, A.; Baglio, V. Methanol-Tolerant M–N–C Catalysts for Oxygen Reduction Reactions in Acidic Media and Their Application in Direct Methanol Fuel Cells. *Catalysts* **2018**, *8*, 650. [CrossRef]
187. Sial, M.A.Z.G.; Din, M.A.U.; Wang, X. Multimetallic nanosheets: Synthesis and applications in fuel cells. *Chem. Soc. Rev.* **2018**, *47*, 6175–6200. [CrossRef]
188. Banham, D.; Kishimoto, T.; Zhou, Y.; Sato, T.; Bai, K.; Ozaki, J.I.; Imashiro, Y.; Ye, S. Critical advancements in achieving high power and stable nonprecious metal catalyst-based MEAs for real-world proton exchange membrane fuel cell applications. *Sci. Adv.* **2018**, *4*, eaar7180. [CrossRef]
189. Pattanayak, P.; Pramanik, N.; Kumar, P.; Kundu, P.P. Fabrication of cost-effective non-noble metal supported on conducting polymer composite such as copper/polypyrrole graphene oxide (Cu2O/PPy–GO) as an anode catalyst for methanol oxidation in DMFC. *Int. J. Hydrogen Energy* **2018**, *43*, 11505–11519. [CrossRef]
190. Das, S.; Dutta, K.; Kundu, P.P. Sulfonated polypyrrole matrix induced enhanced efficiency of Ni nanocatalyst for application as an anode material for DMFCs. *Mater. Chem. Phys.* **2016**, *176*, 143–151. [CrossRef]
191. Park, K.W.; Choi, J.H.; Kwon, B.K.; Lee, S.A.; Sung, Y.E.; Ha, H.Y.; Hong, S.A.; Kim, H.; Wieckowski, A. Chemical and electronic effects of Ni in Pt/Ni and Pt/Ru/Ni alloy nanoparticles in methanol electrooxidation. *J. Phys. Chem. B* **2002**, *106*, 1869–1877. [CrossRef]
192. Das, S.; Dutta, K.; Kundu, P.P. Nickel nanocatalysts supported on sulfonated polyaniline: Potential toward methanol oxidation and as anode materials for DMFCs. *J. Mater. Chem. A* **2015**, *3*, 11349–11357. [CrossRef]
193. Li, K.; Jin, Z.; Ge, J.; Liu, C.; Xing, W. Platinum nanoparticles partially-embedded into carbon sphere surfaces: A low metal-loading anode catalyst with superior performance for direct methanol fuel cells. *J. Mater. Chem. A* **2017**, *5*, 19857–19865. [CrossRef]
194. Yuan, W.; Zhang, Y.; Zhang, N.; Yin, C.; Zhang, X.; Liu, X. Carbon riveted Pt–MnO_2/reduced graphene oxide anode catalyst for DMFC. *Catal. Commun.* **2017**, *100*, 66–70. [CrossRef]
195. Rethinasabapathy, M.; Kang, S.M.; Haldorai, Y.; Jankiraman, M.; Jonna, N.; Choe, S.R.; Huh, Y.S.; Natesan, B. Ternary PtRuFe nanoparticles supported N-doped graphene as an efficient bifunctional catalyst for methanol oxidation and oxygen reduction reactions. *Int. J. Hydrogen Energy* **2017**, *42*, 30738–30749. [CrossRef]
196. Rethinasabapathy, M.; Kang, S.M.; Haldorai, Y.; Jonna, N.; Jankiraman, M.; Lee, G.W.; Jang, S.C.; Natesan, B.; Roh, C.; Huh, Y.S. Quaternary PtRuFeCo nanoparticles supported N-doped graphene as an efficient bifunctional electrocatalyst for low-temperature fuel cells. *J. Ind. Eng. Chem.* **2019**, *69*, 285–294. [CrossRef]
197. Zhao, S.; Yin, H.; Du, L.; Yin, G.; Tang, Z.; Liu, S. Three dimensional N-doped graphene/PtRu nanoparticle hybrids as high performance anode for direct methanol fuel cells. *J. Mater. Chem. A* **2014**, *2*, 3719–3724. [CrossRef]
198. Thiagarajan, V.; Karthikeyan, P.; Thanarajan, K.; Neelakrishnan, S.; Manoharan, R.; Chen, R.; Fly, A.; Anand, R.; Karuppa Raj, T.R.; Sendhil Kumar, N. Experimental investigation on DMFCs using reduced noble metal loading with NiTiO3 as supportive material to enhance cell performances. *Int. J. Hydrogen Energy* **2019**, *44*, 13415–13423. [CrossRef]
199. Fard, H.F.; Khodaverdi, M.; Pourfayaz, F.; Ahmadi, M.H. Application of N-doped carbon nanotube-supported Pt–Ru as electrocatalyst layer in passive direct methanol fuel cell. *Int. J. Hydrogen Energy* **2021**, *45*, 25307–25316. [CrossRef]
200. Kulkarni, A.; Siahrostami, S.; Patel, A.; Nørskov, J.K. Understanding Catalytic Activity Trends in the Oxygen Reduction Reaction. *Chem. Rev.* **2018**, *118*, 2302–2312. [CrossRef]

201. Kang, S.Y.; Kim, H.J.; Chung, Y.H. Recent developments of nano-structured materials as the catalysts for oxygen reduction reaction. *Nano Converg.* **2018**, *5*, 1–15. [CrossRef] [PubMed]
202. Stacy, J.; Regmi, Y.N.; Leonard, B.; Fan, M. The recent progress and future of oxygen reduction reaction catalysis: A review. *Renew. Sustain. Energy Rev.* **2017**, *69*, 401–414. [CrossRef]
203. Dai, L.; Xue, Y.; Qu, L.; Choi, H.J.; Baek, J.B. Metal-Free Catalysts for Oxygen Reduction Reaction. *Chem. Rev.* **2015**, *115*, 4823–4892. [CrossRef] [PubMed]
204. Wang, L.; Holewinski, A.; Wang, C. Prospects of Platinum-Based Nanostructures for the Electrocatalytic Reduction of Oxygen. *ACS Catal.* **2018**, *8*, 9388–9398. [CrossRef]
205. Zhang, C.; Shen, X.; Pan, Y.; Peng, Z. A review of Pt-based electrocatalysts for oxygen reduction reaction. *Front. Energy* **2017**, *11*, 268–285. [CrossRef]
206. Sakthivel, M.; Drillet, J.F. An extensive study about influence of the carbon support morphology on Pt activity and stability for oxygen reduction reaction. *Appl. Catal. B Environ.* **2018**, *231*, 62–72. [CrossRef]
207. Yarlagadda, V.; Carpenter, M.K.; Moylan, T.E.; Kukreja, R.S.; Koestner, R.; Gu, W.; Thompson, L.; Kongkanand, A.A.A. Boosting Fuel Cell Performance with Accessible Carbon Mesopores. *ACS Energy Lett.* **2018**, *3*, 618–621. [CrossRef]
208. Mora-Hernández, J.M.; Luo, Y.; Alonso-Vante, N. What can we learn in electrocatalysis, from nanoparticulated precious and/or non-precious catalytic centers interacting with their support? *Catalysts* **2016**, *6*, 145. [CrossRef]
209. Shahgaldi, S.; Hamelin, J. Improved carbon nanostructures as a novel catalyst support in the cathode side of PEMFC: A critical review. *Carbon* **2015**, *94*, 705–728. [CrossRef]
210. Zhao, G.; Zhao, T.S.; Xu, J.; Lin, Z.; Yan, X. Impact of pore size of ordered mesoporous carbon FDU-15-supported platinum catalysts on oxygen reduction reaction. *Int. J. Hydrogen Energy* **2017**, *42*, 3325–3334. [CrossRef]
211. Tesfu-Zeru, T.; Sakthivel, M.; Drillet, J.F. Investigation of mesoporous carbon hollow spheres as catalyst support in DMFC cathode. *Appl. Catal. B Environ.* **2017**, *204*, 173–184. [CrossRef]
212. Yang, Z.; Ling, Y.; Zhang, Y.; Yang, M. Highly methanol-tolerant platinum electrocatalyst derived from poly(vinylpoyrrolidone) coating. *Nanotechnology* **2017**, *28*, 055404. [CrossRef] [PubMed]
213. Yang, Z.; Nakashima, N. A simple preparation of very high methanol tolerant cathode electrocatalyst for direct methanol fuel cell based on polymer-coated carbon nanotube/platinum. *Sci. Rep.* **2015**, *5*, 1–9. [CrossRef] [PubMed]
214. Liu, J.; Liu, C.T.; Zhao, L.; Zhang, J.J.; Zhang, L.M.; Wang, Z.B. Effect of different structures of carbon supports for cathode catalyst on performance of direct methanol fuel cell. *Int. J. Hydrogen Energy* **2016**, *41*, 1859–1870. [CrossRef]
215. Guo, S.; Zhang, S.; Sun, S. Tuning Nanoparticle Catalysis for the Oxygen Reduction Reaction. *Angew. Chem. Int. Ed.* **2013**, *52*, 8526–8544. [CrossRef]
216. Mistry, H.; Varela, A.S.; Kühl, S.; Strasser, P.; Cuenya, B.R. Nanostructured electrocatalysts with tunable activity and selectivity. *Nat. Rev. Mater.* **2016**, *1*, 1–14. [CrossRef]
217. Lu, Y.; Du, S.; Steinberger-Wilckens, R. One-dimensional nanostructured electrocatalysts for polymer electrolyte membrane fuel cells—A review. *Appl. Catal. B Environ.* **2016**, *199*, 292–314. [CrossRef]
218. Calle-Vallejo, F.; Pohl, M.D.; Reinisch, D.; Loffreda, D.; Sautet, P.; Bandarenka, A.S. Why conclusions from platinum model surfaces do not necessarily lead to enhanced nanoparticle catalysts for the oxygen reduction reaction. *Chem. Sci.* **2017**, *8*, 2283–2289. [CrossRef]
219. Shao, M.; Peles, A.; Shoemaker, K. Electrocatalysis on platinum nanoparticles: Particle size effect on oxygen reduction reaction activity. *Nano Lett.* **2011**, *11*, 3714–3719. [CrossRef]
220. Li, M.; Zhao, Z.; Cheng, T.; Fortunelli, A.; Chen, C.Y.; Yu, R.; Zhang, Q.; Gu, L.; Merinov, B.V.; Lin, Z.; et al. Ultrafine jagged platinum nanowires enable ultrahigh mass activity for the oxygen reduction reaction. *Science* **2016**, *354*, 1414–1419. [CrossRef]
221. Stephens, I.E.L.; Rossmeisl, J.; Chorkendorff, I. Toward sustainable fuel cells. *Science* **2016**, *354*, 1378–1379. [CrossRef] [PubMed]
222. Park, J.; Kwon, T.; Kim, J.; Jin, H.; Kim, H.Y.; Kim, B.; Joo, S.H.; Lee, K. Hollow nanoparticles as emerging electrocatalysts for renewable energy conversion reactions. *Chem. Soc. Rev.* **2018**, *47*, 8173–8202. [CrossRef] [PubMed]
223. Kim, S.; Park, J.E.; Hwang, W.; Cho, Y.H.; Sung, Y.E. A hierarchical cathode catalyst layer architecture for improving the performance of direct methanol fuel cell. *Appl. Catal. B Environ.* **2017**, *209*, 91–97. [CrossRef]
224. Glass, D.E.; Prakash, G.K.S. Effect of the Cathode Catalyst Layer Thickness on the Performance in Direct Methanol Fuel Cells. *Electroanalysis* **2019**, *31*, 718–725. [CrossRef]
225. Hunt, S.T.; Román-Leshkov, Y. Principles and Methods for the Rational Design of Core-Shell Nanoparticle Catalysts with Ultralow Noble Metal Loadings. *Acc. Chem. Res.* **2018**, *51*, 1054–1062. [CrossRef]
226. Stamenkovic, V.; Mun, B.S.; Mayrhofer, K.J.J.; Ross, P.N.; Markovic, N.M.; Rossmeisl, J.; Greeley, J.; Nørskov, J.K. Changing the Activity of Electrocatalysts for Oxygen Reduction by Tuning the Surface Electronic Structure. *Angew. Chemie Int. Ed.* **2006**, *45*, 2897–2901. [CrossRef]
227. Calle-Vallejo, F.; Martínez, J.I.; Rossmeisl, J. Density functional studies of functionalized graphitic materials with late transition metals for oxygen reduction reactions. *Phys. Chem. Chem. Phys.* **2011**, *13*, 15639–15643. [CrossRef]
228. Li, J.; Alsudairi, A.; Ma, Z.F.; Mukerjee, S.; Jia, Q. Asymmetric volcano trend in oxygen reduction activity of Pt and non-Pt catalysts: In situ identification of the site-blocking effect. *J. Am. Chem. Soc.* **2017**, *139*, 1384–1387. [CrossRef]
229. Stamenkovic, V.R.; Mun, B.S.; Arenz, M.; Mayrhofer, K.J.J.; Lucas, C.A.; Wang, G.; Ross, P.N.; Markovic, N.M. Trends in electrocatalysis on extended and nanoscale Pt-bimetallic alloy surfaces. *Nat. Mater.* **2007**, *6*, 241–247. [CrossRef]

230. Greeley, J.; Stephens, I.E.L.; Bondarenko, A.S.; Johansson, T.P.; Hansen, H.A.; Jaramillo, T.F.; Rossmeisl, J.; Chorkendorff, I.; Nørskov, J.K. Alloys of platinum and early transition metals as oxygen reduction electrocatalysts. *Nat. Chem.* **2009**, *1*, 552–556. [CrossRef]
231. Stamenkovic, V.R.; Fowler, B.; Mun, B.S.; Wang, G.; Ross, P.N.; Lucas, C.A.; Markovic, N.M. Improved oxygen reduction activity on Pt3Ni(111) via increased surface site availability. *Science* **2007**, *315*, 493–497. [CrossRef] [PubMed]
232. Gan, L.; Rudi, S.; Cui, C.; Heggen, M.; Strasser, P. Size-Controlled Synthesis of Sub-10 nm PtNi 3 Alloy Nanoparticles and their Unusual Volcano-Shaped Size Effect on ORR Electrocatalysis. *Small* **2016**, *12*, 3189–3196. [CrossRef] [PubMed]
233. Strasser, P.; Koh, S.; Anniyev, T.; Greeley, J.; More, K.; Yu, C.; Liu, Z.; Kaya, S.; Nordlund, D.; Ogasawara, H.; et al. Lattice-strain control of the activity in dealloyed core-shell fuel cell catalysts. *Nat. Chem.* **2010**, *2*, 454–460. [CrossRef] [PubMed]
234. Escudero-Escribano, M.; Malacrida, P.; Hansen, M.H.; Vej-Hansen, U.G.; Velázquez-Palenzuela, A.; Tripkovic, V.; Schiøtz, J.; Rossmeisl, J.; Stephens, I.E.L.; Chorkendorff, I. Tuning the activity of Pt alloy electrocatalysts by means of the lanthanide contraction. *Science* **2016**, *352*, 73–76. [CrossRef]
235. Chen, C.; Kang, Y.; Huo, Z.; Zhu, Z.; Huang, W.; Xin, H.L.; Snyder, J.D.; Li, D.; Herron, J.A.; Mavrikakis, M.; et al. Highly crystalline multimetallic nanoframes with three-dimensional electrocatalytic surfaces. *Science* **2014**, *343*, 1339–1343. [CrossRef]
236. Bu, L.; Zhang, N.; Guo, S.; Zhang, X.; Li, J.; Yao, J.; Wu, T.; Lu, G.; Ma, J.Y.; Su, D.; et al. Biaxially strained PtPb/Pt core/shell nanoplate boosts oxygen reduction catalysis. *Science* **2016**, *354*, 1410–1414. [CrossRef]
237. Wang, G.; Jiang, J.; Huang, Q.; Zhou, Y.; Zou, Z.; Yang, H. Interconnected nanoparticle-stacked platinum-based nanosheets as active cathode electrocatalysts for passive direct methanol fuel cells. *J. Electroanal. Chem.* **2018**, *828*, 50–58. [CrossRef]
238. Choi, B.; Nam, W.H.; Chung, D.Y.; Park, I.S.; Yoo, S.J.; Song, J.C.; Sung, Y.E. Enhanced methanol tolerance of highly Pd rich Pd-Pt cathode electrocatalysts in direct methanol fuel cells. *Electrochim. Acta* **2015**, *164*, 235–242. [CrossRef]
239. Yan, X.H.; Zhao, T.S.; An, L.; Zhao, G.; Zeng, L. A novel cathode architecture with a thin reaction layer alleviates mixed potentials and catalyst poisoning in direct methanol fuel cells. *Int. J. Hydrogen Energy* **2015**, *40*, 16540–16546. [CrossRef]
240. Shao, Y.; Dodelet, J.; Wu, G.; Zelenay, P. PGM-Free Cathode Catalysts for PEM Fuel Cells: A Mini-Review on Stability Challenges. *Adv. Mater.* **2019**, *31*, 1807615. [CrossRef]
241. Goswami, C.; Hazarika, K.K.; Bharali, P. Transition metal oxide nanocatalysts for oxygen reduction reaction. *Mater. Sci. Energy Technol.* **2018**, *1*, 117–128. [CrossRef]
242. Zhang, C.; Wang, Y.-C.; An, B.; Huang, R.; Wang, C.; Zhou, Z.; Lin, W. Networking Pyrolyzed Zeolitic Imidazolate Frameworks by Carbon Nanotubes Improves Conductivity and Enhances Oxygen-Reduction Performance in Polymer-Electrolyte-Membrane Fuel Cells. *Adv. Mater.* **2017**, *29*, 1604556. [CrossRef]
243. Nie, Y.; Li, L.; Wei, Z. Recent advancements in Pt and Pt-free catalysts for oxygen reduction reaction. *Chem. Soc. Rev.* **2015**, *44*, 2168–2201. [CrossRef] [PubMed]
244. Singh, S.K.; Takeyasu, K.; Nakamura, J. Active Sites and Mechanism of Oxygen Reduction Reaction Electrocatalysis on Nitrogen-Doped Carbon Materials. *Adv. Mater.* **2019**, *31*, 1804297. [CrossRef] [PubMed]
245. Wu, Z.; Song, M.; Wang, J.; Liu, X. Recent Progress in Nitrogen-Doped Metal-Free Electrocatalysts for Oxygen Reduction Reaction. *Catalysts* **2018**, *8*, 196. [CrossRef]
246. Sa, Y.J.; Kim, J.H.; Joo, S.H. Recent progress in the identification of active sites in pyrolyzed Fe–N/C catalysts and insights into their role in oxygen reduction reaction. *J. Electrochem. Sci. Technol.* **2017**, *8*, 169–182. [CrossRef]
247. Wu, G.; Santandreu, A.; Kellogg, W.; Gupta, S.; Ogoke, O.; Zhang, H.; Wang, H.L.; Dai, L. Carbon nanocomposite catalysts for oxygen reduction and evolution reactions: From nitrogen doping to transition-metal addition. *Nano Energy* **2016**, *29*, 83–110. [CrossRef]
248. Zhang, J.; Xia, Z.; Dai, L. Carbon-based electrocatalysts for advanced energy conversion and storage. *Sci. Adv.* **2015**, *1*, e1500564. [CrossRef]
249. Jaouen, F.; Proietti, E.; Lefèvre, M.; Chenitz, R.; Dodelet, J.P.; Wu, G.; Chung, H.T.; Johnston, C.M.; Zelenay, P. Recent advances in non-precious metal catalysis for oxygen-reduction reaction in polymer electrolyte fuel cells. *Energy Environ. Sci.* **2011**, *4*, 114–130. [CrossRef]
250. Martinez, U.; Babu, S.K.; Holby, E.F.; Zelenay, P. Durability challenges and perspective in the development of PGM-free electrocatalysts for the oxygen reduction reaction. *Curr. Opin. Electrochem.* **2018**, *9*, 224–232. [CrossRef]
251. Banham, D.; Kishimoto, T.; Sato, T.; Kobayashi, Y.; Narizuka, K.; Ozaki, J.-i.; Zhou, J.Y.; Marquez, E.; Bai, K.; Ye, S. New insights into non-precious metal catalyst layer designs for proton exchange membrane fuel cells: Improving performance and stability. *J. Power Sources* **2017**, *344*, 39–45. [CrossRef]
252. Banham, D.; Ye, S.; Pei, K.; Ozaki, J.I.; Kishimoto, T.; Imashiro, Y. A review of the stability and durability of non-precious metal catalysts for the oxygen reduction reaction in proton exchange membrane fuel cells. *J. Power Sources* **2015**, *285*, 334–348. [CrossRef]
253. Zagal, J.H.; Recio, F.J.; Gutierrez, C.A.; Zuñiga, C.; Páez, M.A.; Caro, C.A. Towards a unified way of comparing the electrocatalytic activity MN4 macrocyclic metal catalysts for O_2 reduction on the basis of the reversible potential of the reaction. *Electrochem. Commun.* **2014**, *41*, 24–26. [CrossRef]
254. Chen, Z.; Higgins, D.; Yu, A.; Zhang, L.; Zhang, J. A review on non-precious metal electrocatalysts for PEM fuel cells. *Energy Environ. Sci.* **2011**, *4*, 3167–3192. [CrossRef]
255. Lefèvre, M.; Proietti, E.; Jaouen, F.; Dodelet, J.P. Iron-Based catalysts with improved oxygen reduction activity in polymer electrolyte fuel cells. *Science* **2009**, *324*, 71–74. [CrossRef] [PubMed]

256. Piela, B.; Olson, T.S.; Atanassov, P.; Zelenay, P. Highly methanol-tolerant non-precious metal cathode catalysts for direct methanol fuel cell. *Electrochim. Acta* **2010**, *55*, 7615–7621. [CrossRef]
257. Serov, A.; Shum, A.D.; Xiao, X.; De Andrade, V.; Artyushkova, K.; Zenyuk, I.V.; Atanassov, P. Nano-structured platinum group metal-free catalysts and their integration in fuel cell electrode architectures. *Appl. Catal. B Environ.* **2018**, *237*, 1139–1147. [CrossRef]
258. Normile, S.J.; Sabarirajan, D.C.; Calzada, O.; De Andrade, V.; Xiao, X.; Mandal, P.; Parkinson, D.Y.; Serov, A.; Atanassov, P.; Zenyuk, I.V. Direct observations of liquid water formation at nano- and micro-scale in platinum group metal-free electrodes by operando X-ray computed tomography. *Mater. Today Energy* **2018**, *9*, 187–197. [CrossRef]
259. Gómez, J.C.; Moliner, R.; Lázaro, M. Palladium-Based Catalysts as Electrodes for Direct Methanol Fuel Cells: A Last Ten Years Review. *Catalysts* **2016**, *6*, 130. [CrossRef]
260. Shao, M. Palladium-based electrocatalysts for hydrogen oxidation and oxygen reduction reactions. *J. Power Sources* **2011**, *196*, 2433–2444. [CrossRef]
261. Wen, C.; Wei, Y.; Tang, D.; Sa, B.; Zhang, T.; Chen, C. Improving the electrocatalytic properties of Pd-based catalyst for direct alcohol fuel cells: Effect of solid solution. *Sci. Rep.* **2017**, *7*, 1–11. [CrossRef]
262. Zhang, L.; Chang, Q.; Chen, H.; Shao, M. Recent advances in palladium-based electrocatalysts for fuel cell reactions and hydrogen evolution reaction. *Nano Energy* **2016**, *29*, 198–219. [CrossRef]
263. Baglio, V.; Aricò, A.S.; Stassi, A.; D'Urso, C.; Di Blasi, A.; Luna, A.M.C.; Antonucci, V. Investigation of Pt–Fe catalysts for oxygen reduction in low temperature direct methanol fuel cells. *J. Power Sources* **2006**, *159*, 900–904. [CrossRef]
264. Salgado, J.R.C.; Antolini, E.; Gonzalez, E.R. Carbon supported Pt–Co alloys as methanol-resistant oxygen-reduction electrocatalysts for direct methanol fuel cells. *Appl. Catal. B Environ.* **2005**, *57*, 283–290. [CrossRef]
265. Gavidia, L.M.R.; García, G.; Anaya, D.; Querejeta, A.; Alcaide, F.; Pastor, E. Carbon-supported Pt-free catalysts with high specificity and activity toward the oxygen reduction reaction in acidic medium. *Appl. Catal. B Environ.* **2016**, *184*, 12–19. [CrossRef]
266. Gavidia, L.R.; Sebastián, D.; Pastor, E.; Aricò, A.; Baglio, V. Carbon-Supported Pd and PdFe Alloy Catalysts for Direct Methanol Fuel Cell Cathodes. *Materials* **2017**, *10*, 580. [CrossRef]
267. Lo Vecchio, C.; Sebastián, D.; Alegre, C.; Aricò, A.S.; Baglio, V. Carbon-supported Pd and Pd-Co cathode catalysts for direct methanol fuel cells (DMFCs) operating with high methanol concentration. *J. Electroanal. Chem.* **2018**, *808*, 464–473. [CrossRef]
268. Hu, Y.; Zhu, J.; Lv, Q.; Liu, C.; Li, Q.; Xing, W. Promotional effect of phosphorus doping on the activity of the Fe-N/C catalyst for the oxygen reduction reaction. *Electrochim. Acta* **2015**, *155*, 335–340. [CrossRef]
269. Karim, N.A.; Kamarudin, S.K.; Loh, K.S. Performance of a novel non-platinum cathode catalyst for direct methanol fuel cells. *Energy Convers. Manag.* **2017**, *145*, 293–307. [CrossRef]
270. Karim, N.A.; Kamarudin, S.K. Novel heat-treated cobalt phthalocyanine/carbon-tungsten oxide nanowires (CoPc/C-W18O49) cathode catalyst for direct methanol fuel cell. *J. Electroanal. Chem.* **2017**, *803*, 19–29. [CrossRef]
271. Karim, N.A.; Kamarudin, S.K. An overview on non-platinum cathode catalysts for direct methanol fuel cell. *Appl. Energy* **2013**, *103*, 212–220. [CrossRef]
272. Karim, N.A.; Kamarudin, S.K.; Shyuan, L.K.; Yaakob, Z.; Daud, W.R.W.; Khadum, A.A.H. Novel cathode catalyst for DMFC: Study of the density of states of oxygen adsorption using density functional theory. *Int. J. Hydrogen Energy* **2014**, *39*, 17295–17305. [CrossRef]
273. Baranton, S.; Coutanceau, C.; Léger, J.M.; Roux, C.; Capron, P. Alternative cathodes based on iron phthalocyanine catalysts for mini- or micro-DMFC working at room temperature. *Electrochim. Acta* **2005**, *51*, 517–525. [CrossRef]
274. Negro, E.; Videla, A.H.A.M.; Baglio, V.; Aricò, A.S.; Specchia, S.; Koper, G.J.M. Fe-N supported on graphitic carbon nano-networks grown from cobalt as oxygen reduction catalysts for low-temperature fuel cells. *Appl. Catal. B Environ.* **2015**, *166–167*, 75–83. [CrossRef]
275. Li, Q.; Wang, T.; Havas, D.; Zhang, H.; Xu, P.; Han, J.; Cho, J.; Wu, G. High-Performance Direct Methanol Fuel Cells with Precious-Metal-Free Cathode. *Adv. Sci.* **2016**, *3*, 1600140. [CrossRef]
276. Park, J.C.; Choi, C.H. Graphene-derived Fe/Co-N-C catalyst in direct methanol fuel cells: Effects of the methanol concentration and ionomer content on cell performance. *J. Power Sources* **2017**, *358*, 76–84. [CrossRef]
277. Serov, A.; Artyushkova, K.; Niangar, E.; Wang, C.; Dale, N.; Jaouen, F.; Sougrati, M.T.; Jia, Q.; Mukerjee, S.; Atanassov, P. Nano-structured non-platinum catalysts for automotive fuel cell application. *Nano Energy* **2015**, *16*, 293–300. [CrossRef]
278. Serov, A.; Artyushkova, K.; Atanassov, P. Fe-N-C Oxygen Reduction Fuel Cell Catalyst Derived from Carbendazim: Synthesis, Structure, and Reactivity. *Adv. Energy Mater.* **2014**, *4*, 1301735. [CrossRef]
279. Videla, A.H.A.M.; Sebastián, D.; Vasile, N.S.; Osmieri, L.; Aricò, A.S.; Baglio, V.; Specchia, S. Performance analysis of Fe–N–C catalyst for DMFC cathodes: Effect of water saturation in the cathodic catalyst layer. *Int. J. Hydrogen Energy* **2016**, *41*, 22605–22618. [CrossRef]
280. Videla, A.H.A.M.; Osmieri, L.; Armandi, M.; Specchia, S. Varying the morphology of Fe-N-C electrocatalysts by templating Iron Phthalocyanine precursor with different porous SiO_2 to promote the Oxygen Reduction Reaction. *Electrochim. Acta* **2015**, *177*, 43–50. [CrossRef]
281. Wang, Y.C.; Huang, L.; Zhang, P.; Qiu, Y.T.; Sheng, T.; Zhou, Z.Y.; Wang, G.; Liu, J.G.; Rauf, M.; Gu, Z.Q.; et al. Constructing a triple-phase interface in micropores to boost performance of Fe/N/C catalysts for direct methanol fuel cells. *ACS Energy Lett.* **2017**, *2*, 645–650. [CrossRef]

282. Wang, Q.; Zhou, Z.Y.; Lai, Y.J.; You, Y.; Liu, J.G.; Wu, X.L.; Terefe, E.; Chen, C.; Song, L.; Rauf, M.; et al. Phenylenediamine-based FeNx/C catalyst with high activity for oxygen reduction in acid medium and its active-site probing. *J. Am. Chem. Soc.* **2014**, *136*, 10882–10885. [CrossRef]
283. Osmieri, L.; Escudero-Cid, R.; Videla, A.H.A.M.; Ocón, P.; Specchia, S. Performance of a Fe-N-C catalyst for the oxygen reduction reaction in direct methanol fuel cell: Cathode formulation optimization and short-term durability. *Appl. Catal. B Environ.* **2017**, *201*, 253–265. [CrossRef]
284. Osmieri, L.; Videla, A.H.A.M.; Armandi, M.; Specchia, S. Influence of different transition metals on the properties of Me–N–C (Me = Fe, Co, Cu, Zn) catalysts synthesized using SBA-15 as tubular nano-silica reactor for oxygen reduction reaction. *Int. J. Hydrogen Energy* **2016**, *41*, 22570–22588. [CrossRef]
285. Sebastián, D.; Baglio, V.; Aricò, A.S.; Serov, A.; Atanassov, P. Performance analysis of a non-platinum group metal catalyst based on iron-aminoantipyrine for direct methanol fuel cells. *Appl. Catal. B Environ.* **2016**, *182*, 297–305. [CrossRef]
286. Sebastián, D.; Serov, A.; Artyushkova, K.; Atanassov, P.; Aricò, A.S.; Baglio, V. Performance, methanol tolerance and stability of Fe-aminobenzimidazole derived catalyst for direct methanol fuel cells. *J. Power Sources* **2016**, *319*, 235–246. [CrossRef]
287. Osmieri, L.; Escudero-Cid, R.; Armandi, M.; Videla, A.H.A.M.; Fierro, J.L.G.; Ocón, P.; Specchia, S. Fe-N/C catalysts for oxygen reduction reaction supported on different carbonaceous materials. Performance in acidic and alkaline direct alcohol fuel cells. *Appl. Catal. B Environ.* **2017**, *205*, 637–653. [CrossRef]
288. Liu, J.; Li, E.; Ruan, M.; Song, P.; Xu, W. Recent progress on Fe/N/C electrocatalysts for the oxygen reduction reaction in fuel cells. *Catalysts* **2015**, *5*, 1167–1192. [CrossRef]
289. Sebastián, D.; Serov, A.; Matanovic, I.; Artyushkova, K.; Atanassov, P.; Aricò, A.S.; Baglio, V. Insights on the extraordinary tolerance to alcohols of Fe-N-C cathode catalysts in highly performing direct alcohol fuel cells. *Nano Energy* **2017**, *34*, 195–204. [CrossRef]
290. Lo Vecchio, C.; Aricò, A.S.; Baglio, V. Application of low-cost Me-N-C (Me = Fe or Co) electrocatalysts derived from edta in direct methanol fuel cells (DMFCs). *Materials* **2018**, *11*, 1193. [CrossRef]
291. Lo Vecchio, C.; Serov, A.; Romero, H.; Lubers, A.; Zulevi, B.; Aricò, A.S.; Baglio, V. Commercial platinum group metal-free cathodic electrocatalysts for highly performed direct methanol fuel cell applications. *J. Power Sources* **2019**, *437*, 226948. [CrossRef]
292. Xu, X.; Xia, Z.; Zhang, X.; Sun, R.; Sun, X.; Li, H.; Wu, C.; Wang, J.; Wang, S.; Sun, G. Atomically dispersed Fe-N-C derived from dual metal-organic frameworks as efficient oxygen reduction electrocatalysts in direct methanol fuel cells. *Appl. Catal. B Environ.* **2019**, *259*, 118042. [CrossRef]
293. Pu, L.; Zhang, H.; Yuan, T.; Zou, Z.; Zou, L.; Li, X.M.; Yang, H. High performance platinum nanorod assemblies based double-layered cathode for passive direct methanol fuel cells. *J. Power Sources* **2015**, *276*, 95–101. [CrossRef]
294. Wang, G.; Lei, L.; Jiang, J.; Zhou, Y.; Huang, Q.; Zou, Z.; Jiang, S.P.; Yang, H. An ordered structured cathode based on vertically aligned Pt nanotubes for ultra-low Pt loading passive direct methanol fuel cells. *Electrochim. Acta* **2017**, *252*, 541–548. [CrossRef]
295. Viva, F.A.; Olah, G.A.; Prakash, G.K.S. Characterization of Pt supported on commercial fluorinated carbon as cathode catalysts for Polymer Electrolyte Membrane Fuel Cell. *Int. J. Hydrogen Energy* **2017**, *42*, 15054–15063. [CrossRef]
296. Pu, L.; Zou, L.; Zhou, Y.; Zou, Z.; Yang, H. High performance MWCNT-Pt nanocomposite-based cathode for passive direct methanol fuel cells. *RSC Adv.* **2017**, *7*, 12329–12335. [CrossRef]
297. Fan, C.; Wang, G.; Zou, L.; Fang, J.; Zou, Z.; Yang, H. Composition- and shape-controlled synthesis of the PtNi alloy nanotubes with enhanced activity and durability toward oxygen reduction reaction. *J. Power Sources* **2019**, *429*, 1–8. [CrossRef]
298. Martinaiou, I.; Videla, A.H.A.M.; Weidler, N.; Kübler, M.; Wallace, W.D.Z.; Paul, S.; Wagner, S.; Shahraei, A.; Stark, R.W.; Specchia, S.; et al. Activity and degradation study of an Fe-N-C catalyst for ORR in Direct Methanol Fuel Cell (DMFC). *Appl. Catal. B Environ.* **2020**, *262*, 118217. [CrossRef]
299. Seh, Z.W.; Kibsgaard, J.; Dickens, C.F.; Chorkendorff, I.; Nørskov, J.K.; Jaramillo, T.F. Combining theory and experiment in electrocatalysis: Insights into materials design. *Science* **2017**, *355*, eaad4998. [CrossRef]
300. Ismail, M.S.; Ingham, D.B.; Ma, L.; Hughes, K.J.; Pourkashanian, M. Effects of catalyst agglomerate shape in polymer electrolyte fuel cells investigated by a multi-scale modelling framework. *Energy* **2017**, *122*, 420–430. [CrossRef]
301. Zawodzinski, T.; Wieckowski, A.; Mukerjee, S.; Neurock, M. Integrated Theoretical and Experimental Studies of Fuel Cell Electrocatalysts. *Electrochem. Soc. Interface* **2007**, *16*, 37–41. [CrossRef]
302. Karim, N.A.; Yahya, N.; Kejuruter, J. A Short Overview Current Research of Catalyst for Methanol Oxidation Reaction in Direct Methanol Fuel Cell (DMFC) from Experimental and Theoretical Aspect. *J. Kejuruter.* **2018**, *1*, 9–17. [CrossRef]
303. Lee, J.; Lee, S.; Han, D.; Gwak, G.; Ju, H. Numerical modeling and simulations of active direct methanol fuel cell (DMFC) systems under various ambient temperatures and operating conditions. *Int. J. Hydrogen Energy* **2017**, *42*, 1736–1750. [CrossRef]
304. Falcão, D.S.; Oliveira, V.B.; Rangel, C.M.; Pinto, A.M.F.R. Experimental and modeling studies of a micro direct methanol fuel cell. *Renew. Energy* **2015**, *74*, 464–470. [CrossRef]
305. Oliveira, V.B.; Rangel, C.M.; Pinto, A.M.F.R. One-dimensional and non-isothermal model for a passive DMFC. *J. Power Sources* **2011**, *196*, 8973–8982. [CrossRef]
306. Oliveira, V.B.; Falcão, D.S.; Rangel, C.M.; Pinto, A.M.F.R. Heat and mass transfer effects in a direct methanol fuel cell: A 1D model. *Int. J. Hydrogen Energy* **2008**, *33*, 3818–3828. [CrossRef]
307. Liu, C.Y.; Chang, C.C.; Ho, J.J.; Li, E.Y. First-Principles Study on CO Removing Mechanism on Pt-Decorated Oxygen-Rich Anode Surfaces (Pt2/o-MO_2(110), M = Ru and Ir) in DMFC. *J. Phys. Chem. C* **2017**, *121*, 9825–9832. [CrossRef]

308. Park, S.; Shao, Y.; Liu, J.; Wang, Y. Oxygen electrocatalysts for water electrolyzers and reversible fuel cells: Status and perspective. *Energy Environ. Sci.* **2012**, *5*, 9331–9344. [CrossRef]
309. Basri, S.; Kamarudin, S.K.; Daud, W.R.W.; Yaakob, Z.H.; Khadum, A.A. Study on kinetic energy of a novel metal composite for anode catalyst in direct methanol fuel cell. *Int. J. Energy Res.* **2015**, *39*, 181–190. [CrossRef]
310. Ghosh, A.; Ramaprabhu, S. An efficient and durable novel catalyst support with superior electron-donating properties and fuel diffusivity for a direct methanol fuel cell. *Catal. Sci. Technol.* **2017**, *7*, 5079–5091. [CrossRef]
311. Liu, L.; Zeng, G.; Chen, J.; Bi, L.; Dai, L.; Wen, Z. N-doped porous carbon nanosheets as pH-universal ORR electrocatalyst in various fuel cell devices. *Nano Energy* **2018**, *49*, 393–402. [CrossRef]